Groundwater equilibration and radionuclide solubility calculations

NWMO TR-2010-02 December 2010

Lara Duro, Vanessa Montoya, Elisenda Colàs and David García

Amphos 21

nwmo

NUCLEAR WASTE MANAGEMENT ORGANIZATION

SOCIÉTÉ DE GESTION DES DÉCHETS NUCLÉAIRES

Nuclear Waste Management Organization
22 St. Clair Avenue East, 6th Floor
Toronto, Ontario
M4T 2S3
Canada

Tel: 416-934-9814
Web: www.nwmo.ca

Groundwater equilibration and radionuclide solubility calculations

NWMO TR-2010-02

December 2010

Lara Duro, Vanessa Montoya, Elisenda Colàs and David García
Amphos 21

ABSTRACT

Title: **Groundwater equilibration and radionuclide solubility calculations**
Report No.: **NWMO TR-2010-02**
Author(s): Lara Duro, Vanessa Montoya, Elisenda Colàs and David García
Company: Amphos 21
Date: December 2010

Abstract
In a geological repository, containers are designed to prevent groundwater from getting in contact with fuel. In the case of a defective container water may contact the fuel and hence radionuclides might be mobilized. The assessment of radionuclide solubility limits in the near field of a repository for used fuel is essential for the safety demonstration of such as a disposal system. The objective of this report is then the study of the solubility of 19 radionuclides (Am, As, Bi, C, Cu, Mo, Nb, Np, Pa, Pb, Pd, Pu, Ra, Se, Sn, Tc, Th, U and Zr) in two different groundwater compositions, considered as representative groundwaters expected in the geological formation likely to host a future Canadian geological repository: the saline crystalline groundwater (CR-10) and the highly saline sedimentary groundwater (SR-270) provided by NWMO.

The crystalline groundwater CR-10 is well known and in previous work it has been (thermodynamically) equilibriated with minerals present at repository depth and with the near field components (bentonite buffer and the container). The sedimentary groundwater SR-270 is not as well established. This report summarise the calculation of the groundwater composition resulting from the interaction of SR-270 sedimentary groundwater with the MX-80 bentonite buffer and the carbon steel insert (SA 516 grade 70) of the Cu-Container.

Solubility calculations have been carried out with groundwaters equilibrated with minerals present at repository depth (*CR-10 eq* and *SR-270 eq*) and groundwaters equilibrated with the bentonite buffer and the container (*CR-10 NF* and *SR-270 NF*).

The Yucca Mountain Pitzer database (data0.ypf.R2) has been used in the solubility assessment of Am, C, Cu, Np, Mo, Pu, Tc, Th, U and Zr. The ThermoChimie v.7b SIT (Specific Ion Interaction Theory) database (released as sit.txt with the code PHREEQC v.17) has been used to compare the results obtained with the Yucca Mountain Pitzer database. The SIT database has been used for the solubility assessment of the elements not included in the Yucca Mountain Pitzer database.

The ThermoChimie SIT database does not include thermodynamic data for the element Bi and the thermodynamic data for the elements As and Cu are not complete. A literature review of the available information has been carried out to find a consistent and alternative thermodynamic dataset for Bi, As and Cu solubilities.

Sensitivity analyses, studying the influence of some key parameters on the solubility of radionuclides, and qualitative uncertainty analysis, describing the conceptual uncertainties that may affect the solubility limits of a radionuclide, are also provided.

TABLE OF CONTENTS

LIST OF TABLES

Page

LIST OF FIGURES

Page

1. INTRODUCTION

Deep geological disposal concepts for used nuclear fuel waste rely on the passive safety functions of a series of engineered and natural barriers. In a geological repository, containers are designed to prevent groundwater from contacting the used fuel and radionuclides in the fuel. In the case of an engineered barrier failure, radionuclides can eventually be released from the waste matrix and migrate through the engineered and natural barriers.

The assessment of radionuclide mobility in these environments is essential for the safety demonstration of the repository. One of the key factors influencing the rate of radionuclide transport out of the repository is the solubility of radionuclides released into the aqueous environment. The ability to model radionuclide dissolution under repository conditions is an important issue when assessing the safety of a disposal system.

Solubility values for several radionuclides of interest for Canada were calculated 15-20 years ago (Lemire and Garisto, 1989) based on a range of water chemistries from Canadian Shield crystalline rock data and using the thermodynamic data available at that time. The purpose of this work is to update the solubility assessment of 19 radionuclides (Am, As, Bi, C, Cu, Mo, Nb, Np, Pa, Pb, Pd, Pu, Ra, Se, Sn, Tc, Th, U and Zr) taking into account current information on new potential groundwater compositions and updated thermodynamic data.

Presently no Canadian site is selected for a repository for used fuel. In order to conduct these solubility assessments, NWMO has selected two different groundwater compositions as representative of the different chemical conditions expected to occur in the surroundings of the potential nuclear waste repository: the saline crystalline groundwater (CR-10) and the highly saline sedimentary groundwater (SR-270).

The changes induced in these groundwater compositions due to its interaction with the bentonite and the metallic canister are also relevant, since it is the modified groundwater that could eventually contact the fuel. In the case of groundwater interaction with, for example, the C-steel insert in the absence of any other active oxidant but water, the C-steel insert starts to corrode through generation of hydrogen due to water reduction. Under these conditions Fe(II) solid phases may form, which very possibly evolve towards the formation of Fe(II)-Fe(III) phases, such as magnetite (Fe_3O_4(s)). When groundwater contacts the bentonite barrier, processes such as ion exchange and groundwater-bentonite surface interactions can also exert an important control on the geochemistry of the system. This effect appears to be more important than the one played by mineral dissolution and/or precipitation processes in the clay.

Other variable which can affect solubility calculations is the salinity, that is, the ionic strength of the selected groundwaters, which varies from saline (0.24 m) to very saline (> 4.5 m). This implies that an appropriate choice of the approach to conduct activity corrections is needed (SIT or Pitzer).

An effort has also been made to use the most adequate thermodynamic database to conduct the solubility calculations. Two different databases have been used: the ANDRA database ThermoChimie v.7b (released as sit.txt with the code PHREEQC v.17) and the Yucca Mountain Project Pitzer database data0.ypf.R2 (Jove-Colon et al., 2007).

The main objectives of this report are:

1) Assessing the effect of the presence of the clay buffer and metallic C-steel insert on the compositions of the SR-270 groundwater;

2) Calculating the solubility of Am, As, Bi, C, Cu, Mo, Nb, Np, Pa, Pb, Pd, Pu, Ra, Se, Sn, Tc, Th, U and Zr under the different conditions of interest; and

3) Comparing the results of the solubility calculations obtained with two different thermodynamic databases associated with the different ionic strength corrections: ThermoChimie v.7b (TC) /SIT approach and Yucca Mountain Project (YMP) / Pitzer approach.

2. DEFINITION OF THE SYSTEM AND MODELLING APPROACH

Geochemical calculations reported in this work have been done by using the geochemical code PHREEQCI v2.17.0 (Parkhurst and Appelo, 2001), an open source code developed by USGS and widely used and tested in many types of geochemical problems. Solubility and speciation calculations have been complemented with the code HYDRA-MEDUSA (Puigdomènech, 2002). The HYDRA-MEDUSA package is a combination of a thermodynamic database and a geochemical code that allows a very easy drawing of many different types of chemical diagrams: predominance, fraction and solubility, among others. The package has been developed by Ignasi Puigdomènech at KTH and can be freely downloaded from http://www.kemi.kth.se/medusa/.

2.1 GENERAL CONSTRAINTS

Calculations have been carried out at 25ºC and no temperature assessment has been conducted.

We have assumed that sulphate to sulphide reduction does not occur whereas any sulphide present in solution can be easily oxidised to sulphate if thermodynamically favoured. We have also neglected the reduction of carbonate to methane and the reduction of nitrate to ammonium or $N_2(g)$. The reason for these assumptions is that all these processes (sulphate reduction, methanogenesis and denitrification) are normally microbiologically mediated (Pedersen, 2000) and the microbial activity has not been considered in this study. The absence of bacterial activity in the clay buffer is supported by the small pore space of the compacted bentonite, which makes the growth of microorganisms very difficult (SKB 2004b).

In the solubility calculations in this report we have assumed the basic Ostwald's principle that the less crystalline phases are kinetically favoured to precipitate and that, consequently, they constitute the most likely solubility limiting solid phases. Equilibration of the corresponding solutions with the pure solid phases has been considered by avoiding changes in the groundwater composition other than those for the elements of interest. This means that for calculating the composition of the groundwater in equilibrium with, i.e., $RaSO_4(s)$, radium has been added to the solution until the saturation index of the target solid ($RaSO_4(s)$) equals 0.

This methodology is different from that used in previous assessments where the equilibration of the solution with the solid was done adding the solid ($RaSO_4(s)$) which resulted in changes to both the sulphate and the radium concentrations in solution. For a more extensive discussion on this issue the reader is referred to Bruno et al. (2001).

2.2 THERMODYNAMIC DATABASES

The YMP dataset data0.ypf.R2 provided by NWMO was developed using the Pitzer approach. This dataset was developed for the YMP by Jove-Colon et al. (2007). The Pitzer database were originally developed for the EQ3/6 codes, but have been converted to the PHREEQC format by NWMO. The dataset contains the elements shown in Figure 1.

The thermodynamic database used to conduct the calculations with SIT ionic strength corrections was the ThermoChimie v.7.b database, developed by Duro and co-workers for ANDRA (Duro et al. 2006; Colàs et al. 2007, Montoya et al. 2008, Grivé et al., 2009). The ThermoChimie v.7.b database is a complete self consistent thermodynamic database that contains the data needed for conducting thermodynamic calculations for the elements and radionuclides shown in Figure 1. The database was developed by using the SIT approach; however, when SIT parameters were not available, the Debye-Hückel (D-H) approach was applied.

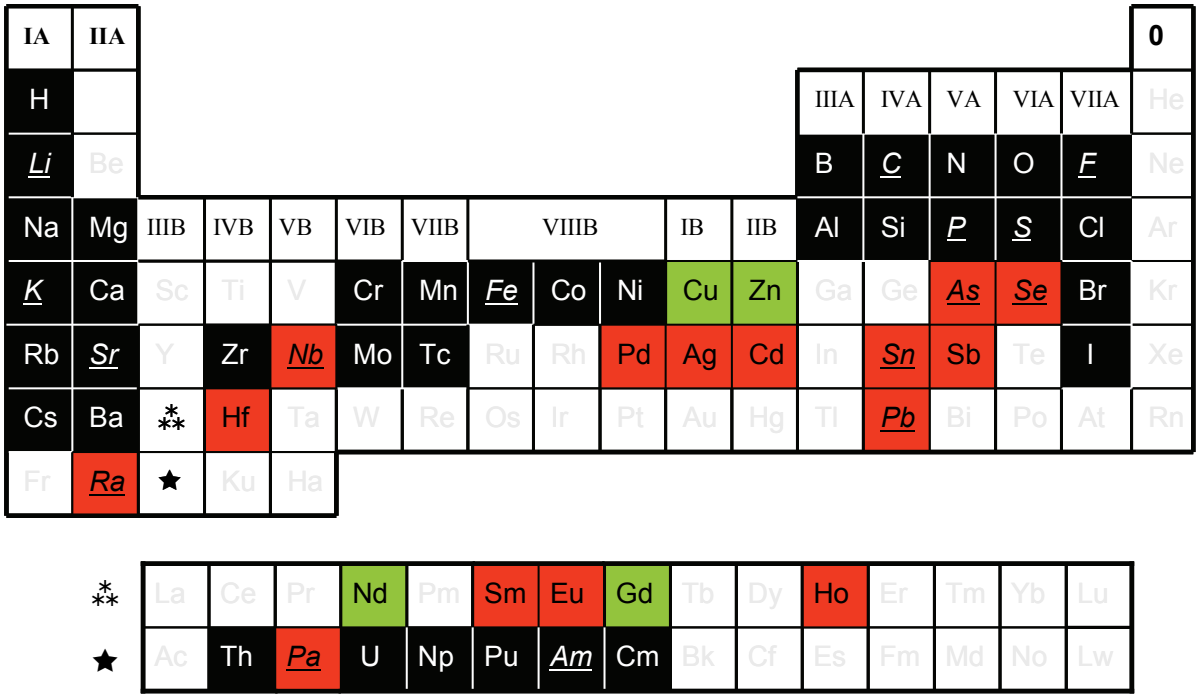

Figure 1: Periodic table showing the elements present in a) ThermoChimie v.7b and YMP databases (black), b) only in ThermoChimie v.7b (red) and c) only in YMP database (green). Elements in the ThermoChimie database where the selection of SIT coefficients is not complete for relevant aqueous species for this work are underlined.

Thermodynamic data originally not included in ThermoChimie SIT database but selected in this work to perform the solubility calculations of As, Bi and Cu are described below.

2.2.1 Arsenic

Only a limited amount of thermodynamic data for As, mainly taken from the NEA compilation (Grenthe et al., 1992) and originally coming from Wagman et al. (1982), are included in ThermoChimie v.7.b/SIT database

Two different oxidation states for arsenic are defined in ThermoChimie v.7.b/SIT: As(V) and As(III). Arsenate species are predominant at moderate and high redox potentials, while arsenite species occur under more reducing conditions.

For As(V) the aqueous species present in ThermoChimie v.7.b/SIT are the free arsenate ion AsO_4^{3-} and the three protonated species. These data have been selected from the auxiliary data of the NEA review (Grenthe et al., 1992).

The As(III) species originally included in ThermoChimie v.7.b/SIT were the protonated forms of AsO_3^{3-}. The data for the aqueous As(III) species has been also taken from the auxiliary data of the NEA review (Grenthe et al., 1992) (Table 1).

Solid arsenates ($M_x(AsO_4)_y$) are also selected in ThermoChimie v.7.b/SIT. Only thermodynamic data for those species that could be present for the groundwaters of interest have been selected (calcium and strontium arsenates). Thermodynamic data for these solids refer to their formation, therefore reaction data have been calculated using the formation data selected from Wagman et al. (1982) (see Table 1). Metal arsenites are much more soluble than the corresponding metal arsenates and they have not been selected for this work.

Both, As(V) and As(III) form different oxide solid phases. Reaction data have been calculated and selected from formation parameters in Grenthe et al., (1992) and Robby and Hemingway, (1995), respectively. Two different As_2O_3 polymorphs are described in the literature. The monoclinic As_2O_3 called claudetite is the low temperature polymorph, and it transforms into arsenolite at 110ºC. Only claudetite has been included in the database.

Arsenic also forms sulphide species for which thermodynamic data have been found in the literature. ThermoChimie v.7.b/SIT includes two different sulphide solids, AsS and As_2S_3, called realgar and orpiment respectively. In all cases reaction data have been calculated from formation parameters in the NBS tables (Robby and Hemingway, 1995) and selected in this work. In the literature, the sulphide solid arsenopyrite (FeAsS) is also described. However, this phase only occurs at high temperatures and hydrothermal systems and has not been selected in this work.

There are several aqueous As(III)-S species described in the literature (Eary, 1992; Helz et al., 1995; Krupp, 1990; Mironova and Zotov, 1980; Spycher and Reed, 1989; Webster, 1990). However, the occurrence of these species has been the subject of considerable debate as no clear stoichiometry is defined for the studied systems. Under low sulphide concentration (10^{-6} M), Helz et al., (1995) defined the presence of the aqueous species $AsS(OH)(HS)^-$ not reported by other authors. As we can see in Figure 2 the incorporation of this species in the database does not agree with the solubility experiments of other authors (Mironova et al., 1984; Webster, 1990) therefore it was not included in the database. For those studies performed under higher

sulphide concentration (10^{-3} M) two sets of results concerning the stoichiometry of As(III)-S aqueous species and the corresponding stability constants defined for the system can be identified. One group of authors (Mironova and Zotov, 1980; Krupp, 1990) supports the idea that dimeric species are governing arsenic sulphide aqueous chemistry. A second group of authors (Spycher and Reed, 1989; Webster, 1990; Eary, 1992) suggests that trimer species are the ones present in solution. By means of ab initio quantum mechanical predictions and EXAFS and Raman spectroscopic data Helz et al. (1995) suggested that the aqueous chemistry of arsenic sulphides is only governed by As-S trimer species. In a more recent report, Bessinger and Apps (2003) recommend selecting trimer species, although the authors highlight that more experimental information would be desired to finally solve this controversy. Finally, in this work we have included the aqueous trimer species $HAs_3S_6^{2-}$, $H_2As_3S_6^-$ and $H_3As_3S_6$ selected by Bessinger and Apps (2003). As we can see in Figure 3, the solubility results of orpiment (As_2S_3) under high sulphide concentration (Eary, 1992) can be explained with the sulphide/arsenic aqueous scheme selected for this work.

No SIT coefficients have been selected for As species so the D-H approach was applied in the calculations.

Table 1: Thermodynamic data selected for arsenic aqueous complexes and solid phases.

Reaction	logK
$AsO_4^{3-} + H^+ = HAsO_4^{2-}$	11.60
$AsO_4^{3-} + 2H^+ = H_2AsO_4^-$	18.37
$AsO_4^{3-} + 3H^+ = H_3AsO_4$	20.63
$AsO_4^{3-} + 3H^+ + 2e^- = HAsO_3^{2-}$	19.80
$AsO_4^{3-} + 4H^+ + 2e^- = H_2AsO_3^-$	30.81
$AsO_4^{3-} + 5H^+ + 2e^- = H_3AsO_3$	40.02
$6HS^- + 3AsO_4^{3-} + 19H^+ + 6e^- = HAs_3S_6^{2-} + 12H_2O$	185.37
$6HS^- + 3AsO_4^{3-} + 20H^+ + 6e^- = H_2As_3S_6^- + 12H_2O$	193.28
$6HS^- + 3AsO_4^{3-} + 21H^+ + 6e^- = H_3As_3S_6 + 12H_2O$	196.86
$2AsO_4^{3-} + 3Ca^{2+} = Ca_3(AsO_4)_2(s)$	18.90
$2AsO_4^{3-} + 3Sr^{2+} = Sr_3(AsO_4)_2(s)$	16.08
$2AsO_4^{3-} + 6H^+ = As_2O_5(s) + 3H_2O$	34.54
$2AsO_4^{3-} + 10H^+ + 4e^- = As_2O_3(s) + 5H_2O$	81.39
$13H^+ + 4e^- + 3HS^- + 2AsO_4^{3-} = As_2S_3(s) + 8H_2O$	127.46
$7H^+ + 3e^- + HS^- + AsO_4^{3-} = AsS(s) + 4H_2O$	67.06

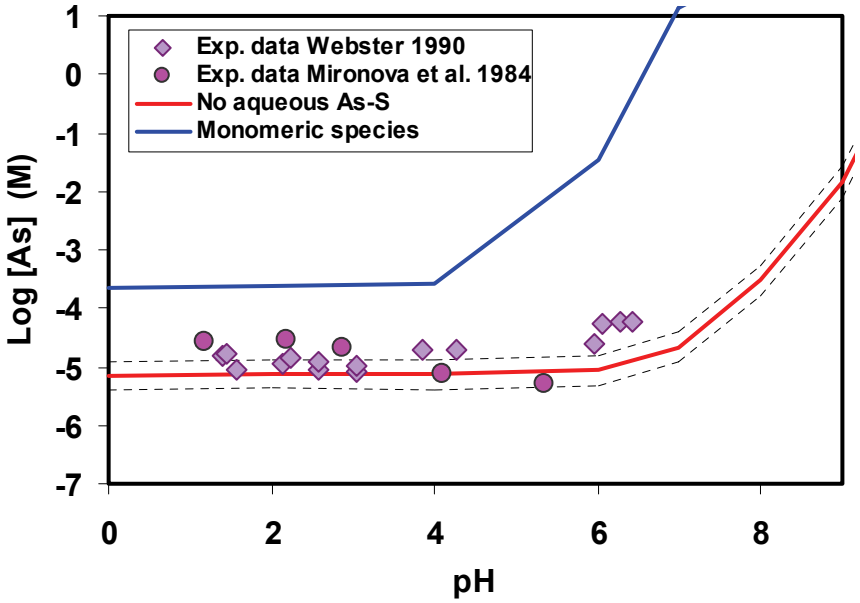

Figure 2: Solubility of orpiment (As_2S_3) as a function of pH and sulphur total concentration of 10^{-5} M. Diamonds represent experimental data of Mironova et al., (1984) and circles experiments of Webster (1990). Blue line is the model taking into account the monomeric species $AsS(OH)(HS)^-$. Red line shows the results without taking into account this monomeric species and only hydrolysis species (see Table 1). Error includes different crystallinity of the solid used in each experiment.

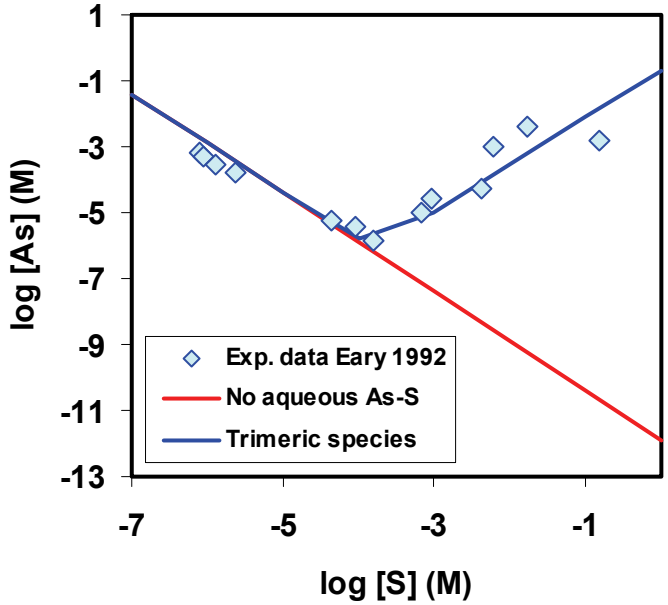

Figure 3: Solubility of orpiment (As_2S_3) as a function of sulphide and pH = 4. Diamonds represent experimental data of Eary (1992). Blue line is the model considering the existence of trimeric species $HAs_3S_6^{2-}$, $H_2As_3S_6^-$ and $H_3As_3S_6$. Red line is the model without this trimeric species and only hydrolysis species (see Table 1).

We have completed the selection with the addition of the redox equilibrium $Bi^{3+} + 3e^- = Bi(cr)$, taken from of Lotenbach et al. (1999)

Lothenbach et al. (1999) did not select any bismuth-sulphide species (solid or aqueous complex). In the literature, only thermodynamic data for the solid sulphide bisthmutinite (Bi_2S_3) are described (Licht, 1988, Bard et al., 1985). Thermodynamic data for this solid have not been selected due to the extremely high stability associated with its crystallinity, which would yield solubilities below 10^{-17} M.

Although in Lothenbach et al. (1999) the SIT correction is used to obtain thermodynamic data at I = 0, only the SIT coefficients for ε(cation, ClO_4^-) can be obtained for those bismuth cations listed in Table 2.

2.2.3 Copper

A review of published thermodynamic data for solid and aqueous species of copper relevant for the system has been performed. Common oxidation states of copper include Cu(I) and Cu(II). Under anoxic and reducing conditions, Cu(I) prevails, whereas Cu(II) dominates the copper speciation under oxidising conditions.

Different compilations of thermodynamic data including copper are available in the literature (Baes and Mesmer, 1976, Puigdomènech and Taxén, 2000, Martell et al., 2004, Blanc et al. 2007). Puigdomènech and Taxén (2000) made one of the most extensive and accurate selection, including chlorides, carbonates, phosphates, sulphates, sulphides and redox aqueous species. We have used this database as the main source of information (see Table 3).

The Cu(II)/Cuº redox equilibrium ($Cu^{2+} + 2e^- = Cu(s)$) has been calculated using the auxiliary data included in NEA thermodynamic selections (Grenthe et al. 1992), and is in agreement with the selection in Puigdomènech and Taxén (2000).

Thermodynamic data for Cu(II) hydrolysis species have been obtained from Puigdomènech and Taxén (2000).

In the case of Cu(I) hydrolysis, we have decided to selected thermodynamic data selected in Puigdomènech and Taxén (2000) but with some minor changes as discussed below.

Thermodynamic data for Cu(I) hydrolysis is very scarce and several data come from studies at high temperatures (>100ºC) (Akinfiev and Zotov, 2001, Var'yash, 1989). Data for hydrolysis species of Cu(I) in Puigdomènech and Taxén (2000) have been selected from Beverskog and Puigdomènech (1997). In this last reference, stability constants for the species CuOH and $Cu(OH)_2^-$ have been calculated by fitting the temperature dependence of the aqueous solubility of Cu_2O/Cu mixtures determined by Var'yash (1989) over the temperature range 150-350ºC at saturated vapour pressure and at 450ºC and 500 bars. The selection of these constants gives the diagram shown in Figure 4.

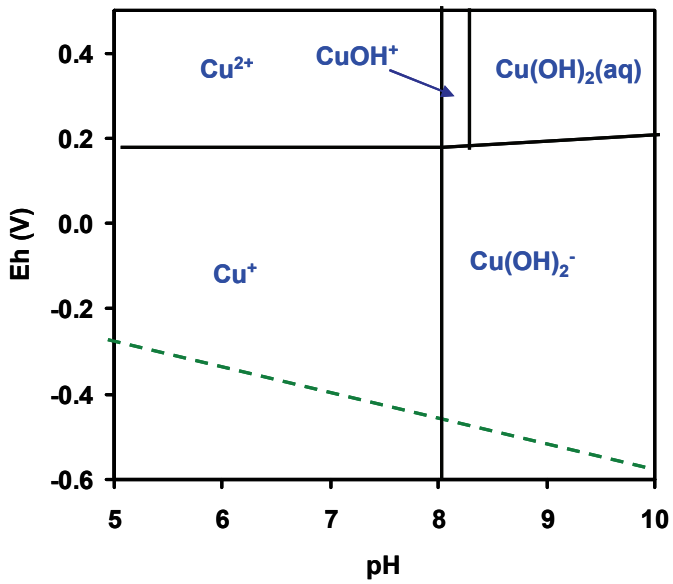

Figure 4: Eh vs pH predominance diagram for copper aqueous species in water. $[Cu]_T=10^{-8}$ mol/L. The diagram has been obtained using the selection from Puigdomènech and Taxén (2000), where $Cu(OH)_2^-$ stability seems to be overestimated (see text).

Properties of Cu(I) have been compared with those of alkaline metals and elements of its same group such as Ag(I), because all these elements have a single valence electron in a s orbital, so their properties should be similar (Dyer and Leddicote, 1961).

Hydrolysis of a metal ion is closely related to its acidity. This is shown in Figure 5, where the acidity of alkaline metals and Ag(I) (related to the Z/r ratio, where Z is the ion charge and r is the ion radius) is correlated with the value of the first hydrolysis constant. The more acidic a metal the higher will be its tendency towards hydrolysis. Taking this premise into account and the data shown in Figure 5, thermodynamic data for the first hydrolysis constants agree with the actual selection of similar elements included in ThermoChimie v7.b/SIT.

In the case of $M(OH)_2^-$ species, only thermodynamic data for Ag(I) are selected in ThermoChimie v.7b/SIT database with logK =-24 (Baes and Mesmer 1976). If we compare this stability constant with the one selected in Puigdomènech and Taxén (2000) for Cu(I) (logK = -16.16) we observe an unexpected difference of 8 log units. For this reason we consider that the stability constant reported in Puigdomènech and Taxén (2000) for $Cu(OH)_2^-$ is overestimated. A stability constant for $M(OH)_2^-$ similar to the one selected for Ag(I) would give a speciation diagram where the species $Cu(OH)_2^-$ would be only relevant at pH > 11. This high pH is not relevant for the present study and for this reason $Cu(OH)_2^-$ has not been included in the database.

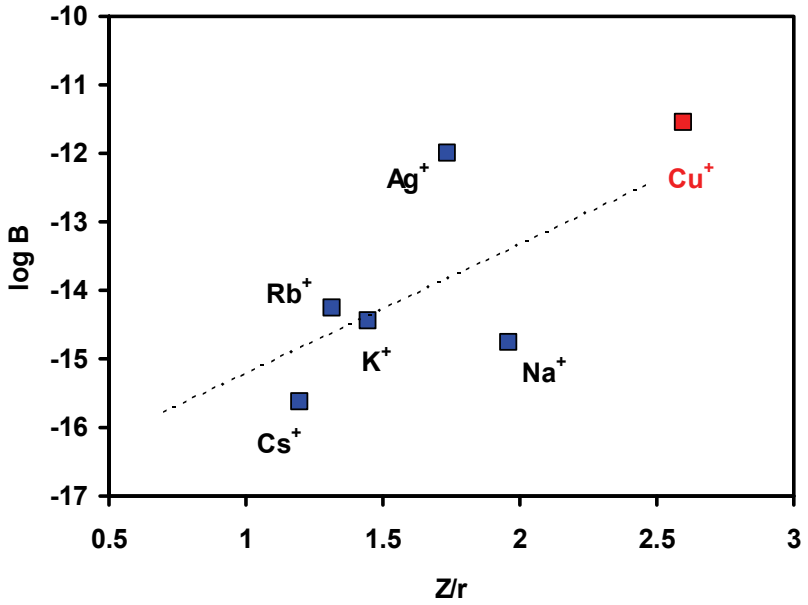

Figure 5: Correlation between Z/r ratio of metal ions and its first hydrolysis constant logβ of (M(OH)). Hydrolysis constant are defined for the reaction $M^+ + H_2O = MOH + H^+$. Dashed line shown to guide the eye in the correlation.

No polynuclear species have been selected in this work as they form at copper concentrations above 1M (Puigdomènech and Taxén, 2000).

No copper(I) carbonates are described in the literature and only carbonate species of Cu(II) have been included from Puigdomènech and Taxén, (2000). Copper(II) carbonate complexes become important at carbonate concentrations above those commonly found in groundwaters.

Phosphate complexes with both Cu(I) and Cu(II) have been included in the database. Only solid Cu(II) phosphates have been found in the literature. Although acknowledging that there is some uncertainty concerning the copper speciation in this system (see discussion in Puigdomènech and Taxén (2000)), this should not be a handicap for the copper solubility assessment, as the phosphate ligand plays a minor role under the studied conditions, due to the very low concentration of this ligand in the reference groundwaters.

Only weak Cu-NO_3^- complexes have been reported in the literature. As nitrate is present only in trace amounts in the groudwaters studied, we have decided not to include them in the database.

Chloride ions may influence copper chemistry by the formation of aqueous complexes and solid phases: copper-chloride complexes can be important under the conditions of the studied groundwaters. Copper(II) forms weaker chloride complexes than Cu(I). Thermodynamic data from Puigdomènech and Taxén (2000) have been selected.

No fluoride species have been selected because the influence of fluoride at the low concentrations expected in the selected groundwaters appears to be unimportant.

Sulphide aqueous species have been seleted from Puigdomènech and Taxén (2000). In terms of solid sulphide phases, a series of different phases are formed with compositions varying between chalcocite (Cu_2S) and covellite (CuS). Thermodynamic data from Puigdomènech and Taxén (2000) have been selected for these two phases. Other intermediate sulphides with a different Cu(I)/Cu(II) ratio are considered by Puigdomènech and Taxén (2000), such as djurleite ($Cu_{1.75}S$) and anilite ($Cu_{1.934}S$). However, only thermodynamic data for pure phases have been selected in this work. In the literature, other sulphide species such as chalcopyrite ($CuFeS_2$) and bornite (Cu_5FeS_4) are reported, but their formation are only expected at high temperatures and so are not considered to occur in the studied systems.

The Cu(II) solids selected in Puigdomènech and Taxén (2000) are not likely to form under the conditions of interest and have not been included in the database.

Puigdomènech and Taxén (2000) reported SIT coefficients for Cu(II) species.

Table 3: Thermodynamic data selected for copper aqueous complexes and solid phases. Data from Puigdomènech and Taxén (2000).

Reaction	logK
$Cu^{2+} + e^- = Cu^+$	2.83
$Cu^{2+} + H_2O = CuOH^+ + H^+$	-7.97
$Cu^{2+} + 2H_2O = Cu(OH)_2 + 2H^+$	-16.24
$Cu^{2+} + 3H_2O = Cu(OH)_3^- + 3H^+$	-26.70
$Cu^{2+} + 4H_2O = Cu(OH)_4^{2-} + 4H^+$	-39.6
$Cu^+ + H_2O = CuOH + H^+$	-11.55
$Cu^{2+} + CO_3^{2-} = CuCO_3$ (aq)	6.77
$Cu^{2+} + 2CO_3^{2-} = Cu(CO_3)_2^{2-}$	10.20
$Cu^{2+} + CO_3^{2-} + H^+ = CuHCO_3^+$	12.13
$Cu^{2+} + H_2PO_4^- = CuH_2PO_4^+$	1.14
$Cu^{2+} + 2H_2PO_4^- = Cu(H_2PO_4)_2$ (aq)	1.94
$Cu^{2+} + 2H_2PO_4^- = Cu(HPO_4)(H_2PO_4)^- + H^+$	-1.86
$Cu^{2+} + 2H_2PO_4^- = Cu(HPO_4)_2^{2-} + 2H^+$	-7.06
$Cu^{2+} + H_2PO_4^- = Cu(HPO_4)$ (aq) $+ H^+$	-3.11
$Cu^+ + H_2PO_4^- = CuH_2PO_4$ (aq)	0.87
$Cu^+ + H_2PO_4^- = Cu(H_2PO_4)_2^-$	1.80
$Cu^+ + 2H_2PO_4^- = Cu(HPO_4)(H_2PO_4)^{2-} + H^+$	-3.00
$Cu^{2+} + SO_4^{2-} = CuSO_4$(aq)	2.31
$Cu^{2+} + Cl^- = CuCl^+$	0.64
Cu^{2+} $2Cl^- = CuCl_2$ (aq)	0.24
Cu^{2+} $3Cl^- = CuCl_3^-$	-1.28
Cu^{2+} $4Cl^- = CuCl_4^{2-}$	-3.98

Reaction	logK
$Cu^{+} + Cl^{-} = CuCl\ (aq)$	3.30
$Cu^{+} + 2Cl^{-} = CuCl_2^{-}$	5.62
$Cu^{+} + 3Cl^{-} = CuCl_3^{2-}$	4.86
$Cu^{+} + HS^{-} = CuHS\ (aq)$	13.00
$Cu^{+} + 2HS^{-} = Cu(HS)_2^{-}$	17.18
$2Cu^{+} + 2HS^{-} = Cu_2S(HS)_2^{2-}$	29.87
$Cu^{2+} + 2e^{-} = Cu(s)$	11.39(1)
$Cu^{2+} + H_2O = CuO(s) + 2H^{+}$	-7.68
$Cu^{2+} + 2H_2O = Cu(OH)_2(s) + 2H^{+}$	-8.64
$2Cu^{2+} + H_2O = Cu_2O(s) + 2H^{+}$	1.49
$Cu^{2+} + CO_3^{2-} = CuCO_3(s)$	11.45
$2Cu^{2+} + CO_3^{2-} + H_2O = Cu_2CO_3(OH)_2(s)$	5.30
$3\ Cu^{2+} + 2H_2PO_4^{-} = Cu_3(PO_4)_2\ (s) + 4H^{+}$	-2.27
$3\ Cu^{2+} + 2H_2PO_4^{-} + 3H_2O = Cu_3(PO_4)_2{\cdot}3H_2O(s) + 4H^{+}$	-4.00
$2Cu^{+} + SO_4^{2-} = Cu_2SO_4(s)$	1.95
$Cu^{2+} + SO_4^{2-} = CuSO_4(s)$	-2.94
$Cu^{2+} + SO_4^{2-} = CuSO_4{\cdot}5H_2O(s)$	2.69
$Cu^{2+} + 2Cl^{-} + 6H_2O = CuCl_2{\cdot}3Cu(OH)_2 + 6H^{+}$	-14.92
$Cu^{+} + Cl^{-} = CuCl(s)$	6.80
$Cu^{2+} + 2Cl^{-} = CuCl_2(s)$	-3.73
$Cu^{+} + HS^{-} = CuS(s) + H^{+}$	-34.02
$2Cu^{+} + HS^{-} = Cu_2S(s) + H^{+}$	-22.06

(1) In agreement with Grenthe et al., 1992

2.3 IONIC STRENGTH CORRECTION APPROACHES

When ionic solutions depart strongly from ideality, this non-ideality effect must be accounted for by the introduction of an activity coefficient, γ_I, relating the concentration m_i of the species *i* with its activity a_i (see eq. 1).

$$a_i = m_i \cdot \gamma_i \qquad \textbf{eq. 1}$$

There exist a number of different semi-empirical methods for the estimation of activity coefficients, mostly based on microscopic physico-chemical descriptions of the interactions between dissolved ions, and sometimes of the interactions between ions and solvent.

However, a consistent theory of ionic solutions is still awaited. Until such a theory is available we have to rely on empirical models. The ones used in this work are all based on extensions of the Debye-Hückel theory (SIT and Pitzer).

The new version of the PHREEQC code (v2.17) can use both the Pitzer and the SIT approaches. The Nuclear Energy Agency (Grenthe and Puigdomenech, 1997) recommends the Specific Ion Interaction Theory (SIT) for activity corrections. The SIT equation accounts for both the electrostatic long-range interactions in dilute solutions and the short-range and non-electrostatic interactions occurring between ions at higher concentrations. According to this theory, the activity coefficient (γ_i) for the species *i* can be calculated with eq. 2 where z_i is the charge of ion *i*, I_m is the molal ionic strength, A and B are the temperature and pressure dependent Debye-Hückel parameters and a_i is the ion size parameter for the hydrated ion *i*. This equation adds to the Debye-Hückel term, the sum of the products of the specific ion interaction parameters, $\varepsilon(i,k,I_m)$, with the molality m_k, for all the ions *k* present in solution. This approximation gives good results for solutions with ionic strengths below 2 m.

$$\log(\gamma_i) = -z_i^2 \left(\frac{A\sqrt{I_m}}{1 + Ba_i\sqrt{I_m}} \right) + \sum_k \varepsilon(i,k,I_m) m_k \qquad \textbf{eq. 2}$$

The Pitzer model in its original form, describes the thermodynamics of electrolyte mixtures where ionic pairing and complex formation are relatively weak. The number of interactions between dissolved species considered in the Pitzer model is higher than in SIT. This improves the description of thermodynamic properties at high ionic strengths (up to 20 m) but requires a large number of empirical parameters. According to this theory, the activity coefficient (γ_i) for the species *i* can be calculated with eq. 3,

$$\begin{aligned} \log(\gamma_i) = -z_i^2 & \left(\frac{A\sqrt{I_m}}{1 + b\sqrt{I_m}} + \frac{2}{b}\ln\left(1 + b\sqrt{I_m}\right) \right) + \sum_c \sum_a m_c m_a B'_{ac} + \sum_c \sum_{c'} m_c m_{c'} \phi'_{cc'} \\ & + \sum_a \sum_{a'} m_a m_{a'} \phi'_{aa'} + \sum_a m_a \left(2B_{ia} + ZC_{ia}\right) + \sum_c m_c \left(2\phi_{ic} + \sum_a m_a \psi_{ica}\right) \\ & + \sum_a \sum_{a'} m_a m_{a'} \psi_{iaa'} + |z_i| \sum_c \sum_a m_c m_a C_{ac} + 2\sum_n m_n \lambda_{ni} \end{aligned} \qquad \textbf{eq. 3}$$

where z_i is the charge of the cation *i* (the corresponding equation for an anion is obtained by exchanging a for c, and c for a throughout); A and b are fixed parameters ($0.3915 kg^{1/2}\ mol^{-1/2}$ and $1.2\ kg^{1/2}$); I_m is the molal ionic strength; c, c', a and a' are subscripts referring to cations (c and c') and anions (a and a') and n denotes neutral species; m_i is the molality for the species present in solution; ϕ_{ic} and λ_{ni} are the second virial coefficients arising from binary interactions between a specific cation i and another cation c, or a neutral species n, respectively; and ψ_{ica} and $\psi_{iaa'}$ are the third virial coefficients representing triple interactions between ions, i, c, a and ions i, a, a', respectively.

The terms B'_{ac}, ϕ'_{cc}, $\phi'_{aa'}$, B_{ia}, C_{ia}, C_{ac} and Z are functions that depend on the ionic strength and other empirical parameters needed for correct implementation of this ionic strength correction approach. The supplementary equations needed for correct implementation of the Pitzer ionic strength approach are shown in eq. 4 to eq. 11.

$$Z = \sum_i m_i |z_i| \qquad \textbf{eq. 4}$$

where z_i is the charge and m_i the molality of the species *i*. The ionic strength dependence of B_{ia} is described as follows:

$$B_{ia} = \beta_{ia}^{(0)} + \beta_{ia}^{(1)} g(I_m) \qquad \textbf{eq. 5}$$

where $\beta^{(0)}$, $\beta^{(1)}$ are constants for each anion-cation pair and the function $g(I_m)$ is defined as:

$$g(I_m) = \frac{2}{\alpha^2 I_m}\left[1 - \left(1 + \alpha\sqrt{I_m}\right)e^{-\alpha\sqrt{I_m}}\right] \qquad \textbf{eq. 6}$$

where α is a fixed parameter (α = 2.0 $Kg^{1/2}\cdot mol^{-1/2}$) for all electrolytes except the 2-2 charge type.

B'_{ac} is the ionic strength derivative of B_{ac}:

$$B'_{ac} = \beta_{ac}^{(1)} \frac{g'(I_m)}{I_m} \qquad \textbf{eq. 7}$$

where function $g'(I_m)$ is defined as:

$$g'(I_m) = -\frac{2}{\alpha^2 I_m}\left[1 - \left(1 + \alpha\sqrt{I_m} + \frac{1}{2}\alpha^2 I_m\right)e^{-\alpha\sqrt{I_m}}\right] \qquad \textbf{eq. 8}$$

C_{ia} is defined as follows:

$$C_{ia} = \frac{C_{ia}^{\Phi}}{2\left|z_i z_a\right|^{1/2}} \qquad \textbf{eq. 9}$$

The virial coefficient $\phi_{cc'}$ has the following form:

$$\phi_{cc'} = \theta_{cc'} + {}^{E}\theta_{cc'}(I_m) \qquad \textbf{eq. 10}$$

and $\phi'_{cc'}$ is the ionic strength derivative of $\phi_{cc'}$:

$$\phi'_{cc'} = {}^{E}\theta'_{cc'}(I_m) \qquad \textbf{eq. 11}$$

$\theta_{cc'}$ is a constant for each unlike cation-cation or anion-anion pair ($\theta_{aa'}$), ${}^{E}\theta_{cc'}(I_m)$ is a function of the ionic strength only (it is zero except for unsymmetrical mixing ions of the same sign) and ${}^{E}\theta'_{cc'}(I_m)$ is the derivative function of ${}^{E}\theta_{cc'}(I_m)$.

The differences between the two approaches to calculating the ionic strength corrections could be important for high ionic strength solutions (I > 1m).

At present, there is no unambiguous thermodynamic method to distinguish between complex formation/ion pairing and other types of short-range interactions between species in solution when the extent of complex formation is small or moderate. It is up to the modeller to decide whether to describe weak interactions between ions in terms of complex formation or by Pitzer type ion interactions.

2.4 GROUNDWATER COMPOSITION

The crystalline groundwater composition CR-10 is representative of the Canadian Shield crystalline rocks at depths and has been chosen to perform the solubility calculations of this work. For this groundwater, two different cases have been considered:

A. **CR-10 Equilibrated (*CR-10 eq*).** Corresponding to the groundwater composition resulting from the pre-equilibration step with the major minerals

B. **CR-10 interacted with bentonite and steel (*CR-10 NF*)**. Corresponding to the equilibrated groundwater composition affected by the influence of both the C-Steel insert and bentonite.

These two groundwater compositions have been provided by NWMO and are shown in Table 4.

The SR-270 groundwater provided by NWMO has also been selected as representative for the present study. This water SR-270 eq has already undergone equilibration with minerals present at repository depth and is shown in Table 4. However the equilibration with the MX-80 bentonite buffer and Cu container with carbon steel insert is required to obtain the groundwater compositions after interacting with bentonite and steel (see section 3).

One parameter that affects the results of the calculations is the density of the solution, which was not provided for the SR-270 eq groundwater. One can appreciate the high salinity of the SR-270 eq groundwater (TDS= 274,833 mg/L). This implies that the density for this groundwater will be higher than that of pure water (1.000 g/mL).

In order to obtain a density value for the SR-270 eq groundwater we have made a correlation between the TDS (mg/L) and the density of different groundwaters (see Figure 6 and Table 5) obtaining a density of 1.192 g/mL for the SR-270 groundwater.

Table 4: Groundwater composition provided by NWMO.

	CR-10 eq	CR-10 NF	SR-270 eq
pH	7.1	8.7	5.8
Environment	Reducing	Reducing	Reducing
Eh (mV)	-194	-575	-200
Density (g/mL)	1.006	1.006	*1.192**
Solutes (mg/L)			
Na	1,899	6,255	50,100
K	15	80	12,500
Ca	2,217	870	32,000
Mg	60	182	8,200
HCO_3	50	4	110
SO_4	1,243	4,314	440
Cl	6,099	6,059	168,500
Br			1,700
Sr	25	25	1,200
Li			5
F	2	2	1
I			3
B			80
Si	5	10	4
Fe	8	7	30
NO_3	1	1	10
PO_4	1	1	
Ionic strength (m)	0.24	0.32	6.47

* Calculated in this work

Table 5: Groundwater density (g/mL) and TDS (mg/L) for different Canadian reference groundwaters.

	Crystalline				Sedimentary			Meltwater
	CR-50	**CR-20**	**CR-10**	**CR-0**	**SR-300**	**SR-160**	**SR-20**	**RM-0**
TDS (mg/L)	55,500	23,000	11,300	500	327,000	157,000	20,000	80
Density (g/mL)	1.041	1.015	1.006	1.000	1.228	1.115	1.013	1.000

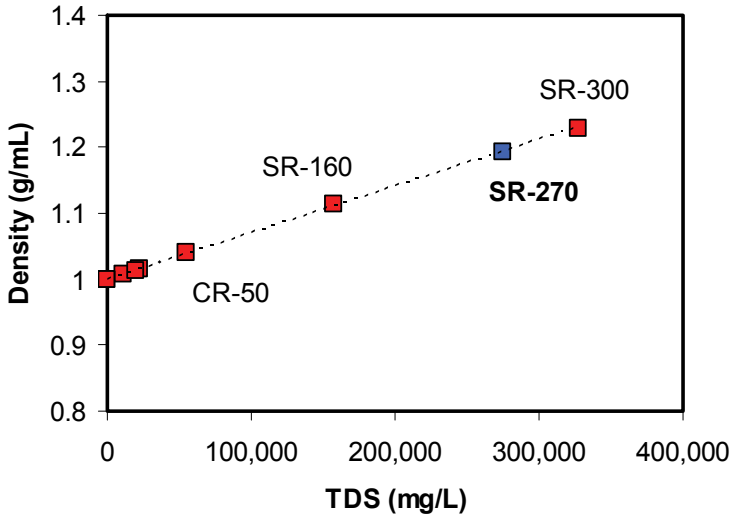

Figure 6: Correlation between TDS and the density for different groundwater compositions.

Minerals likely to be in equilibrium with groundwater compositions present a saturation index close to 0. For SR-270 eq groundwater has been preequilibrated with calcite and gypsum by NWMO using the YMP Pitzer database data0.ypf.R2 (see Figure 7).

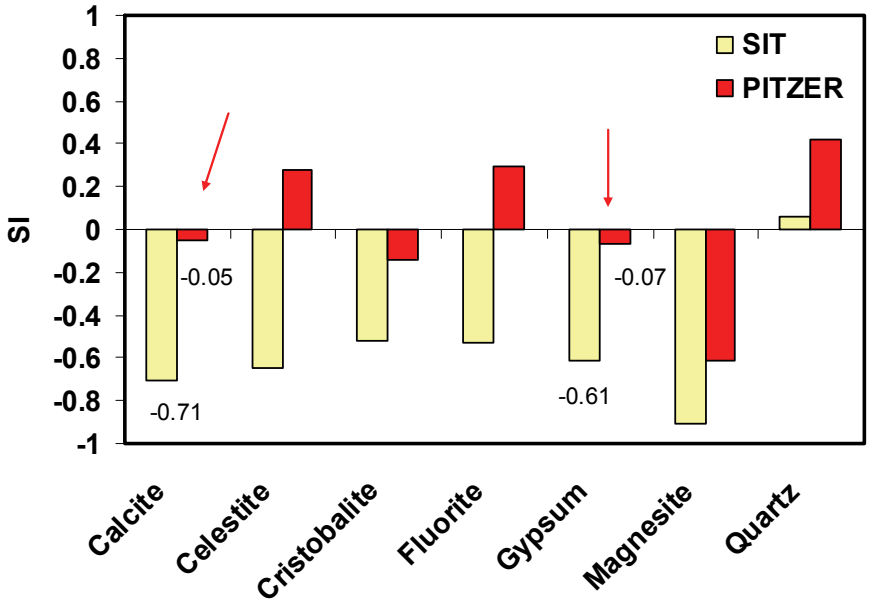

Figure 7: Calculated saturation indices of calcite ($CaCO_3$), celestite ($SrSO_4$), cristobalite (SiO_2), fluorite (CaF_2), gypsum ($CaSO_4$) magnesite ($MgCO_3$) and quartz (SiO_2) for SR-270 groundwater using ThermoChimie v.7b/SIT (yellow) and YMP Pitzer (red) databases.

The saturation indices have been compared with the ones obtained when using the ThermoChimie v.7b/SIT database. As we can see in Figure 7, the (absolute) saturation indices for calcite and gypsum are less than one.

We have recalculated the composition of the SR-270 eq groundwater using the ThermoChimie v.7b/SIT database in order to avoid effects due to initial re-equilibration when calculating the SR-270 groundwater composition after interacting with bentonite and the C-steel insert (see section 3). In Table 6, the re-equilibriated groundwater compositions, calculated using the two TDBs, are shown.

Table 6: Comparison between the re-equilibrated composition of SR-270 eq groundwater sample using ThermoChimie v.7b database/ SIT association and the YMP Pitzer database. Concentrations in mg L^{-1}.

	Yucca Mountain/PITZER	ThermoChimie v.7b/SIT
pH	5.8	6.3
Environment	Reducing	Reducing
Eh (mV)	-200	-200
Density (g/mL)*	*1.192*	*1.192*
Solutes (mg/L)		
Na	50,100	50,025
K	12,500	12,486
Ca	32,000	32,494
Mg	8,200	8,173
HCO_3	110	135
SO_4	440	1,784
Cl	168,500	168,058
Br	1,700	1,698
Sr	1,200	1,198
Li	5	5
F	1	1
I	3	3
B	80	80
Si	4	4
Fe	30	30
NO_3	10	10
Equilibration with*	Calcite, gypsum	Calcite, gypsum
Ionic strength (mol kgw^{-1})	6.47	4.51

* Calculated in this work

The main differences between the two compositons in Table 6 are related to the sulphate concentration. This difference is due to the different aqueous sulphate speciation calculated in the two TDBs. For the calculations performed with the YMP Pitzer database, SO_4^{2-} is the main

aqueous species in solution for sulphate with minor contribution of the $CaSO_4$ species. However when calculations are performed with ThermoChimie v.7b/SIT the complex $NaSO_4^-$ is the main aqueous species in solution with a minor contribution of the $CaSO_4$ species. Specially, it must be noticed that ThermoChimie SIT database includes both $NaSO_4^-$ and the SIT interaction coefficient $\varepsilon(Na^+, SO_4^{2-})$, which results in enhanced gypsum dissolution and high sulphate concentrations in solution.

3. EFFECT OF THE NEAR FIELD ON THE SR-270 GROUNDWATER COMPOSITION

In this section, different geochemical calculations have been performed to study the interaction of the SR-270 eq groundwater with the C-steel insert and the bentonite barrier. Calculations have been done by using the latest version of PHREEQC (PHREEQCI v2.17.) (Parkhurst and Appelo, 2001) and the YMP Pitzer database data0.ypf.R2 (Jove-Colon et al. 2007) based on the Pitzer ionic strength corrections approach.

A comparison with the calculations performed by applying the ThermoChimie v.7b database (Duro et al. 2006; Colàs et al. 2007, Montoya et al. 2008, Grivé et al. 2009), and SIT corrections has been done.

3.1 CHARACTERIZATION OF BENTONITE MINERALOGY AND PROCESSES

The composition of the Wyoming MX-80 bentonite has been used in the calculations of this work. Karnland et al. (2006) performed a coherent study of Wyoming bentonite (see Figure 8). A final but important conclusion of this work is that there are bentonite materials with quite different geological origin, which have the same basic mineralogical characteristics and thereby the same sealing properties. For this reason, the mineral composition of the bentonite considered in SKB (2004) has been selected in this work as representative. The mineral composition together with the initial composition of bentonite exchange positions is shown in Table 7.

As seen in Table 7, the nominal amount of calcite and siderite in montmorillonite is 0 %wt. However, different analyses of MX-80 bentonite conclude that both the calcite and siderite content of montmorillonite is about 0.7% wt (Madsen 1998). The role of carbonate minerals in the buffering capacity of the system as well as in the radionuclide complexation capacity of groundwater is very significant. Therefore, we have considered in the calculations the initial mineral composition of bentonite shown in Table 7, supplemented with 0.7 wt% of calcite and 0.7wt% of siderite.

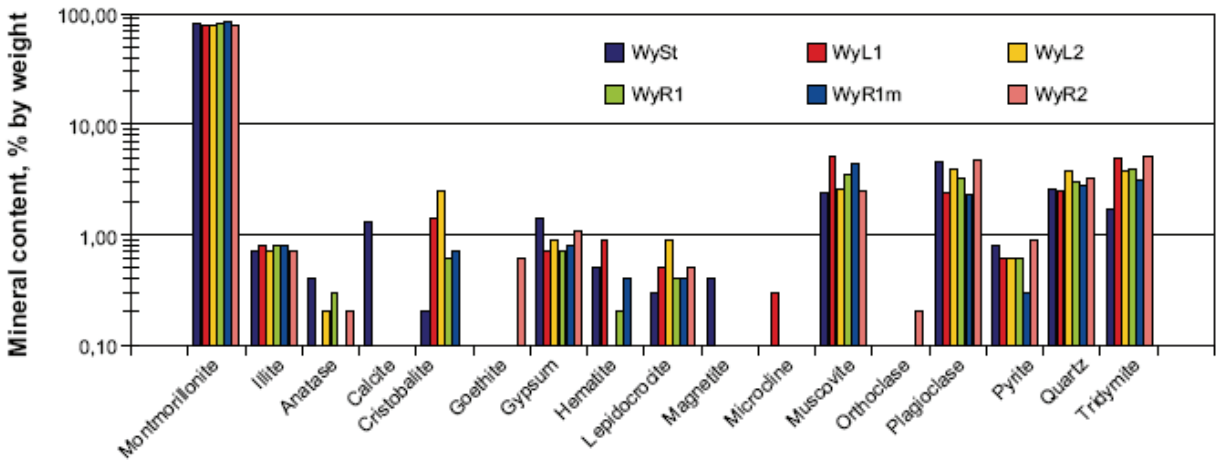

Figure 8: Results from Karnland et al. (2006) showing the mineral content in five consignments representing over 20 years of production of MX-80 bentonite (WySt, WyL1, WyL2, WyR1 and WyR2). Note the logarithmic scale.

Table 7: Mineralogical composition and cation exchange capacity of the clay fraction of bentonite MX-80. The uncertainties are mainly related to the precision of the analytical method used. From SKB (2004).

Mineral (wt%)	
Montmorillonite	87±3
Quartz	3.0±0.5
Cristobalite	2.0±0.5
Mica	4±1
Albite	3±1
Anortoclase	0±1
Calcite+ siderite	0±1
Pyrite	0.07±0.05
Gypsum	0.7±0.2
Organic carbon	0.2
CEC = 75 ± 2 meq/100g	
NaX (%)	72±5
KX (%)	2±1
CaX_2 (%)	18±5
MgX_2 (%)	8±5

The main component of bentonite is montmorillonite. However, its dissolution rate is very slow under near neutral pH (Cama et al. 2000) so that we consider that montmorillonite dissolution is a minor process that will hardly affect the geochemical evolution of the system. The illitization of montmorillonite is also believed to have minor influences on the pore water chemistry in the repository (Karnland 1995, Benbow et al. 2000). Therefore, both montmorillonite dissolution and montmorillonite illitization have not been explicitly included in the calculations.

We have not distinguished between cristobalite and quartz in the calculations. Groundwater compositions are equilibrated with 5%wt of SiO_2 (quartz), considering this amount as the sum of initial quartz and cristobalite content in MX-80 bentonite (3%wt and 2%wt, respectively).

Precipitation / dissolution of gypsum may control the calcium availability in the system, directly affecting those reactions where calcium is involved: precipitation of calcium carbonate (buffering the pH) and Ca-exchange reactions. Therefore, precipitation (or dissolution) of gypsum has been considered in the calculations. This process can be affected by other processes competing for sulphate to form other sulphate minerals/species.

Pyrite is considered to dissolve according to a kinetic rate law. The rate law most commonly used is the one described by Williamson and Rimstidt (1994) (eq. 12) which shows the influence of oxygen and pH on the pyrite dissolution rate. The oxidation of pyrite consumes oxygen and produces Fe(III) and sulphate. Fe(III) can precipitate in the form of Fe(III) oxy-hydroxides (r 1) whose rate of formation will mainly depend on the pH of the system.

$$R_{py}(mol\ m^{-2}s^{-1}) = 10^{-8.19(\pm 0.10)} \frac{\left[O_2(aq)\right]^{0.50(\pm 0.04)}}{\left[H^+\right]^{0.11(\pm 0.01)}} \qquad \textbf{eq. 12}$$

$FeS_2(s) + 3.75O_2(g) + 3.5H_2O \rightarrow Fe(OH)_3(s) + 2SO_4^{2-} + 4H^+$ r 1

Different secondary minerals can precipitate after the interaction of a given groundwater with bentonite. The most common minerals that can precipitate and that have been considered in the calculations are calcite and iron minerals (siderite, FeS(am), and Fe oxy-hydroxides).

Table 8 shows the initial composition of the bentonite selected for the calculations performed in this work. To obtain the moles of mineral per dm^{-3}, a porosity of 0.43 and a dry density of 1,570 kg m^{-3} have been used in the calculations according to Ochs et al. (2001).

Table 8: Initial mineralogical composition of MX-80 bentonite (in mol dm^{-3}) used in the calculations. The last column represents the moles of mineral per dm^{-3} of water under repository conditions (porosity of 0.43 and a dry density of 1,570 kg m^{-3}).

Mineral		mol dm^{-3}
Montmorillonite	Not reactive	-
Quartz + cristobalite	Equilibrium	3.04
Mica	Not reactive	-
Albite	Not reactive	-
Calcite	Equilibrium	0.25
Siderite	Equilibrium	0.22
Pyrite	Kinetics	0.021
Gypsum	Equilibrium	0.1484

Other process that could have a significant role in the geochemical evolution of the system is the surface protonation of montmorillonite. The protonation of the surface edge of montmorillonite contributes to pH buffering according to the reactions r 2 and r 3, where ">sOH" stands for the surface groups of the solid.

$>sOH + H^+ \leftrightarrow >sOH_2^+$ r 2

$>sOH \leftrightarrow >sO^- + H^+$ r 3

The density of surface sites and the constants associated with the surface reactions (r 2 and r3) depend on the type of bentonite. Bradbury and Baeyens (2002) considered two different types of weak protonation-deprotonation surface sites, $S_{w1}OH$ and $S_{w2}OH$ for MX-80 montmorillonite. They obtained the log K for the protonation-deprotonation reactions and the capacities of each site ($S_{w1}OH$ and $S_{w2}OH$) from the analyses of batch titration experiments on dispersed systems. The surface area of MX-80 montmorillonite is 31.3 $m^2\ g^{-1}$ (Bradbury and Baeyens, 2002). The log K values and site capacities used in this report are those of Bradbury and Baeyens (2002), listed in Table 9.

Table 9: Properties of montmorillonite surface sites. Log K of protonation and deprotonation reactions, from Bradbury and Baeyens (2002). Site capacities in moles per dm^3 of water have been calculated for repository conditions (porosity of 0.43 and a dry density of 1,570 kg m^{-3}).

SURFACE	Log K	Site capacities	
		mol kg^{-2}	mol dm^{-3}
$S_{W1}OH$		4.00×10^{-2}	0.12
$>S_{W1}OH + H^+ \leftrightarrow >S_{W1}OH_2^+$	4.5		
$>S_{W1}OH \leftrightarrow >S_{W1}O^- + H^+$	-7.9		
$S_{W2}OH$		4.00×10^{-2}	0.12
$>S_{W2}OH + H^+ \leftrightarrow >S_{W2}OH_2^+$	6.0		
$>S_{W2}OH \leftrightarrow >S_{W2}O^- + H^+$	-10.5		

Selectivity exchange coefficients for cation exchange reactions (r 4 to r 6) have also been selected from Bradbury and Baeyens (2002). Partial substitution of interlayer major cations by Fe^{2+} in montmorillonite would also be expected, according to reaction r 7 (Kamei et al., 1999). In the literature (Charlet and Tournassat, 2005, Géhin et al., 2007, Kamei et al. 1999), selectivity constants in the range 0.27-0.8 are reported for the exchange of Fe^{2+} onto Na-montmorillonite. We have used an average value of 0.4 (Charlet and Tournassat, 2005) in the calculations.

$2\ NaX + Ca^{2+} \leftrightarrow CaX_2 + 2Na^+$	log K = 0.41	r 4
$2\ NaX + Mg^{2+} \leftrightarrow MgX_2 + 2Na^+$	log K = 0.34	r 5
$NaX + K^+ \leftrightarrow KX + Na^+$	log K = 0.60	r 6
$2\ NaX + Fe^{2+} \leftrightarrow FeX_2 + 2Na^+$	log K = 0.40	r 7

Table 10 shows the initial exchange composition used in the calculations.

Table 10: Initial exchange composition of MX-80 bentonite (meq/100g) used in the calculations. Values in moles per dm^{-3} of water have been calculated for repository conditions (porosity of 0.43 and a dry density of 1,570 kg m^{-3}).

	meq/100 g	mol dm^{-3}
NaX	54	1.723
KX	1.5	0.048
MgX_2	6.0	0.095
CaX_2	13.5	0.214
FeX_2	0	0

3.2 CHARACTERIZATION OF C-STEEL INSERT CORROSION

Based on the properties of the selected groundwater SR-270, the corrosion of the C-steel inserts occurs under anaerobic conditions.

As the main component of C-steel is Fe(0), steel corrosion is usually explained in terms of Fe(0) corrosion. When Fe(0) corrodes anoxically, it forms in a first step, $Fe(OH)_2$ (r 8) which then transforms into magnetite via the Schikorr reaction (r 9). The overall reaction is summarised in r 10

$$Fe + 2H_2O = Fe(OH)_2 + H_2 \qquad \text{r 8}$$

$$3Fe(OH)_2 = Fe_3O_4 + 2\,H_2O + H_2 \qquad \text{r 9}$$

$$3\,Fe + 4\,H_2O = Fe_3O_4 + 4\,H_2 \qquad \text{r 10}$$

C-steel corrosion (and therefore, Fe(0) corrosion) is considered to be kinetically controlled. Corrosion rates can be affected by different parameters, such as temperature, chloride, CO_2(aq) concentrations, gamma radiation or the hydrodynamics of the system.

In the present study we have used corrosion rates from Smart and Hochs (2006), who presented a compilation of steel corrosion rates under anoxic and oxic conditions. They observed that instantaneous electrochemical measurements gave much higher corrosion rates than long-term weight loss and hydrogen evolution measurements. Smart et al. (2001) and references therein also state that during the first hours of C-steel corrosion (<1500 hours) the hydrogen evolution rates are high but then rapidly decrease. After this first period, the hydrogen evolution rates can be considered constant.

Smart and Hochs (2006) selected a C-steel corrosion rate for each of the scenarios they considered (Table 11).

Table 11: C-Steel corrosion rates reported in Smart and Hochs (2006) for different scenarios. (E_a: activation energy).

Scenarios considered in Smart and Hochs (2006)		C-Steel corrosion rates (k_a, k_c)
Atmospheric	Short-term	Not required
	Long-term	Not required
Aerobic, low chloride	Short-term	Arrhenius variation of k_S=200μm yr^{-1} at 20 ºC, E_a=19 kJ mol^{-1}; t_a=0.003 yr
	Long-term	Arrhenius variation of k_L=0.1μm yr^{-1} at 20 ºC, E_a=19 kJ mol^{-1}; t_a=∞
Anaerobic, low chloride	Short-term	Arrhenius variation of k_S=0.5μm yr^{-1} at 30 ºC, E_a=56 kJ mol^{-1}; t_a=0.5 yr
	Long-term	k_L=0.005 μm yr^{-1}; no temperature dependence t_a=∞
Anaerobic, high chloride	Short-term	Arrhenius variation of k_s=0.5μm yr^{-1} at 30 ºC, E_a=56 kJ mol^{-1}; t_a=0.5 yr
	Long-term	k_L =0.005 μm yr^{-1}; no temperature dependence t_a=∞

The reference corrosion rate selected in this work is the one that Smart and Hochs (2006) used for the case of C-steel corrosion rate under high chloride anaerobic conditions (0.005 μm yr^{-1}). According to Smart and Hochs (2006) this value comes from Smart et al. (2004) and was determined from H_2(g) evolution measurements. It was taken equal to the corrosion rate under anaerobic low chloride solutions because the anaerobic corrosion rates are only weakly affected by the presence of chloride (Smart et al. 2004).

Due to the input characteristics of the code PHREEQCI (Parkhurst and Appelo, 2001), the C-steel corrosion rate in μm yr^{-1} must be converted to mol_{Fe} m^{-2} s^{-1}. By assuming a composition of C-steel equal to that reported in Table 12 and a density of 7,860 kg m^{-3} the corrosion rate 0.005 μm yr^{-1} is equivalent to 2.2×10^{-11} mol_{Fe} m^{-2} s^{-1}.

We can calculate the geometric area of the inner steel vessel of the C-steel insert, which for a cylinder of 3.6 m height and 1.05 m diameter, is of 25.7 m^2. This surface area assumes that both the inner and outer surfaces of the C-steel insert are in contact with the bentonite buffer, i.e., it neglects the isolation provided by the presence of the outer copper canister. By considering the porosity of the bentonite barrier equal to 0.43 and a thickness of the buffer of 3.5 dm, the amount of water surrounding the inner steel vessel would be 4,976 m^3, which makes the ratio of the steel surface area to the water volume equal to 25.7m^2/4,976 m^3, or 0.005 m^2/dm^3 of water. For conservatism, the surface area exposed to corrosion is doubled in the calculations to 0.01 m^2 of steel per dm^3 of water. We have assumed that the initial amount of steel in the media is sufficiently high not to be exhausted.

Calculations presented in this report are batch calculations. That means that neither advective nor diffusive transport has been considered.

Table 12: C-steel composition (from Sriram and Tromans, 1985).

element	CARBON STEEL (SA 516 grade 70)	
	Range (%wt)	Selected (%wt)
Mn	0.85-1.20	1.16
Si	0.13-0.45	0.23
C	0.19-0.31	0.19
S	0.08	0.08
P	0.021	0.021
Fe	balance	98

C-steel corrosion is assumed to produce $H_2(g)$, which is lost from the system (Vines, 2002). According to King (2007) some of this $H_2(g)$ would sorb on the steel surface and diffuse through the container wall to the near field or would be accumulated and transported away from the canister. However, the transport of $H_2(g)$ is limited by its low solubility and the low permeability of the bentonite barrier. When the partial pressure of hydrogen, pH_2, is higher than a threshold value determined by the system, $H_2(g)$ is transported through bentonite by a mechanism still not well-understood. The permeability of bentonite returns to its original low value once the H_2 pressure is released.

The maximum hydrogen pressure will depend on factors such as the hydrostatic pressure at the depth of the repository, and likely the swelling pressure of the bentonite buffer. In the absence of a specific site, we have used 10 MPa as the maximum value allowed for $pH_2(g)$[1]

Although magnetite is considered to be the main corrosion product (r 10), we have also considered the possible precipitation of secondary minerals such as goethite, siderite, calcite and gypsum.

3.3 CALCULATIONS RESULTS: SR-270 NF GROUNDWATER COMPOSITION

In this section we present the results of the interaction of the SR-270 eq groundwater with the buffer and the C-steel insert simultaneously.

Calculations have been done with the SR-270 eq groundwater provided by NWMO (see Table 4) using the YMP Pitzer database data0.ypf.R2 which uses Pitzer equations for the ionic strength correction. Results have been compared with the reequilibrated water obtained in

[1] In PHREEQCI v2.17 (Parkhurst and Appelo, 2001), the $H_2(g)$ pressure is calculated from the hydrogen concentration in water using Henry's law.

section 2.4 using the ThermoChimie v.7b/SIT database (see Table 6). In the modelling we have considered that the SR-270 eq groundwater reacts with C-steel insert and equilibrates with bentonite. The following assumptions have been taken into account as reported in section 3.1 and 3.2:

- bentonite contains 0.7% wt of calcite and 0.7% wt siderite in its initial mineral composition. Exchange and surface reactions in bentonite are considered to occur in equilibrium as well as dissolution of primary minerals and precipitation of secondary minerals;
- gypsum, quartz, pyrite, calcite and siderite have been considered as bentonite reactive minerals. These minerals are allowed to dissolve or to re-precipitate in equilibrium;
- goethite, magnetite, $Fe(OH)_3(am)$, $Fe(OH)_2(s)$ and FeS (am) are considered secondary minerals and their precipitation have been allowed;
- pyrite dissolution is considered to be kinetically controlled;
- montmorillonite surface protonation and deprotonation and the exchange capacity of bentonite have been implemented according to section 3.1;
- the reactive area of C-steel is 0.01 m^2 dm^{-3}. As C-steel corrosion is kinetically controlled, groundwater compositions change constantly and calculations have been done until a maximum pressure of $H_2(g)$ = 10 MPa is achieved;
- aqueous sulphate is not allowed to be reduced to sulphide, aqueous carbonate is not allowed to be reduced to methane and aqueous nitrate is not allowed to be reduced to ammonium or $N_2(g)$.

Table 13 shows the results of the interaction of the equilibrated water (Table 6) with bentonite and with the corroding C-steel insert using two sets of databases with different ionic strength corrections: **a)** YMP Pitzer database; and **b)** ThermoChimie v.7b database/SIT database.

In both cases when C-steel corrosion starts, the redox potential decreases and pH increases (Table 13). At pH 7.4 and pe around -8.37 the precipitation of magnetite starts when using the YMP Pitzer database. Higher pH values and more reducing conditions are required to precipitate magnetite when using ThermoChimie v.7b/SIT (pe =-9.06, pH = 8.1). In both cases, $H_2(g)$ is accumulated in solution and the calculation stops when $H_2(g)$ reaches a pressure of 10 MPa (around 10,500 years).

The oxidative dissolution of pyrite does not occur due to the low Eh groundwater. Therefore, no sulphide is generated and there is no precipitation of FeS(am). Aqueous concentrations of Fe increase due to the corrosion of C-steel and siderite dissolution. Consequently, Fe occupies some bentonite exchange positions (see Table 14). Differences between the iron concentrations in the two calculations are due to the different ionic strength corrections as SIT coefficients are not implemented in ThermoChimie v.7b/SIT for the Fe^{2+}/Cl^- interaction.

Table 13: Comparison of the SR-270 composition after interacting with bentonite and C-steel insert (after $pH_2(g)$ =10 MPa) for the two databases.

	SR-270 equilibrated				SR-270 bentonite- C-steel insert equilibration			
	(YM_PITZER)*		(TC_SIT)*		(YM_PITZER)*		(TC_SIT)*	
pH	5.8		6.2		7.4		8.1	
pe	-3.38		-3.38		-8.37		-9.06	
Eh (mV)	-200		-200		-494		-535	
log(pCO_2) (atm)	-2.14		-1.81		-5.24		-5.48	
	mg L^{-1}	**mol dm^{-3}**	**mg L^{-1}**	**mol dm^{-3}**	**mg L^{-1}**	**mol dm^{-3}**	**mg L^{-1}**	**mol dm^{-3}**
Na	50,100	2.18	50,025	2.18	52,972	2.30	48,673	2.12
K	12,500	$3.20\cdot10^{-1}$	12,486	$3.19\cdot10^{-1}$	4,052	$1.04\cdot10^{-1}$	3,482	$8.91\cdot10^{-2}$
Ca	32,000	$7.98\cdot10^{-1}$	32,494	$8.11\cdot10^{-1}$	31,942	$7.97\cdot10^{-1}$	37,285	$9.30\cdot10^{-1}$
Mg	8,200	$3.37\cdot10^{-1}$	8,173	$3.37\cdot10^{-1}$	8,745	$3.60\cdot10^{-1}$	9,940	$4.09\cdot10^{-1}$
HCO_3	110	$1.80\cdot10^{-3}$	135	$2.22\cdot10^{-3}$	5	$7.52\cdot10^{-5}$	3	$4.34\cdot10^{-5}$
SO_4	440	$4.58\cdot10^{-3}$	1,784	$1.86\cdot10^{-2}$	522	$5.43\cdot10^{-3}$	1,813	$1.89\cdot10^{-2}$
S^{2-}	-	-	-	-	-	-	-	-
Cl	168,500	4.75	168,058	4.74	168,744	4.76	168,744	4.76
Br	1,700	$2.13\cdot10^{-2}$	1,698	$2.13\cdot10^{-2}$	1,702	$2.13\cdot10^{-2}$	1,703	$2.13\cdot10^{-2}$
Sr	1,200	$1.37\cdot10^{-2}$	1,198	$1.37\cdot10^{-2}$	1,202	$1.37\cdot10^{-2}$	1,200	$1.37\cdot10^{-2}$
Li	5	$7.20\cdot10^{-4}$	5	$7.19\cdot10^{-4}$	5	$7.21\cdot10^{-4}$	5	$7.21\cdot10^{-4}$
F	1	$5.26\cdot10^{-5}$	1	$5.25\cdot10^{-5}$	1	$5.27\cdot10^{-5}$	1	$5.27\cdot10^{-5}$
I	3	$2.36\cdot10^{-5}$	3	$2.36\cdot10^{-5}$	3	$2.37\cdot10^{-5}$	3	$2.36\cdot10^{-5}$
B	80	$7.40\cdot10^{-3}$	80	$7.39\cdot10^{-3}$	80	$7.41\cdot10^{-3}$	80	$7.42\cdot10^{-3}$
Si	4	$1.42\cdot10^{-4}$	4	$1.42\cdot10^{-4}$	2	$5.94\cdot10^{-5}$	10	$3.64\cdot10^{-4}$
Fe	30	$5.37\cdot10^{-4}$	30	$5.36\cdot10^{-4}$	4,094	$7.33\cdot10^{-2}$	579	$1.13\cdot10^{-2}$
Fe(II)	30	$5.37\cdot10^{-4}$	30	$5.36\cdot10^{-4}$	4,094	$7.33\cdot10^{-2}$	579	$1.13\cdot10^{-2}$
Fe(III)	-	-	-	-	-	-	-	-
NO_3	10	$1.61\cdot10^{-4}$	10	$1.61\cdot10^{-4}$	10	$1.62\cdot10^{-4}$	10	$1.62\cdot10^{-4}$
Ionic strength (mol kgw^{-1})	6.47		4.51		6.48		4.50	
Time to achieve $pH_2(g)$ = 10 Mpa (y)					10344		10972	

YM_PITZER = Yucca Mountain database and Pitzer ionic strength correction; TC_SIT = ThermoChimie v.7b database and SIT ionic strength correction

The total aqueous concentrations of Na^+, K^+ and Mg^{2+} are controlled by the exchange reactions in bentonite. Due to the high concentration of K^+ in groundwater this cation partially displaces Na^+ and Mg^{2+} from the exchange positions (see Table 14). The aqueous concentration of K^+ decreases while the Mg^{2+} and Na^+ concentrations increase (see Table 13). Changes in the exchange composition of Ca^{2+} are small. Calcium concentration is controlled by the precipitation/dissolution of primary phases. Initially, due to the availability of Ca^{2+}, calcite precipitates causing the dissolution of siderite and gypsum. Therefore, the sulphate aqueous concentration increases.

The aqueous silicon concentration is controlled by quartz dissolution / precipitation. When using the ThermoChimie SIT database the dissolution of quartz is higher than when using the YMP Pitzer database. This is due to the fact that ThermoChimie SIT does not include interaction coefficients for neutral aqueous species while the YMP Pitzer database incorporates Pitzer coefficients for the dominant species of silicon in solution, $Si(OH)_4(aq)$.

The other major difference observed relates to the concentration of aqueous Fe. $FeCl^+$ is the dominant aqueous species when using the YMP Pitzer database data0.ypf.R2, while for the ThermoChimie SIT database Fe^{2+} dominates the aqueous iron speciation. The different speciation scheme obtained is mainly related to:

- the different free Cl^- concentration calculated when using the two databases (the free chloride concentration calculated with YMP Pitzer database is much higher than that calculated with ThermoChimie SIT database),

- the different log K^o values for the formation of $FeCl^+$ in the databases (Log K^o=-0.16 in YMP Pitzer databse, and log K^o=0.14 in ThermoChimie v.7b/SIT database), and

- the lack of SIT coefficients in ThermoChimie SIT database for the interaction Fe^{2+}/Cl^-

All these differences result in a calculated dissolved iron concentration one order of magnitude higher with the YMP Pitzer database

Table 14: Variation of the exchange composition of bentonite after interacting with the equilibrated SR-270 groundwater considering C-steel insert corrosion for the two database / ionic strength correction associations.

	Initial exchange composition (mol kgw^{-1})	SR_270 (YM_PITZER)	SR_270 (TC_SIT)
NaX	1.715	1.584	1.788
CaX_2	0.214	0.185	0.128
KX	0.048	0.284	0.300
MgX_2	0.098	0.071	0.017
FeX_2	0	0.002	0.002

3.4 SUMMARY OF NEAR FIELD INTERACTIONS

From the assessment reported in this section we can conclude that in general terms, both the presence of bentonite and the corrosion of the C-steel insert will affect the composition of the sedimentary SR-270 groundwater. Summarising:

- pH increases and Eh decreases due to the corrosion of the C-steel insert, achieving values around ~ 8 and ~-500mV, respectively.

- Exchange reactions in bentonite control the aqueous concentration of Na, Mg and K. Due to the high K^+ concentration of this groundwater, the exchange positions of MX-80 bentonite become richer in KX and depleted in CaX_2 and MgX_2.

- The high calcium aqueous concentration enhances the precipitation of calcite, which in turn causes dissolution of siderite and gypsum.

- The Fe concentration is controlled by C-steel corrosion, its incorporation on exchange positions (FeX_2) and the equilibrium with siderite and magnetite

- The role of pyrite is not significant in this system.

- In all cases, groundwater compositions are equilibrated with quartz.

Moreover, differences are observed when using the Yucca Mountain database / Pitzer or ThermoChimie v.7b database / SIT association, as described below:

- Differences observed in the final SO_4 aqueous concentration are mainly related to the different results obtained with the two databases when equilibrating the groundwater with gypsum (see for example Table 6).

- Differences observed in the calculated iron concentrations which are due to siderite dissolution. The initial dissolution of siderite is higher when using the YMP Pitzer database, producing more Fe(II) in solution, than in the other approach due to complexation of Fe by chloride, which is not modelled in the Thermochimie v.7b/SIT database.

- Differences in the exchange positions mainly related to the fact that the exchanger is enriched in Na when using Thermochimie v.7b/SIT while it is depleted when the YMP Pitzer database is used. This is a consequence of the higher concentration of Ca available in solution when using the Pitzer approach, which displaces Na from the exchanger.

- Differences observed in the Si concentration are due to the different approach used to calculate interactions with neutral aqueous species.

The pH and Eh values obtained for SR-270 groundwater under the different assumptions considered are plotted in Figure 9.

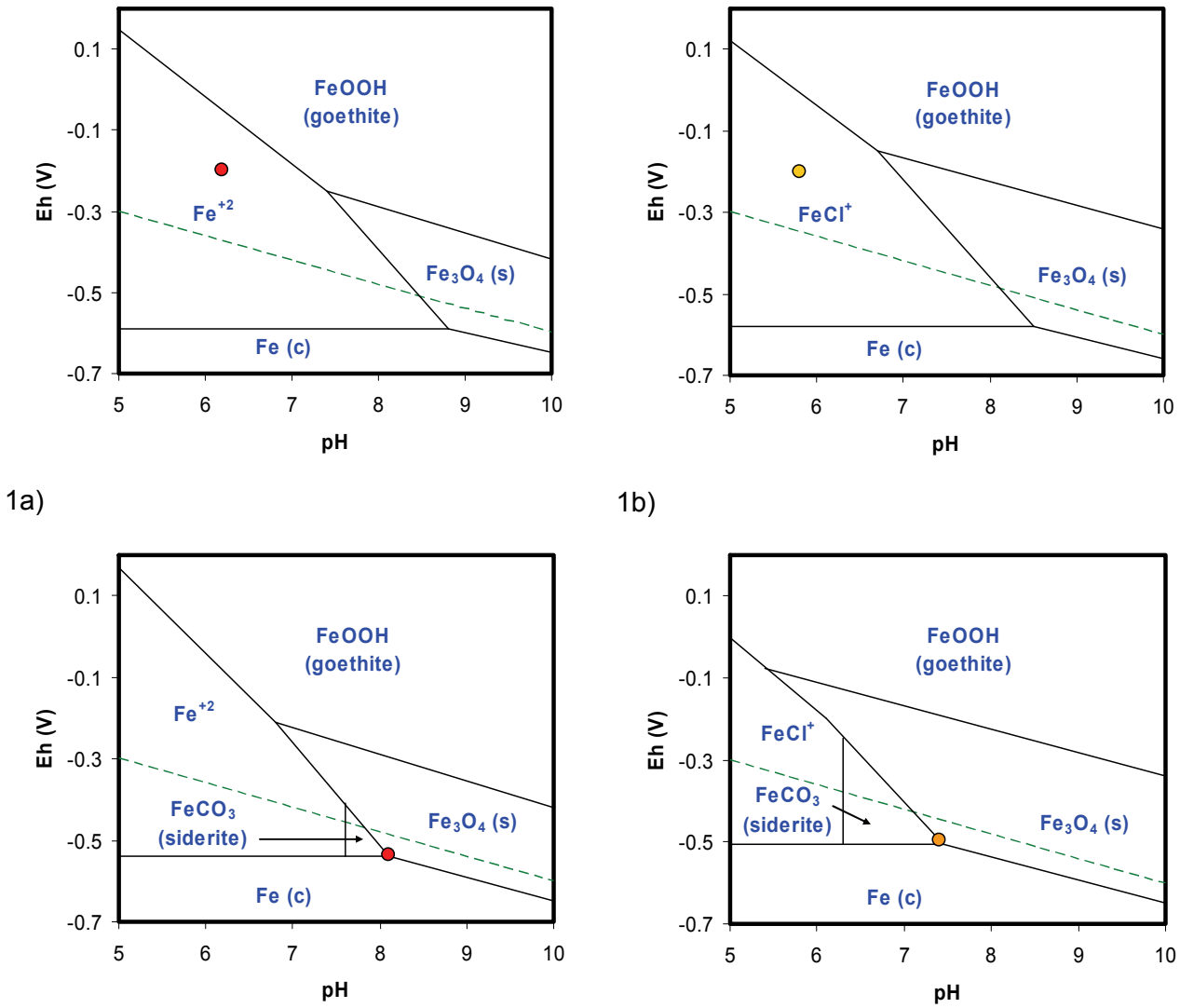

Figure 9: Predominance diagram pH vs Eh (in V) of iron under the composition of the SR-270 groundwater. 1a) Using ThermoChimie v.7b/SIT and the composition of SR-270 groundwater equilibrated in this work, 1b) Using Yucca Mountain/Pitzer and the composition of SR-270 groundwater supplied by NWMO, 2a) Using ThermoChimie v.7b/SIT and the composition of SR-270 groundwater after the bentonite-C-steel insert interactions and 2b) Using Yucca Mountain/Pitzer and the composition of SR-270 groundwater after the bentonite-C-steel insert interactions. Dots represent pH and Eh for the different groundwaters. Composition of the different groundwaters are provided in Table 13).

4. SOLUBILITY CALCULATIONS FOR THE SELECTED RADIONUCLIDES

In this section we present the results of the solubility calculations of Am, As, Bi, C, Cu, Mo, Nb, Np, Pa, Pb, Pd, Pu, Ra, Se, Sn, Tc, Th, U and Zr in the two reference groundwaters, CR-10 and SR-270, at 25ºC.

For each of the selected groundwater compositions, we have considered two different cases:

A. Equilibrated (eq). This case assumes that the groundwater composition is the one resulting from the equilibration of the groundwater composition with major minerals (see section 2.4) (Table 4).

B. Bentonite + C-steel insert (NF). This case assumes that the groundwater composition is the one resulting from the interaction of the near field components with the equilibrated groundwaters (see section 2.4 and 3.3) (Table 4 and Table 13).

The YMP Pitzer database (supplied by NWMO) has been used in the solubility assessment of Am, C, Cu, Mo, Np, Pu, Tc, Th, U and Zr (see Table 15). The ThermoChimie v7.b /SIT database (released as sit.txt with the code PHREEQC v.17) has been used to check the results obtained with the Yucca Mountain Pitzer database. This database has also been used for the solubility assessment for elements not included in the YMP Pitzer database.

The ThermoChimie v.7.b/SIT database does not include thermodynamic data for bismuth and the sets of thermodynamic data for arsenic and copper are not complete. In these cases, a review of available information has been carried out to find a consistent thermodynamic data set for the calculations of Bi, As and Cu solubilities (see section 2.2).

ThermoChimie v.7.b has been applied with the SIT ionic strength correction approach while the YMP dataset provided by NWMO uses the Pitzer approach for activity corrections.

Table 15: Availability of thermodynamic data in the two databases used in the assessment. In yellow are those elements whose thermodynamic data have been compiled especially for this work.

Database	Elements																		
	Am	As	Bi	C	Cu	Mo	Nb	Np	Pa	Pb	Pd	Pu	Ra	Se	Sn	Tc	Th	U	Zr
Yucca Mountain	✓			✓	✓	✓		✓				✓				✓	✓	✓	✓
ThermoChimie v,7b		✓*	✓*	✓	✓*	✓	✓	✓	✓	✓	✓	✓	✓	✓	✓	✓	✓	✓	✓

* Thermodynamic data for these elements are not complete. A review of available information has been carried out in the context of this work.

Sensitivity analyses have been also considered by studying the influence of some key parameters on the solubility of some radionuclides. The most influencial parameters are, besides Eh and pH, the aqueous concentration of Ca^{2+}, Fe(II), CO_3^{2-}, SO_4^{2-} and $Si(OH)_4$. In several cases, the presence of phosphate and sulphide ions can have a very important effect on the assessed solubility.

A qualitative, and when possible, a quantitative analysis of the uncertainties affecting solubility calculations is also provided. The conceptual uncertainties that may affect the solubility of a radionuclide (e.g., sulphate to sulphide reduction or coprecipitation) are also described.

4.1 AMERICIUM

The only relevant redox state under the conditions of interest for this work is Am(+III) although other redox states between 0 and (+VI) are described in the literature.

Am aqueous speciation can be affected by pH and by the groundwater carbonate, chloride, fluoride and sulphate concentrations. Silicates have also been identified to form strong aqueous complexes with Am(III) (Guillamount et al. 2003). However, americium silicate aqueous species are not included in the YMP Pitzer database. Figure 10 shows the influence of carbonate concentration on americium aqueous speciation considering the equilibrated CR-10 groundwater composition ($[Si]_T$ ~10^{-4} M and high sulphate concentration (0.013 M)). As seen, differences in the aqueous speciation are observed when using the different databases.

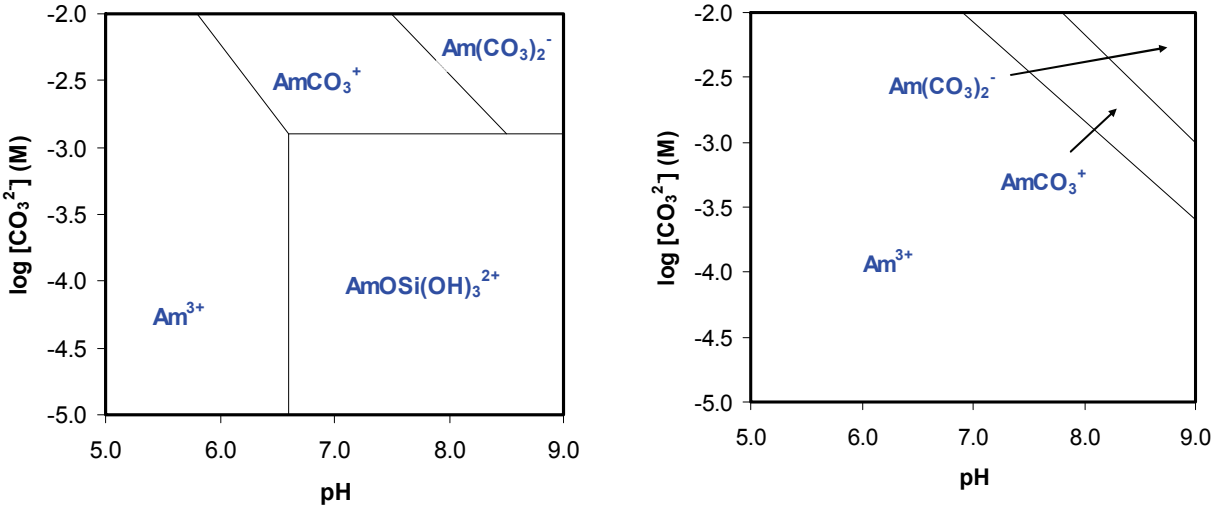

Figure 10: Predominance diagram pH versus $[CO_3^{2-}]_T$ of Am aqueous species with a) ThermoChimie v.7b /SIT b) YMP Pitzer. $[Am]_T = 1 \cdot 10^{-7}$ M, $[Si]_T = 1.7 \cdot 10^{-4}$ M, $[SO_4]_T$ = 0.013 M at I = 0.24.

When using the ThermoChimie v.7b /SIT database, the species $AmOSi(OH)_3^{2+}$ is the main aqueous species in solution for the CR-*10 eq* and CR-*10 NF* groundwaters, although the composition of the *CR-10 eq* is very close to the silicate/carbonate stability boundary (see Table 16). After the groundwater has interacted with bentonite and C-steel insert (*CR-10 NF*), the carbonate concentration becomes lower, so that the dominating aqueous species is the aqueous americium silicate. Minor Am species present in solution are predicted to be americium sulphates or hydroxides (see Table 16). The SR-270 groundwater interacted with bentonite and C-steel insert (*SR-270 NF*) has low carbonate and high chloride concentrations.

In this case, $AmOSi(OH)_3^{2+}$ is the main aqueous species in solution with minor contributions of hydroxide and chloride species. For the groundwater with the lowest pH (*SR-270 eq*), the free cation Am^{3+} is the predominant species in solution with minor contributions of silicate, chloride and carbonate species.

With the YMP Pitzer database, the free cation Am^{3+} is the main aqueous species in solution, with minor contributions of the species $Am(CO_3)^+$ for the equilibrated groundwaters *CR-10 eq and SR-270 eq*. The fluoride complex is also present in *SR-270 eq* groundwater (see Table 16). For those groundwaters interacted with bentonite and the C-steel insert, the aqueous speciation unexpectedly depends on the chloride content of the groundwater (see Figure 11). The sulphate concentration in the *CR-10 NF* groundwater is so high (4,314 mg/l) that the ionic interactions between Am^{3+} and SO_4^{2-} prevent the formation of other complexes in solution and only the free cation Am^{3+} is present (see Figure 11). This high ionic interaction between Am^{3+} and SO_4^{2-} can only be shielded by high chloride concentrations since interaction of other species like $Am(OH)_2^+$ with chloride would be higher than the interaction between Am^{3+} and sulphate (see Figure 11).

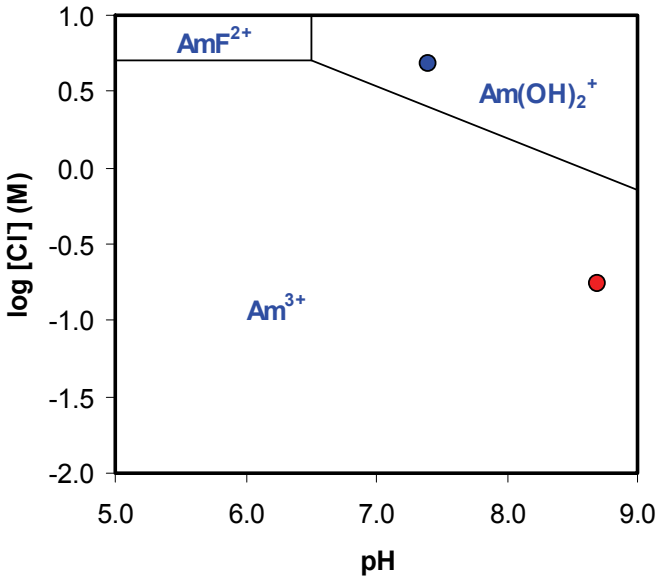

Figure 11: Predominance diagram pH versus $[Cl^-]_T$ of Am aqueous species for CR-10 and SR-270 groundwater calculated with YMP Pitzer. $[Am]_T = 1 \cdot 10^{-7}$ M. Red symbol corresponds to conditions of *CR-10 NF* groundwater and blue symbol to *SR-270 NF* groundwater.

Differences in the calculated aqueous speciation when using the two different databases are attributed to differences in both the selected thermodynamic data in the two databases and the approach used to perform activity corrections.

Table 16: Am aqueous speciation under the different selected conditions using both databases.

	TC / SIT	YMP / PITZER
Equilibrated		
CR-10 eq	$AmOSi(OH)_3^{2+}$ (40%), $Am(CO_3)^+$ (26%), Am^{3+} (19%), $Am(SO_4)^+$ (5%)	Am^{3+} (85%), $Am(CO_3)^+$ (12%)
SR-270 eq	Am^{3+} (64%), $AmCl^{2+}$ (19%), $AmOSi(OH)_3^{2+}$ (9%), $Am(HCO_3)^{2+}$ (5%)	Am^{3+} (53%), AmF^{2+} (28%), $Am(CO_3)^+$ (9%),
Bentonite + C-steel insert		
CR-10 NF	$AmOSi(OH)_3^{2+}$ (73%), $Am(OH)_2^+$ (12%), $AmOH^{2+}$ (5%)	Am^{3+} (100%)
SR-270 NF	$AmOSi(OH)_3^{2+}$ (51%), Am^{3+} (18%), $AmOH^{2+}$ (16%), $Am(OH)_2^+$ (7%), $AmCl^{2+}$ (7%)	$Am(OH)_2^+$ (78%), $Am(OH)^{2+}$ (13%), Am^{3+} (5%)

In the range of pH of interest (pH= 6 – 9), different solids are able to control the solubility of americium: carbonate phases ($AmCO_3OH$(am), $Am_2(CO_3)_3$(cr) or $Am(CO_3)_2Na\cdot 5H_2O$), phosphate phases ($AmPO_4\cdot xH_2O$) or hydroxide phases ($Am(OH)_3$(s)), depending on the groundwater conditions. Phosphates have been identified to form stable Am(III) solid phases leading to lower Am concentrations than those calculated considering equilibrium with carbonate or hydroxide solid phases. Therefore, an Am (III)-bearing phosphate solid phase can be the one controlling the solubility in neutral and reducing waters if phosphates are present, as in the case of the CR-10 groundwater for all the selected conditions (see Table 17).

One of the main uncertainties affecting americium is the effect of the phosphate concentration in the selected groundwater. The concentration of phosphate considered in the calculations is the phosphate detection limit, which is reported as an upper limit in the groundwater compositions (< 1ppm = 10^{-5} mol/L). Thus, using this value certainly overestimates the actual concentration of phosphate in the groundwater. A decrease of this concentration will result in an increase of the americium concentration in solution in equilibrium with the phosphate solid phase. Concentrations of phosphate in groundwaters are in many cases likely to be controlled by equilibrium with hydroxyapatite (for a discussion on this issue see Bruno et al. (2001)). By assuming that the concentration of phosphate in groundwater is given by equilibrium with this calcium phosphate, the resulting phosphate aqueous concentrations will be of $6.4\cdot 10^{-7}$ mol/L for the *CR-10 eq* groundwater and 2.49 10^{-8} mol/L for the *CR-10 NF* groundwater. This would result in americium concentrations in equilibrium with americium phosphate of $8.2\cdot 10^{-11}$ mol/L and $1.06\cdot 10^{-9}$ mol/L respectively (see Table 17).

If we do not consider phosphate in the groundwater, or if we assume that americium phosphate is not formed, other phases, such as carbonates or hydroxides, could control the solubility of this element (see Table 17). Formation of carbonate phases ($AmCO_3OH$(am), $Am_2(CO_3)_3$(cr) or $Am(CO_3)_2Na\cdot 5H_2O$) would lead to americium concentrations on the order of 10^{-5} m for the *CR-10 eq* groundwater. Under similar pH but a lower carbonate concentration (*SR-270 NF*) these carbonate phases are more soluble (see Table 17) and it can be considered that americium would not be solubility limited by those phases. In the case of more acidic waters, such as *SR-270 eq,* carbonate phases become more soluble (10^{-2}-10^{-3} m) and americium concentration

would not be solubility limited. In the case of more alkaline waters, such as *CR-10 NF*, americium hydroxide ($Am(OH)_3(s)$) could be the limiting solid phase producing americium concentrations in the order of 10^{-6} m (see Table 17)

Table 17: Am solid phases and concentration values (m) under the different selected conditions and using both databases.

	Equilibrated (eq)		Bentonite + C-steel insert (NF)	
	TC / SIT	**YMP / PITZER**	**TC / SIT**	**YMP / PITZER**
CR-10	**$AmPO_4 \cdot xH_2O$ (am)** **$5.14 \cdot 10^{-12}$** $AmPO_4 \cdot xH_2O$ (am)* $8.2 \cdot 10^{-11}$ **$AmOHCO_3(s)$** **$2.23 \cdot 10^{-5}$**	**$AmPO_4$ (am)** **$7.94 \cdot 10^{-12}$** **$AmOHCO_3(s)$** **$8.51 \cdot 10^{-6}$**	**$AmPO_4 \cdot xH_2O$ (am)** **$2.63 \cdot 10^{-12}$** $AmPO_4 \cdot xH_2O$ (am)* $1.06 \cdot 10^{-9}$ **$Am(OH)_3(s)$** **$1.51 \cdot 10^{-6}$**	**$AmPO_4$ (am)** **$3.64 \cdot 10^{-11}$** **$Am(OH)_3(s)$** **$2.8 \cdot 10^{-7}$**
SR-270	**n.s.l[1]** $AmOHCO_3(s)$ $1.18 \cdot 10^{-2}$ $Am_2(CO_3)_3$ (s) $2.17 \cdot 10^{-3}$	**n.s.l** $AmOHCO_3(s)$ $2.53 \cdot 10^{-4}$ $Am_2(CO_3)_3$ (s) $9.83 \cdot 10^{-4}$	**n.s.l.** $AmOHCO_3(s)$ $2.32 \cdot 10^{-4}$ $Am(OH)_3$ (s) $6.13 \cdot 10^{-4}$	**n.s.l** $AmOHCO_3(s)$ $6.20 \cdot 10^{-5}$ $Am(OH)_3$ (s) $4.95 \cdot 10^{-4}$

* indicate results obtained for phosphate concentrations given by equilibrium with hydroxyapatite
[1] n.s.l: no solubility limited

The main uncertainty in the Am solubility is related to the possible formation of a solid-solution of Am with calcite. This would limit the solubility of americium, giving more realistic and lower aqueous Am concentrations than equilibrium with pure Am carbonate or hydroxide solids. This process is expected to occur in the light of the very high partition coefficient of Am with calcite (Curti 1999).

4.2 ARSENIC

Arsenic is a redox sensitive element. Arsenate (+V) and arsenite (+III) are the two forms of arsenic commonly found in groundwater. Arsenate (AsO_4^{3-}) generally predominates under oxidizing conditions. Arsenite (AsO_3^{3-}) predominates under anoxic and reducing conditions (see Figure 12).

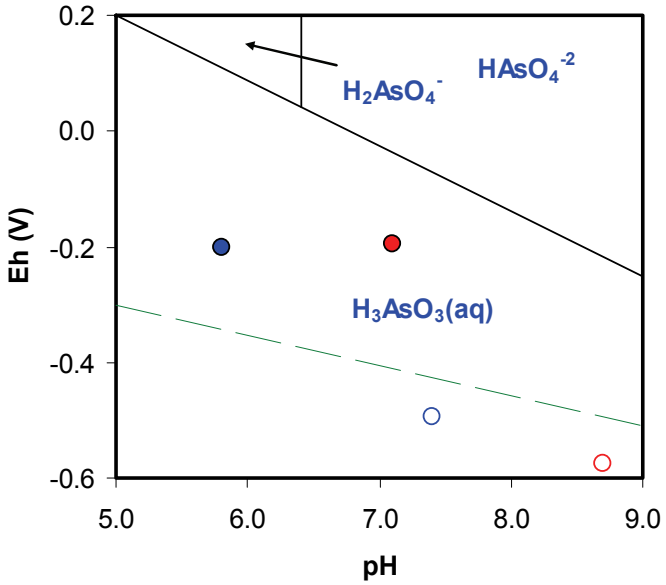

Figure 12: Aqueous predominance diagram (Eh-pH) in the selected groundwaters. $[As]_T = 1 \cdot 10^{-7}$ M. pH and Eh values of the CR-10 groundwater: *CR-10 eq* (●) and the *CR-10 NF* (○) and the SR-270 groundwater: *SR-270 eq* (●) and the *SR-270 NF* (○). Calculations using ThermoChimie v.7b/SIT. Dashed line: reduction of water to H_2.

The formation of aqueous species and solid phases depends on the master variables Eh and pH. Under the reducing conditions studied in this work, arsenic is mainly found as H_3AsO_3 with minor contribution of the species $H_2(AsO_3)^-$ for the CR-10 groundwater equilibrated with C-steel insert and bentonite due to its higher pH (see Table 18).

Table 18: As aqueous speciation under the different selected conditions.

	TC / SIT
Equilibrated	
CR-10 eq	H_3AsO_3 (99%)
SR-270 eq	H_3AsO_3 (100%)
Bentonite + C-steel insert	
CR-10 NF	$H_3(AsO_3)$ (67%), $H_2(AsO_3)^-$ (30%)
SR-270 NF	H_3AsO_3 (97%)

Arsenic is not solubility limited under the studied conditions given the high solubilities of the common alkali and alkali earth salts of AsO_3^{3-} oxyanions. As(0) has been disregarded as a solid likely to limit the solubility because its precipitation occurs only under hydrothermal conditions (Mandal and Suzuki, 2002).

Table 19: As solid phases and concentration values (m) under the different selected conditions using both databases.

	Equilibrated (eq)		Bentonite + C-steel insert (NF)	
	TC / SIT	**YMP / PITZER**	**TC / SIT**	**YMP / PITZER**
CR-10	n.s.l.*	-	n.s.l.	-
SR-270	n.s.l.	-	n.s.l	-

**n.s.l.: no solubility limited.*

An important conceptual uncertainty that could potentially affect As solubility is the reduction of sulphate to sulphide. This process has not been considered here due to its very slow kinetics, although it is favoured in the presence of sulphate reducing bacteria. Reduction of sulphate to sulphide due to bacterial activity would cause the precipitation of different arsenic sulphides. There are many different arsenic sulphide minerals, such as arsenopyrite (FeAsS), orpiment (As_2S_3) and realgar (As_4S_4), occurring primarily in hydrothermal and magmatic ore deposits (O'Day, 2006). Recently, spectroscopic methods have verified the formation of orpiment and realgar type structures in low-temperature, sulphate-reducing environments, probably related to microbiological sulphur and arsenic reduction (O'Day et al. 2004). If sulphate is reduced to sulphide, the formation of orpiment would give solubilities of arsenic around ~10^{-4} M for the CR-10 eq groundwater. For the CR-10 *NF* groundwater where polynuclear species of As/S could be present in solution (see section 2.2.1) a concentrations of ~10^{-3} M could be expected. Solubilities of orpiment under the SR-270 groundwater would be around ~10^{-6} M (see Figure 13).

Concentration of As in groundwaters may be governed by other processes such as co-precipitation or sorption onto major phases, leading to smaller arsenic concentrations than the ones predicted from the solubilities of solids containing arsenic as a major component (Hinkle and Polette, 1999). Arsenic often coprecipitates with metal oxides, especially iron oxides, and is adsorbed to clay mineral surfaces and associated with sulphide minerals, although arsenite is generally less strongly adsorbed than arsenate (Welch et al., 1988, Welch et al., 2006, O'Day, 2006).

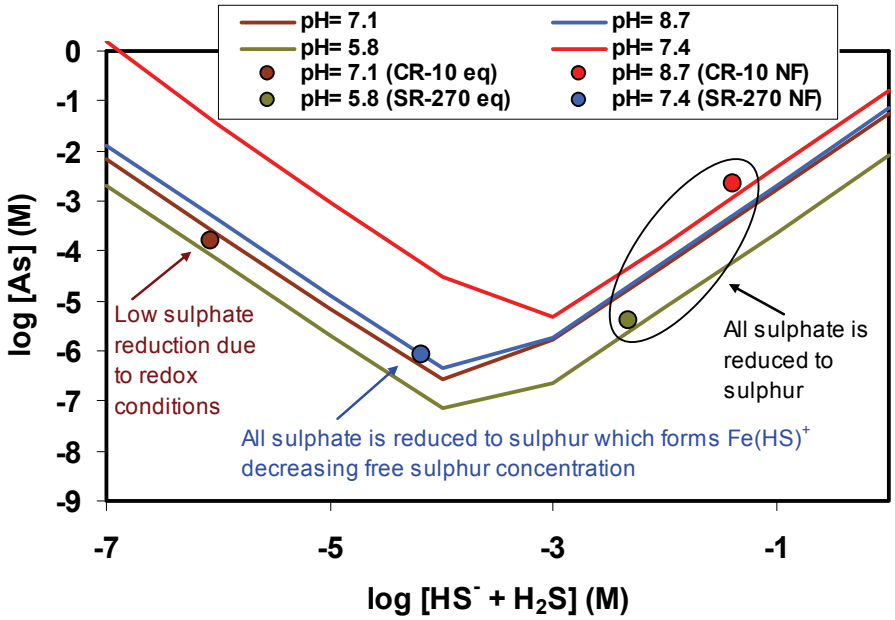

Figure 13: Solubility of orpiment (As_2S_3) as a function of sulphide under all the selected conditions.

4.3 BISMUTH

The most stable oxidation state of bismuth is +III. Pentavalent bismuth is a strong oxidant able to oxidize water.

Thermodynamic data for this element are included in neither the YMP Pitzer nor the ThermoChimie v.7.b/SIT databases. For this reason the alternative thermodynamic data set described in this work has been used to perform solubility calculations of Bi (see section 2.2.2).

The main aqueous species for bismuth under all the selected conditions except for the *SR-270 eq* groundwater is the hydroxocomplex $Bi(OH)_3$ (aq). For the *SR-270 eq* groundwater with lower pH and high chloride concentration, bismuth is less hydrolyzed and chloride species are the main aqueous species in solution (see Table 20 and Figure 14). Concerning the solid phases, the bismuth oxide Bi_2O_3 (s) has been selected as the solid phase limiting the bismuth solubility (see Table 21). Bismuth is not solubility limited in *SR-270 eq* groundwater.

Table 20: Bi aqueous speciation under the different selected conditions.

	TC / SIT
Equilibrated	
CR-10 eq	$Bi(OH)_3$ (100%)
SR-270 eq	$BiCl_6^{3-}$ (75%), $BiCl_5^{2-}$ (18%), $Bi(OH)_3$ (5%)
Bentonite + C-steel insert	
CR-10 NF	$Bi(OH)_3$ (100%)
SR-270 NF	$Bi(OH)_3$ (100%)

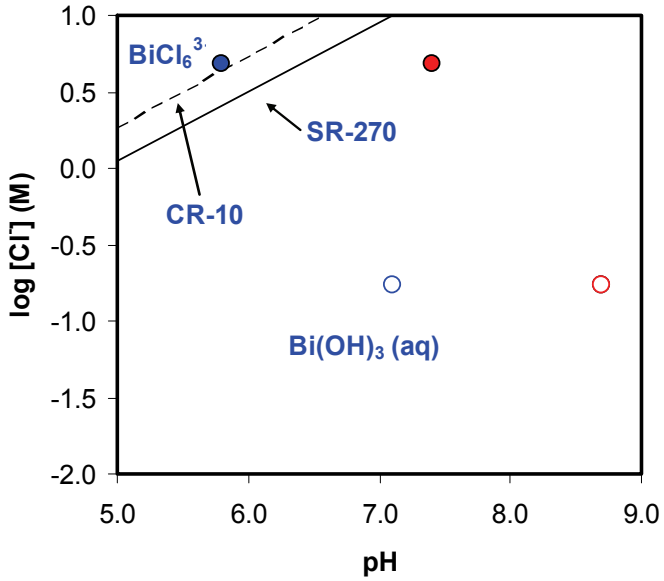

Figure 14: Predominance diagram pH versus $[Cl^-]_T$ of Bi aqueous species for the selected groundwaters. $[Bi]_T = 1 \cdot 10^{-6}$ M. $[Cl^-]_T$ and pH values of the CR-10 groundwater: *CR-10 eq* (●) and the *CR-10 NF* (○) and the SR-270 groundwater: *SR-270 eq* (●) and the *SR-270 NF* (○). Calculations using thermodynamic data selected in this work

Bismuth can also form species with sulphide. In this work, we have assumed that sulphide is not formed from sulphate due to the lack of microbial activity, although this is an uncertainty that should be considered when analysing the behaviour of bismuth. In this sense, we have to advise that very few thermodynamic data are available in the literature for bismuth sulphides, which make it difficult to predict the bismuth concentration in equilibrium with sulphide solids.

Table 21: Bi solid phases and concentration values (m) under the different selected conditions.

	Equilibrated		Bentonite + C-steel insert	
	TC / SIT	**YMP / PITZER**	**TC / SIT**	**YMP / PITZER**
CR-10	Bi_2O_3 (s) $1.17 \cdot 10^{-5}$	-	Bi_2O_3 (s) $1.16 \cdot 10^{-5}$	-
SR-270	n.s.l[1]		Bi_2O_3 (s) $9.33 \cdot 10^{-6}$	

[1]:n.s.l.: no solubility limit

4.4 CARBON

Redox processes are important in the carbon system. C(+IV) is stable under oxidising conditions and occurs as CO_2(g) or CO_3^{2-} solid or aqueous species. The most reduced form of carbon is C(-IV) represented by methane (CH_4). The reduction of carbonate to form methane would be thermodynamically plausible under the studied conditions (see Figure 15) although it is kinetically hindered.

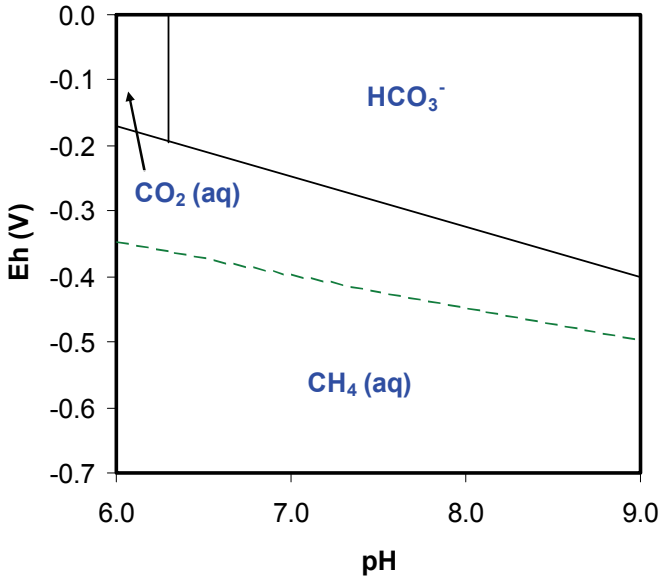

Figure 15: Predominance diagram pH versus Eh of C aqueous species in water. $[CO_3^{2-}]_T = 8 \cdot 10^{-4}$ M. Dashed line: reduction of water to H_2.

The formation of methane needs high temperatures or the presence of biological activity (Kudo and Komatsu, 1999, West and McKinley, 2001). Kudo and Komatsu (1999) indicate that the yield of methane reaches a maximum of 17% at 400ºC and does not occur in the absence of biological activity until the temperature exceeds 150-200ºC. Although biological activity may be present in the repository environment, we have not considered the reduction to methane as feasible for the purpose of the calculations presented in this report.

Another reduced species of carbon is carbon monoxide (CO). The formation of this species has also been disgarded since the reduction of carbonate to form CO is kinetically hindered and needs high temperatures or the presence of biological activity (Bott and Thauer, 1987)

The carbon aqueous speciation for CR-10 groundwaters depends on the master variable pH and to a minor extent the Ca and Fe concentrations in solution. In the case of the more saline SR-270 groundwater, formation of aqueous species depends on pH, and the Ca, Fe and Mg concentrations. In contrast to CR-10 groundwaters, aqueous complexation with the major aqueous species is more important in SR-270 groundwaters due to the high concentration of major cations. The YMP Pitzer database does not include the formation of the aqueous sodium carbonate complexes which were included in ThermoChimie SIT database (i.e., $NaCO_3^-$) because they are considered as ion pairs and not as true complexes in solution. The complex $CaHCO_3^+$ is also not included in the YMP Pitzer database and the complex $MgHCO_3^+$.has not been included in the present calculations (see Table 22).

Table 22: C aqueous speciation under the different selected conditions using both databases.

	TC / SIT	YMP / PITZER
Equilibrated		
CR-10 eq	HCO_3^- (73%), $CaHCO_3^+$ (13%), CO_2 (10%)	HCO_3^- (88%), CO_2 (10%)
SR-270 eq	CO_2 (41%), $CaHCO_3^+$ (25%), HCO_3^- (18%), $NaHCO_3$ (10%), $MgHCO_3^+$ (5%)	HCO_3^- (75%), CO_2 (22%)
Bentonite + C-steel insert		
CR-10 NF	HCO_3^- (62%), $FeCO_3$ (11%), $CaCO_3$ (7%), $NaCO_3^-$ (5%), CO_3^{2-} (4%)	HCO_3^- (74%), $CaCO_3$ (10%), $FeCO_3$ (6%), CO_3^{2-} (6%)
SR-270 NF	$CaHCO_3^+$ (28%), $FeCO_3$ (27%), HCO_3^- (20%), $NaHCO_3$ (11%), $MgHCO_3^+$ (6%)	$FeCO_3$ (27%), HCO_3^- (27%), $CaCO_3$ (25%), $MgCO_3$ (9%), CO_3^{2-} (8%)

For the CR-10 groundwater, under all the studied conditions (CR-*10 eq* and CR-*10 NF*), HCO_3^- dominates the aqueous carbon speciation (see Table 22). In the *CR-10 eq* groundwater, dissolved CO_2 also appears in minor proportion (10%). In the case of the *CR-10 NF* groundwater presenting higher pH, carbonate (CO_3^{2-}), iron and calcium species appear in similar minor proportion independently on the database used. For the SR-270 groundwater, only the aqueous speciation obtained with ThermoChimie SIT will be discussed for the reasons explained above. For the *SR-270 eq*, with the lower pH, CO_2 species dominates the aqueous speciation. Hydrogencarbonate complexes ($CaHCO_3^+$, $NaHCO_3$, $MgHCO_3^+$) also appear in minor proportion. For the *SR-270 NF* groundwater different complexes of carbonate and the free bicarbonate ligand appear with similar proportion (see Table 22). Differences of calculated aqueous speciation depend on the activity models implemented in each database (complex formation vs ion interaction).

The solubility of carbon under the chemical conditions of interest, in the absence of carbonate reduction, will be basically determined by calcite saturation (see Table 23). The predicted solubility limiting phases and carbon concentrations do not differ between the two thermodynamic databases.

Table 23: C solid phases and concentration values (m) under the different selected conditions using both databases.

	Equilibrated (eq)		Bentonite + C-steel insert (NF)	
	TC / SIT	**YMP / PITZER**	**TC / SIT**	**YMP / PITZER**
CR-10	$CaCO_3$ (calcite) $8.29 \cdot 10^{-4}$	$CaCO_3$ (calcite) $8.98 \cdot 10^{-4\ (*)}$	$CaCO_3$ (calcite) $7.01 \cdot 10^{-5}$	$CaCO_3$ (calcite) $8.80 \cdot 10^{-5\ (*)}$
SR-270	$CaCO_3$ (calcite) $2.22 \cdot 10^{-3(**)}$	$CaCO_3$ (calcite) $1.80 \cdot 10^{-3}$	$CaCO_3$ (calcite) $4.34 \cdot 10^{-5(**)}$	$CaCO_3$ (calcite) $7.52 \cdot 10^{-5}$

* carbonate concentration in equilibrium with calcite using Yucca Mountain/Pitzer, This carbonate concentration is not used for solubility calculations for other radionuclides
** carbonate concentration in equilibrium with calcite using ThermoChimie SIT. This carbonate concentration is not used for solubility calculations for other radionuclides

As stated before, the main uncertainty affecting the carbon solubility calculations is related to the possibility of methane generation, which is not taken into account in this work. The methane formation process would lead to an enhancement of calcite dissolution resulting in a very high solubility for total carbon. This high solubility for carbon could be explained by the continuos calcite dissolution due to the formation of methane gas which would act as a driving force for calcite dissolution (see r 11).

$$CaCO_3(s) + 10H^+ + 8e^- \rightarrow CH_4(g) + 3H_2O + Ca^{2+} \qquad \text{r 11}$$

4.5 COPPER

Copper compounds are known in several oxidation states in aqueous solution (+I, +II). The most stable state of copper under oxidising conditions is +II but at anoxic and reducing environments Cu(+I) species becomes predominant (see Figure 16).

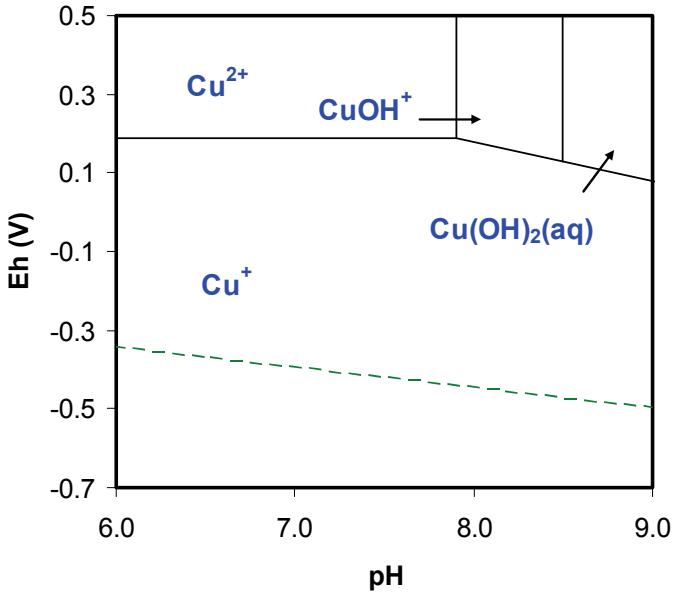

Figure 16: Predominance diagram pH versus Eh of Cu aqueous species in pure water calculated with the thermodynamic data selected in this work. $[Cu]_T = 1 \cdot 10^{-6}$ M. Dashed line: reduction of water to H_2.

Thermodynamic data for copper are only available in the YMP Pitzer database. However, only Cu^{2+} solid species and interactions between Cu^{2+} and different ions are available in this database. Cu^{+} forms a weak hydrolysis species (CuOH). This species is considered quite irrelevant in most reviews of copper chemistry. However, chloride can react with Cu^{+} ion to form CuCl, which subsequently hydrolyzes to form Cu_2O(s). Studies utilizing X-ray diffraction and surface analysis techniques support the formation of a Cu_2O(s) scale in the presence of chloride under various water quality conditions (Palit and Pehkonen, 2000).

In order to compare the results obtained with the YMP Pitzer database, the alternative thermodynamic data set described in this work has been used (see section 2.2.3).

The Cu aqueous speciation in the different groundwaters is different and depends on the database used to perform the calculations (see Table 24). In order to obtain reliable results under reducing conditions, Cu^{+} species must be included in the database. Thus the results obtained with the YMP Pitzer database are not correct. For this reason, only those calculations done with the thermodynamic data selected in this work (see section 2.2.3) will be discussed.

The main parameter affecting copper aqueous speciation under the different groundwater compositions is the chloride aqueous concentration. As we can see in Table 24, the aqueous speciation of copper for the selected groundwater compositions is mainly dominated by chloride complexes, specially $CuCl_2^{-}$ for the CR-10 groundwaters and $CuCl_3^{2-}$ for the more saline SR-270 groundwaters.

Table 24: Cu aqueous speciation under the different selected conditions using both databases.

	TC / SIT	YMP / PITZER*
Equilibrated		
CR-10 eq	$CuCl_2^-$ (92%), $CuCl_3^{2-}$ (6%)	Cu^{2+} (100%)
SR-270 eq	$CuCl_3^{2-}$ (82%), $CuCl_2^-$ (18%)	Cu^{2+} (100%)
Bentonite + C-steel insert		
CR-10 NF	$CuCl_2^-$ (92%), $CuCl_3^{2-}$ (6%)	Cu^{2+} (100%)
SR-270 NF	$CuCl_3^{2-}$ (82%), $CuCl_2^-$ (18%)	Cu^{2+} (100%)

* No Cu^+ species are defined in the database

Aqueous copper concentrations under reducing conditions are expected to be controlled by the precipitation of Cu(I) oxide or formation of Cu(s) (see Figure 17). Under the reducing conditions of the selected groundwater Cu(s) has been selected as a possible solubility limiting phase (see Table 25).

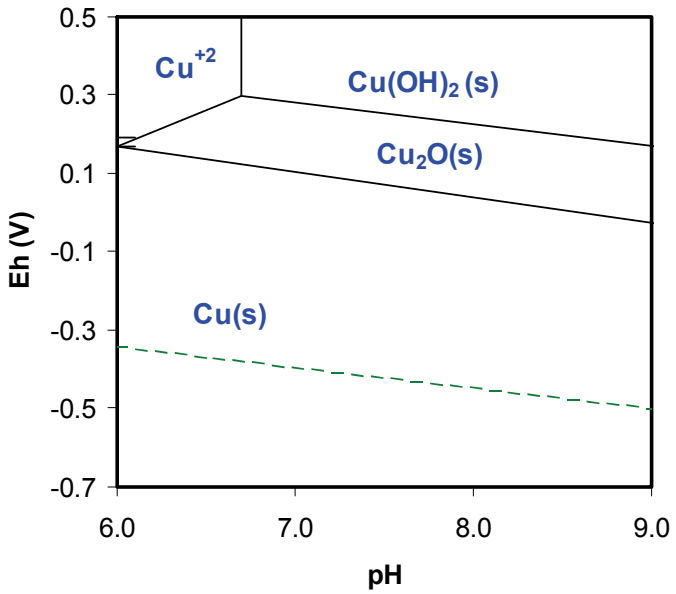

Figure 17: Predominance diagram pH versus Eh of Cu in pure water calculated with the thermodynamic data selected in this work. $[Cu]_T = 1 \cdot 10^{-6}$ M. Dashed line: reduction of water to H_2.

Table 25: Cu solid phases and concentration values (m) under the different selected conditions using both databases.

	Equilibrated (eq)		Bentonite + C-steel insert (NF)	
	TC / SIT	**YMP / PITZER***	**TC / SIT**	**YMP / PITZER***
CR-10	Cu(cr) $1.36 \cdot 10^{-8}$	--	Cu(cr) $5.22 \cdot 10^{-15}$	--
SR-270	Cu(cr) $2.64 \cdot 10^{-5}$	--	Cu(cr) $3.06 \cdot 10^{-10}$	--

* No Cu^{+} species are defined in the database. Unreliable low Cu concentration

One uncertainty to take into consideration is related to the reduction of sulphate to sulphide. Indeed, if sulphate were reduced to sulphide, sulphide solid phases (Cu_2S) might exert solubility control at reducing Eh values giving concentrations of copper around $\sim 10^{-11}$ m and $\sim 10^{-8}$ m for the equilibrated groundwater *CR-10 eq* and *SR-270 eq*, respectively and $\sim 10^{-7}$ m and $\sim 10^{-10}$ m for the *CR-10 NF* and *SR-270 NF* groundwaters, respectively. In all cases, copper speciation would be governed by sulphide complexes.

4.6 MOLYBDENUM

Molybdenum is a redox sensitive element that presents a rather complex chemistry due to the formation of polynuclear complexes conformed in cluster configurations. Although molybdenum can be present in different redox states, thermodynamic data for this element are very scarce and only species in the redox state +VI are defined in the YMP Pitzer database. In the case of ThermoChimie v.7b/SIT, only aqueous species in the redox state +VI are present (MoO_4^{2-}). For solid phases, both Mo(+VI) and Mo(+IV) phases are defined.

The main aqueous Mo species is MoO_4^{2-} for all the selected conditions. No differences in the aqueous speciation are observed when using the different databases, although major differences are found in the data for solid phases, e.g., no Mo(IV) solids are included in the YMP Pitzer database. The predominance diagram calculated by assuming a total Mo concentration of 10^{-5} mol/L, when using Thermochimie v.7b/SIT is shown in Figure 18.

The main parameters that may control molybdenum solubility are pH, Eh and calcium concentration. The solubility of the two solid phases likely to control the aqueous Mo concentration is shown in Figure 19 as a function of the pH of the medium for the two different groundwater compositions considered for the CR-10 groundwater. It can be appreciated that the solubility of MoO_2(s) is very sensitive to pH and that the Mo solubility is extremely sensitive to the redox potential due to the change in the solid phase controlling the solubility.

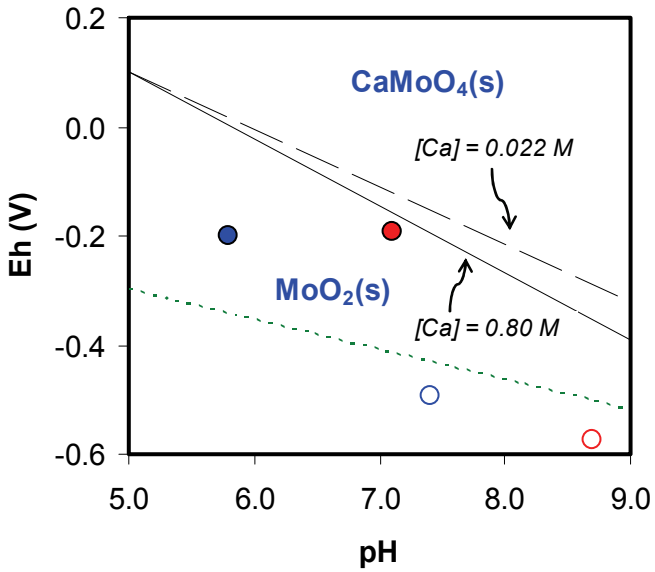

Figure 18. Predominance diagram Eh/pH of Mo solid phases under different groundwater composition: *CR-10 eq* (●) and the *CR-10 NF* (○) and the SR-270 groundwater: *SR-270 eq* (●) and the *SR-270 NF* (○) Calculations using ThermoChimie v.7b/SIT. Formation of polynuclear species has not been considered.

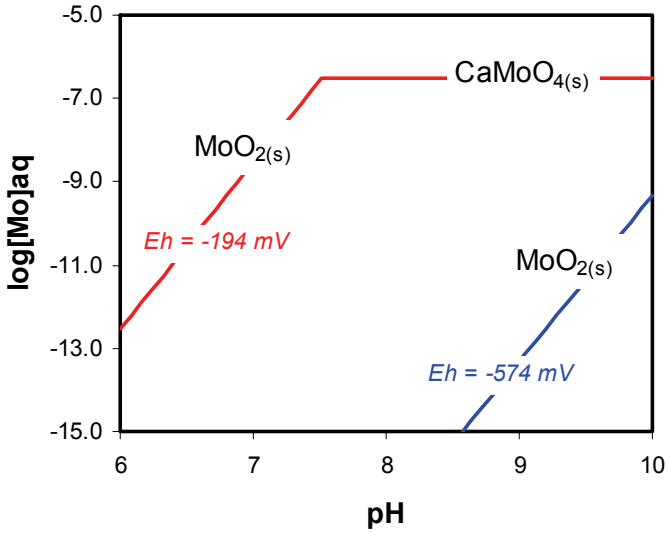

Figure 19. Sensitivity of the Mo solubility to pH and Eh. The solubility has been calculated under the conditions of the *CR-10 eq* (red) and the *CR-10 NF* (blue) groundwaters. The inserts in the calculated curves indicate the solid phases exerting the solubility control in each section of the curves. Calculations have been conducted by using the ThermoChimie v.7b/SIT database.

In Table 26 the solubilities of the possible solid phases controlling the molybdenum aqueous concentration are shown. When using ThermoChimie v.7b/SIT the solubility of MoO_2(s) is calculated, while in the case of the YMP Pitzer database only the solubility of $CaMoO_4$(s) can be computed. The YMP Pitzer database does not provide a full set of thermodynamic data for molybdenum, therefore, solubility assessments can only be done with ThermoChimie v.7b/SIT.

Table 26: Mo solid phases and concentration values (m) under the different selected conditions and using both databases.

	Equilibrated (eq)		Bentonite + C-steel insert (NF)	
	TC / SIT	**YMP / PITZER***	**TC / SIT***	**YMP / PITZER***
CR-10	MoO_2 $8.72 \cdot 10^{-9}$	--	MoO_2 $3.64 \cdot 10^{-15}$	--
SR-270	MoO_2 $2.34 \cdot 10^{-13}$	--	MoO_2 $6.29 \cdot 10^{-17}$	--

* Unrealistic results as no redox species are selected

The most important uncertainty concerning molybdenum is the scarcity of thermodynamic data available in the literature.

4.7 NIOBIUM

Niobium is mainly found in the pentavalent oxidation state in natural waters. There is a general lack of thermodynamic data in the literature on niobium, which constitutes an important drawback when studying the behaviour of this element. This element is not included in the YMP Pitzer database.

The main parameter affecting niobium aqueous speciation under the selected groundwater compositions is pH. The main aqueous species under the studied conditions are hydroxide complexes $Nb(OH)_5$ (aq), $Nb(OH)_6^-$ and $Nb(OH)_7^{2-}$ whose distribution depends on the pH of the system (see Figure 20 and Table 27).

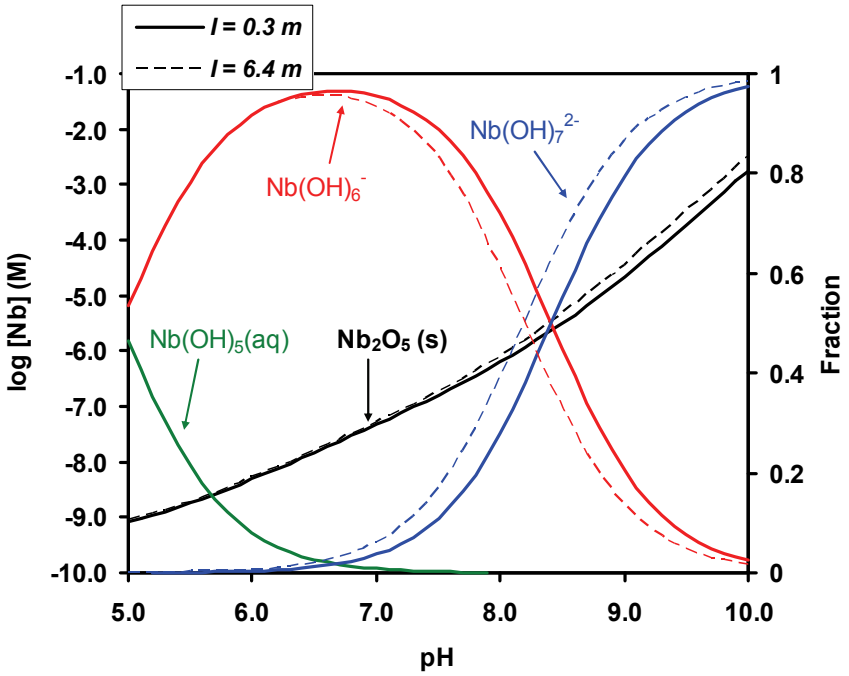

Figure 20: Nb_2O_5(s) solubility and underlying aqueous speciation for the CR-10 (I = 0.3) and SR-270 (I = 6.4 m) groundwater as a function of pH. The solubility is not redox sensitive in the Eh range of the studied waters. Calculations done by using the ThermoChimie SIT database. Left y-axis indicate the solubility and right y-axis the relative fraction of aqueous species. Solid lines present results at 0.3 m ionic strength and dashed lines those obtained at 6.4 m.

Table 27: Nb aqueous speciation under the different selected groundwater compositions.

	TC / SIT
Equilibrated	
CR-10 eq	$Nb(OH)_6^-$ (96%)
SR-270 eq	$Nb(OH)_6^-$ (89%), $Nb(OH)_5$ (11%)
Bentonite + C-steel insert	
CR-10 NF	$Nb(OH)_7^{2-}$ (66%), $Nb(OH)_6^-$ (34%)
SR-270 eq	$Nb(OH)_6^-$ (85%), $Nb(OH)_7^{2-}$ (15%)

Nb(V) oxide is very insoluble in the pH range of interest and niobium solubility will probably be controlled by Nb_2O_5(s) (see Table 28). The influence of pH on the solubility of Nb_2O_5(s) is also shown in Figure 20.

Table 28: Nb solid phases and concentration values (m) under the different selected conditions.

	Equilibrated (eq)		Bentonite + C-steel insert (NF)	
	TC / SIT	**YMP / PITZER**	**TC / SIT**	**YMP / PITZER**
CR-10	$Nb_2O_5(s)$ $1.07 \cdot 10^{-7}$	--	$Nb_2O_5(s)$ $1.30 \cdot 10^{-5}$	--
SR-270	$Nb_2O_5(s)$ $4.90 \cdot 10^{-9}$	--	$Nb_2O_5(s)$ $2.01 \cdot 10^{-7}$	--

The most important uncertainty concerning niobium is the scarcity of thermodynamic data. Formation of $CaNb_4O_{11} \cdot 8H_2O$ (hochelagaite) or $CaNbO_6 \cdot xH_2O$ at alkaline pH values has been reported in the literature (Talerico et al. 2004), although no thermodynamic data for these solids are described. Talerico et al. (2004) obtained an empirical relationship between calcium concentration, pH and niobium solubility:

$$[Nb]_{calculated} = 1.4643 e^{-1.3402\, pH} \times \frac{[Ca]^{-0.8922}}{10^{2.6766}}$$

Taking into account this empirical relationship, niobium concentration in solution for *CR-10 NF* groundwater would be lower ($\approx 8 \cdot 10^{-7}$ M). However, the formation of this kind of solid phases has not been studied at pH values below 9.2, so that the applicability of the former expression under the conditions of interest is not tested.

4.8 NEPTUNIUM

Neptunium presents different oxidation states depending on the redox conditions of the surrounding environment: Np(+III), Np(+IV), Np(+V) and Np(+VI) although Np(+IV) is the most stable redox state under all selected groundwater compositions (see Figure 21).

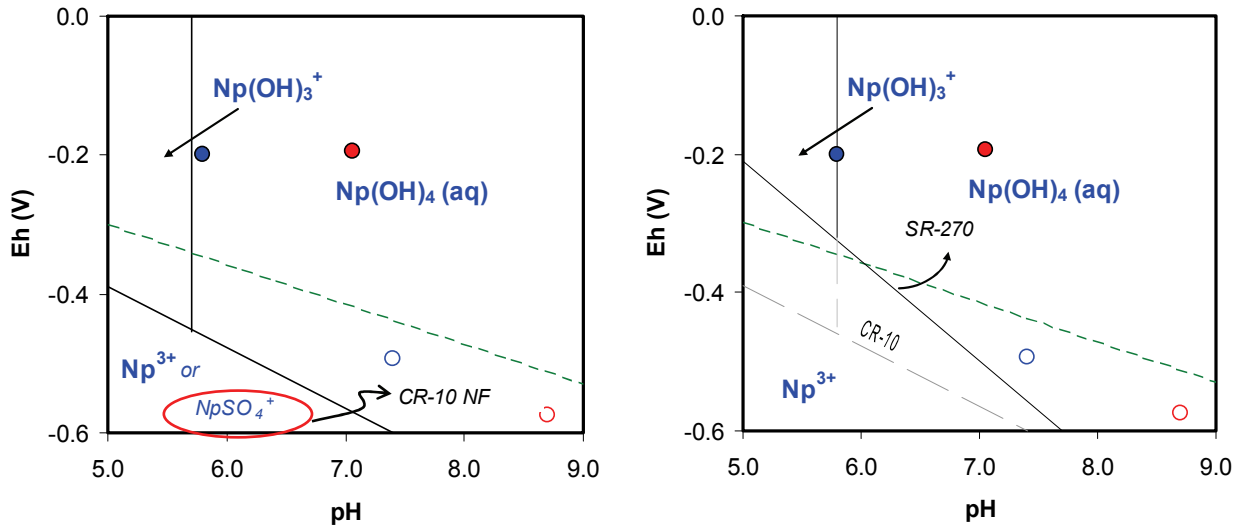

a) b)

Figure 21: Predominance diagram (Eh-pH) of Np aqueous species: a) Calculations using ThermoChimie v.7b/SIT and b) YMP Pitzer database. In red composition of the CR-10 groundwater: *CR-10 eq* (●) and the *CR-10 NF* (○), in blue: composition of the SR-270 groundwater: *SR-270 eq* (●) and the *SR-270 NF* (○).

The aqueous speciation of neptunium for all the selected groundwater compositions is mainly dominated by the species $Np(OH)_4$ (see Table 29), although the composition of *SR-270 eq,* groundwater, which has the lowest pH of all selected groundwaters, is very close to the $Np(OH)_4/Np(OH)_3^+$ boundary.

Table 29: Np aqueous speciation under the different selected conditions using both databases.

	TC / SIT	YMP / PITZER
Equilibrated		
CR-10 eq	$Np(OH)_4$ (93%)	$Np(OH)_4$ (96%)
SR-270 eq	$Np(OH)_4$ (58%), $Np(OH)_3^+$ (39%)	$Np(OH)_3^+$ (51%), $Np(OH)_4$ (44%)
Bentonite + C-steel insert		
CR-10 NF	$Np(OH)_4$ (100%)	$Np(OH)_4$ (100%)
SR-270 NF	$Np(OH)_4$ (98%)	$Np(OH)_4$ (97%)

Aqueous neptunium concentrations under the conditions of interest for this work are expected to be controlled by the precipitation of neptunium(IV) dioxide. This solid is stable over a relatively wide range of redox potential, from very reducing to slightly oxidising conditions. According to the Ostwald's rule, the amorphous phase will be kinetically favoured to precipitate over the most crystalline phase, so amorphous NpO_2 is the phase selected to control the Np solubility (see Table 30).

Table 30: Np solid phases and concentration values (m) under the different selected conditions using both databases.

	Equilibrated (eq)		Bentonite + C-steel insert (NF)	
	TC / SIT	**YMP / PITZER**	**TC / SIT**	**YMP / PITZER**
CR-10	$NpO_2(am)$ $1.08 \cdot 10^{-9}$	$NpO_2(am)$ $1.26 \cdot 10^{-9}$	$NpO_2(am)$ $1.00 \cdot 10^{-9}$	$NpO_2(am)$ $1.21 \cdot 10^{-9}$
SR-270	$NpO_2(am)$ $1.72 \cdot 10^{-9}$	$NpO_2(am)$ $2.73 \cdot 10^{-9}$	$NpO_2(am)$ $1.02 \cdot 10^{-9}$	$NpO_2(am)$ $1.24 \cdot 10^{-9}$

No important differences are observed in the solubility calculations when using the different databases, which is mainly due to the fact that the controlling aqueous species is the neutral $Np(OH)_4(aq)$ in all cases, so that there are no important activity corrections.

4.9 PROTACTINIUM

Protactinium can occur in two oxidation states: +IV and +V, although Pa(IV) is very sensitive to oxidation and it is only stabilized in very strong acids and at very low Eh. Thus, the most common redox state is Pa(V) (see Figure 22).

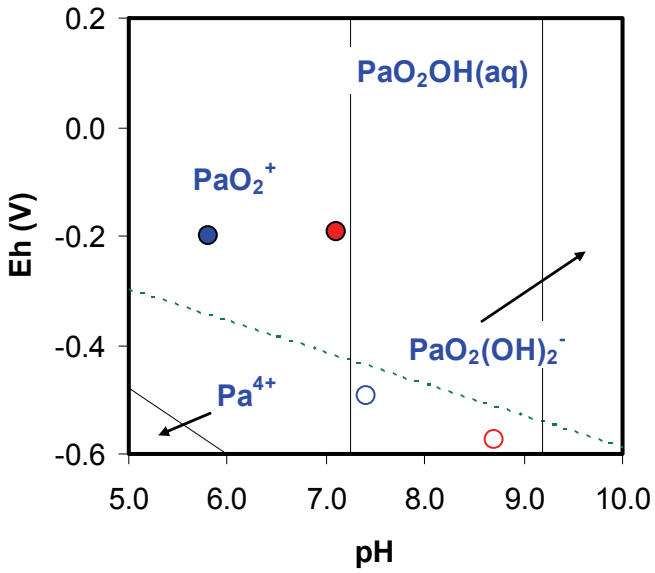

Figure 22: Aqueous predominance diagram (Eh-pH) for protactinium aqueous species under the compositions of the CR-10 groundwater: *CR-10 eq* (●) and the *CR-10 NF* (○), and the SR-270 groundwater: *SR-270 eq* (●) and the *SR-270 NF* (○). Calculations using ThermoChimie v.7b/SIT.

Protactinium thermodynamic data available in the literature are scarce, and its chemical characteristics avoid direct comparison with other actinides. This element is not included in the YMP Pitzer database.

The formation of aqueous species and solid phases under the selected conditions depends on pH. In the equilibrated groundwaters *CR-10 eq* and *SR-270 eq* the cation PaO_2^+ is the main aqueous species for protactinium. Although the composition of *CR-10 eq* is very close to the PaO_2^+/ $PaO_2(OH)$ boundary. Under the more alkaline *CR-10 NF* and *SR-270 NF* groundwaters the hydroxocomplex $PaO_2(OH)$ is the main aqueous species, although the composition of the *SR-270 NF* is also very close to the PaO_2^+/ $PaO_2(OH)$ boundary. The species $PaO(OH)^{2-}$ is present in the CR-10 NF groundwater in minor amounts (see Table 31)

Table 31: Pa aqueous speciation under the different selected conditions.

	TC / SIT
Equilibrated	
CR-10 eq	PaO_2^+ (55%), $PaO_2(OH)$ (45%)
SR-270 eq	PaO_2^+ (97%)
Bentonite + C-steel insert	
CR-10 NF	$PaO_2(OH)$ (76%), $PaO(OH)^{2-}$ (22%)
SR-270 NF	$PaO_2(OH)$ (54%), PaO_2^+ (45%)

Protoactinium solubility will be controlled by Pa_2O_5(s) under the studied conditions (see Table 32).

Table 32: Pa solid phases and equilibrium concentrations (m) under the different selected conditions.

	Equilibrated (eq)		**Bentonite + C-steel insert (NF)**	
	TC / SIT	**YMP / PITZER**	**TC / SIT**	**YMP / PITZER**
CR-10	Pa_2O_5(s) $2.22 \cdot 10^{-9}$	--	Pa_2O_5(s) $1.31 \cdot 10^{-9}$	--
SR-270	Pa_2O_5(s) $3.20 \cdot 10^{-8}$	--	Pa_2O_5(s) $1.72 \cdot 10^{-9}$	--

The most important uncertainty concerning protactinium is the scarcity of thermodynamic data.

4.10 LEAD

The relevant redox state under the conditions of interest is Pb(II) although Pb(IV) has also been described under oxidising conditions. Thermodynamic data for lead are available in the ThermoChimie v.7b/SIT database, but not in the YMP Pitzer database.

Lead aqueous speciation is mainly affected by pH and by the concentration of different ligands such as chloride, sulphate and carbonate (see Figure 23). In the *CR-10 eq* groundwater, the

cation $PbCl^+$ dominates the aqueous speciation. Carbonates ($PbCO_3$), sulphates ($PbSO_4$), the free Pb^{2+} and other chloride species ($PbCl_2$) can also appear in different proportion (see Table 33). Under more alkaline conditions, such as in *CR-10 NF* groundwater, the hydrolysis species $PbOH^+$ appears as a main contributor to the lead aqueous concentration. Other species such as chloride, sulphate, carbonate and free Pb^{2+} are present in lower proportion. Due to the lower concentration of carbonate in this groundwater carbonate species have a lower predominance under these conditions (see Figure 23). In the case of the SR-270 groundwater, with very high chloride concentration (5.18 m) the chloride species $PbCl_4^{2-}$ dominates the aqueous speciation under all the selected conditions with minor contribution of other chloride species ($PbCl_3^-$).

Table 33: Pb aqueous speciation under the different selected conditions.

	TC / SIT
Equilibrated	
CR-10 eq	$PbCl^+$ (33%), Pb^{2+} (26%), $PbCO_3$ (17%), $PbCl_2$ (11%), $PbSO_4$ (8%)
SR-270 eq	$PbCl_4^{2-}$ (86%), $PbCl_3^-$ (10%)
Bentonite + C-steel insert	
CR-10 NF	$PbOH^+$ (47%), $Pb(CO_3)$ (15%), $PbCl^+$ (10%), Pb^{2+} (9%), $Pb(SO_4)$ (8%)
SR-270 NF	$PbCl_4^{2-}$ (87%), $PbCl_3^-$ (9%)

The most likely solubility limiting phases under low carbonate concentration and in the presence of phosphate, as in the case of *CR-10 NF* groundwater, are phosphates of Pb(+II) (Cao et al. 2008). In the absence of phosphates, cerussite ($Pb(CO_3)$(s) and hydrocerussite $Pb_3(CO_3)_2(OH)_2$) will control the lead solubility in the CR-*10 NF* groundwater giving lead concentrations around 10^{-6} m. Under the conditions of *CR-10 eq* groundwater, with higher carbonate content, lead carbonates (cerussite ($Pb(CO_3)$(s), hydrocerussite $Pb_3(CO_3)_2(OH)_2$) and phosphates ($Pb_3(PO_4)_2$(s)) are the most likely solids controlling lead solubility, resulting in similar Pb concentrations in solution (see Table 34). In the case of the SR-270 groundwater, lead is not solubility limited by any solid phase as no phosphates are present in solution and free carbonate in solution is very low. For the *SR-270 NF* groundwater, free carbonate is not available as the total carbonate concentration is low. The free carbonate concentration is low in this groundwater due to the low pH of the solution and carbonate is mainly present as CO_2.

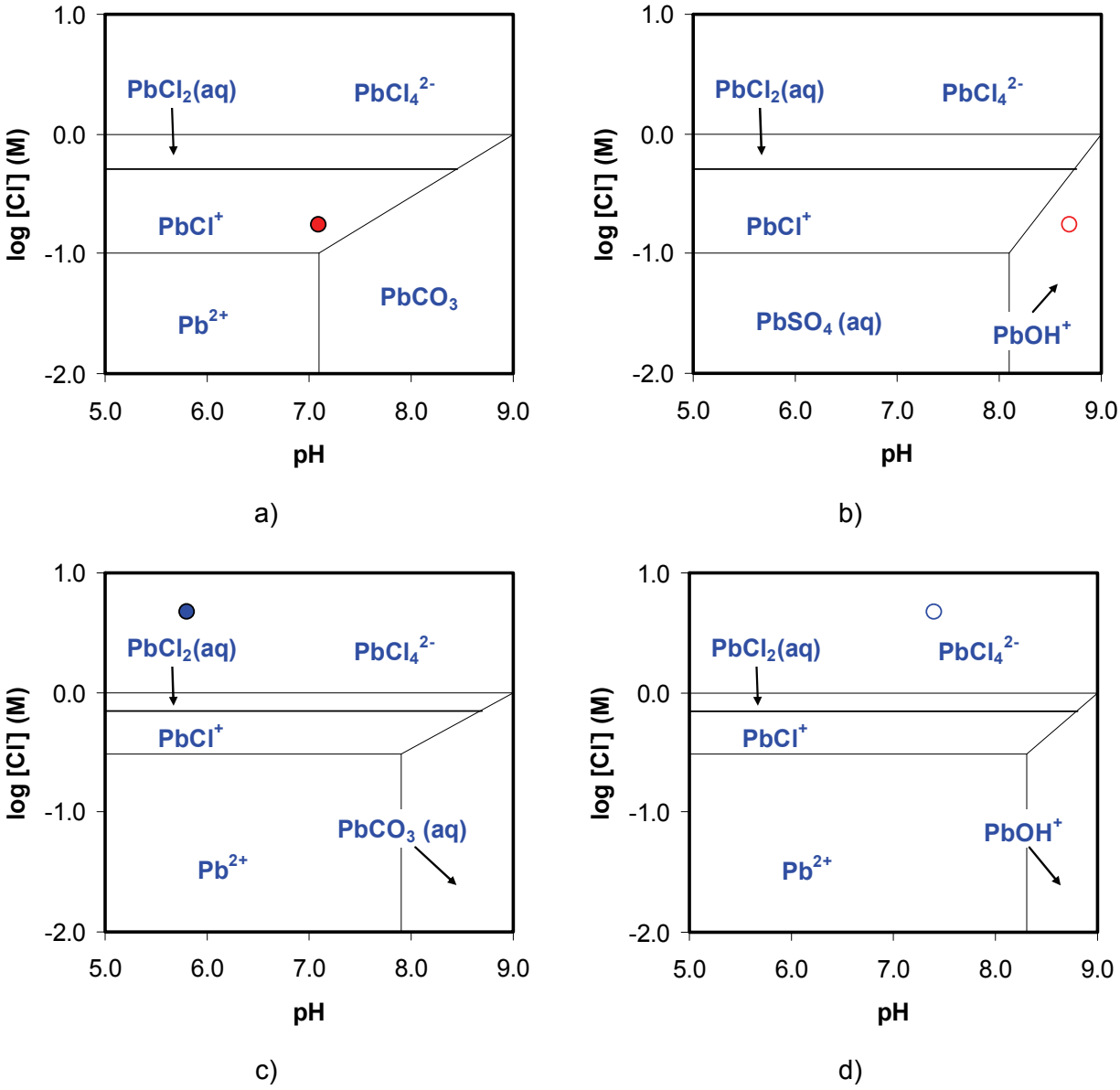

Figure 23. Predominance diagrams pH versus $[Cl^-]_T$ of Pb aqueous species under the compositions of the selected groundwater a) *CR-10 eq* (●) b) *CR-10 NF* (○), c) *SR-270 eq* (●) and d) *SR-270 NF* (○). Symbols are referred to the specific $[Cl]_T$ and pH of each groundwater. Calculations using ThermoChimie SIT.

Table 34: Pb solid phases and concentration values (m) under the different selected conditions.

	Equilibrated (eq)		Bentonite + C-steel insert (NF)	
	TC / SIT	**YMP / PITZER**	**TC / SIT**	**YMP / PITZER**
CR-10	**$Pb(CO_3)(s)$** **$3.11 \cdot 10^{-6}$** **$Pb_3(CO_3)_2(OH)_2$** **$7.89 \cdot 10^{-6}$** **$Pb_3(PO_4)_2(s)$** **$1.09 \cdot 10^{-6}$** $Pb_3(PO_4)_2(s)$* $7.1 \cdot 10^{-6}$	--	**$Pb(CO_3)(s)$** **$3.45 \cdot 10^{-6}$** **$Pb_3(CO_3)_2(OH)_2$** **$1.01 \cdot 10^{-6}$** **$Pb_3(PO_4)_2(s)$** **$2.54 \cdot 10^{-7}$** $Pb_3(PO_4)_2(s)$* $1.4 \cdot 10^{-5}$	--
SR-270	n.s.l.[1]		n.s.l	

[1]: n.s.l.: no solubility limit.

* indicate solubility calculated when the concentration of phosphate in the groundwater is fixed by equilibrium with hydroxyapatite

As in the case of Am, the precipitation of solid phosphate phases is uncertain in the sense that the concentration of phosphate in solution is given as an upper limit. If the groundwaters are assumed to be equilibrated with hydroxyapatite, phosphate concentrations are $6.4 \cdot 10^{-7}$ mol/L for the *CR-10 eq* and 2.49 10^{-8} mol/L for the *CR-10 NF* groundwater. In this case, the concentration of lead in equilibrium with $Pb_3(PO_4)_2(s)$ increases to $7.1 \cdot 10^{-6}$ and $1.4 \cdot 10^{-5}$ mole/L respectively.

Another uncertainty affecting the assessment of lead solubility refers to the reduction of sulphate to sulphide; in that case, lead may precipitate as galena (PbS(s)). Formation of galena would lead to Pb concentrations in the order of 10^{-14} m for *CR-10 eq* groundwater, 10^{-12} m for *SR-270 NF* groundwater and 10^{-10} m for *CR-10 NF and SR-270 eq* groundwaters. Lead may also be incorporated in other major sulphides, which will also cause a decrease of its solubility.

4.11 PALLADIUM

Palladium may be found at several valence states, Pd(II) being the most common redox state in aqueous media. Thermodynamic data for palladium are available in ThermoChimie v.7b/SIT database but not in the YMP Pitzer database.

Calculations indicate that the palladium aqueous speciation in the CR-10 groundwater, under all the studied conditions, will be controlled by the hydrolysis species $Pd(OH)_2(aq)$ (see Table 35). Palladium chlorides are only relevant at chloride concentrations in solutions higher than 0.3 M (see Figure 24). In the case of the SR-270 groundwater with high chloride concentration (4.75 M), $PdCl_4^{2-}$ will be the main aqueous species.

Table 35: Pd aqueous speciation under the different selected conditions.

	TC / SIT
Equilibrated	
CR-10 eq	$Pd(OH)_2(aq)$ (97%), $PdCl_4^{2-}$(2%)
SR-270 eq	$PdCl_4^{2-}$(98%)
Bentonite + C-steel insert	
CR-10 NF	$Pd(OH)_2(aq)$ (100%)
SR-270 NF	$PdCl_4^{2-}$(98%)

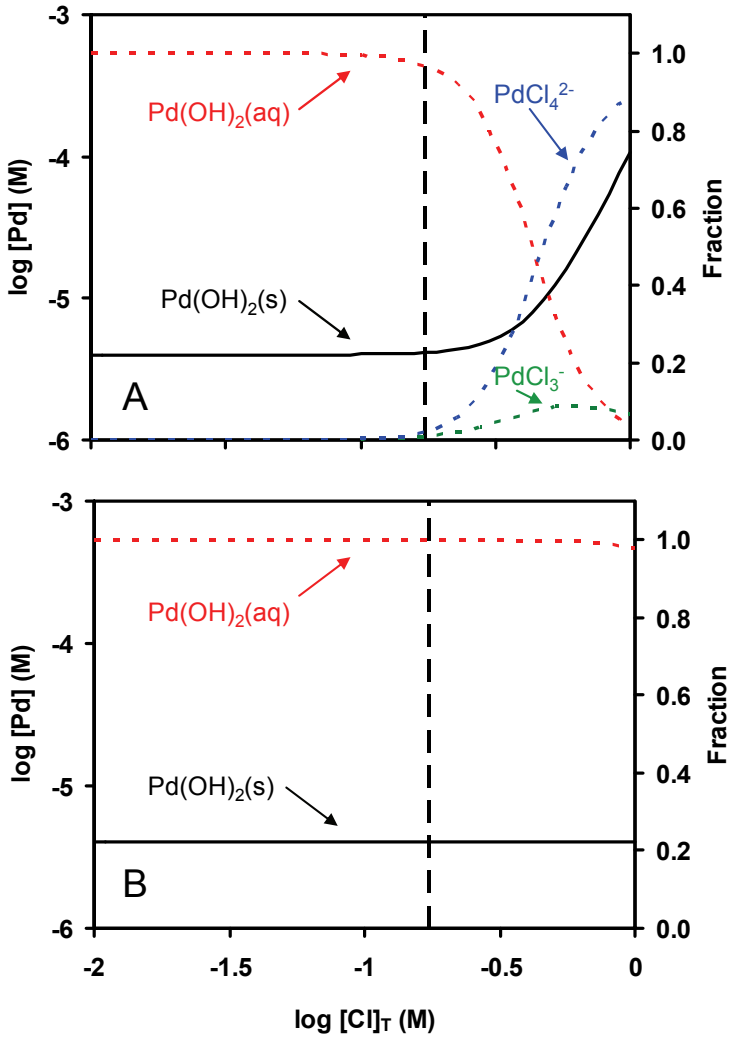

Figure 24: Fractional diagram of palladium aqueous species in equilibrium with $Pd(OH)_2(s)$, as a function of chloride concentration in solution A) for *CR-10 eq* water B) for *CR-10 NF* water. Vertical line corresponds to real chloride concentration in each groundwater.

$Pd(OH)_2(s)$ is the most likely solid controlling the Pd solubility under the studied conditions, giving the aqueous concentrations shown in Table 36. For the SR-270 groundwater, $Pd(OH)_2(s)$ has a high solubility due to the formation of aqueous Pd chlorides in solution and Pd is not solubility limited (see Table 36). The possibility that pure palladium controls the solubility under reducing conditions seems unrealistic due to the slow kinetics of the formation of metallic Pd from solution.

A conceptual uncertainty affecting Pd solubility is the reduction of sulphate to sulphide. If sulphate were allowed to be reduced to sulphide, sulphide solid phases (PdS) might exert solubility control at reducing Eh values. The equilibration with PdS(s) in the calculations results in extremely low aqueous palladium concentrations. Note that the thermodynamic data for solid Pd sulphide have been derived from high temperature experiments done with visotskite (PdS) which is a solid phase formed under high temperature conditions, not expected under the studied conditions of this work.

Table 36: Pd solid phases and concentration values (m) under the different selected conditions.

	Equilibrated (eq)		Bentonite + C-steel insert (NF)	
	TC / SIT	**YMP / PITZER**	**TC / SIT**	**YMP / PITZER**
CR-10	$Pd(OH)_2(s)$ $4.11 \cdot 10^{-6}$	--	$Pd(OH)_2(s)$ $3.98 \cdot 10^{-6}$	--
SR-270	n.s.l*	--	n.s.l	

*:n.s.l.: no solubility limit

4.12 PLUTONIUM

Plutonium presents different redox states (+III, +IV, +V and +VI) in solution. Under the conditions of the selected groundwater compositions (near neutral pH and reducing conditions), plutonium will mainly appear in the oxidation states (+III) and (+IV) (see Figure 25).

The formation of aqueous species and solid phases depends on the master variables Eh and pH. Nevertheless, the presence of carbonates and/or sulphates will also have an important role in determining the aqueous complexes dominating Pu speciation in solution. Phosphates have also been identified to form strong aqueous complexes with Pu(III), although Pu-phosphate aqueous species are not included in the YMP Pitzer database.

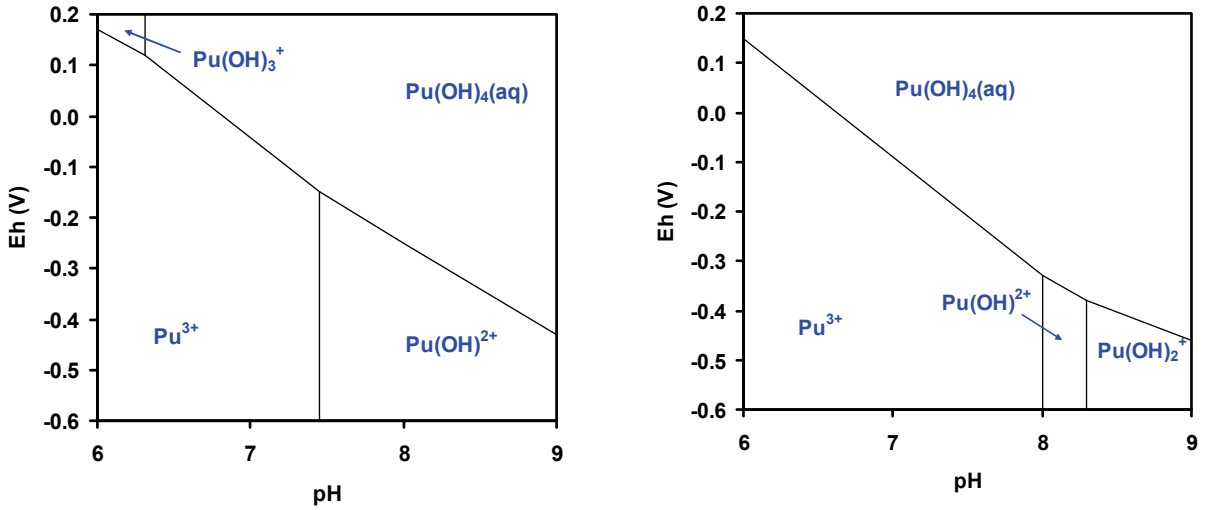

a) b)

Figure 25: Predominance diagram (Eh-pH) of Pu aqueous species calculated with a) ThermoChimie v.7b/SIT database and b) YMP Pitzer database in pure water. $[Pu]_T=1\cdot10^{-7}$ M. Carbonate, silicate or sulfate species are not taken into account in this diagram.

Due to the reducing conditions prevailing under the selected conditions and the pH range, Pu(III) species dominate the aqueous Pu speciation (see Table 37)

In *CR-10 eq* groundwater, the cation Pu^{3+} dominates the aqueous speciation. Carbonates, sulphates and hydrolyzed Pu(III) species ($PuSO_4^+$, $PuCO_3^+$, $Pu(OH)^{2+}$) also appear but their concentrations depend on the thermodynamic database (see Table 37).

In the case of *CR-10 NF* groundwater, due to the higher pH value, $Pu(OH)^{2+}$ dominates the aqueous speciation when using ThermoChimie v.7b/SIT database. Carbonates, sulphates, hydroxides and phosphates ($PuSO_4^+$, $PuCO_3^+$, $Pu(OH)_2^+$, $PuPO_4$) also appear in solution. When using the YMP Pitzer database, only the aqueous species Pu^{3+} is present.

In *SR-270 eq* groundwater the free cation Pu^{3+} dominates the aqueous speciation when using both databases and no major differences are observed between the two calculations. In the case of *SR-270 NF* groundwater, $PuOH^{2+}$ dominates the aqueous speciation when using ThermoChimie SIT. The free cation Pu^{3+} also appears in solution. When using the YMP Pitzer database, the aqueous species $Pu(OH)_2^+$ is the major species in solution with minor contributions from $PuOH^{2+}$ and the free cation Pu^{3+}.

In this case, differences in the calculated Pu aqueous speciations for the different databases are attributed to differences in both the stability constant selected for each database and the approach used to calculate activity corrections.

Table 37: Pu aqueous speciation under the different selected conditions using both databases.

	TC / SIT	YMP / PITZER
CR-10 eq	$PuSO_4^+$ (31%), Pu^{3+} (31%), $PuCO_3^+$ (22%), $Pu(OH)^{2+}$ (9%)	Pu^{3+} (85%), $PuCO_3^+$ (12%)
SR-270 eq	Pu^{3+} (91%), $PuOH^{2+}$ (4%)	Pu^{3+} (79%), $PuCO_3^+$ (9%), $PuOH^{2+}$ (6%)
CR-10 NF	$Pu(OH)^{2+}$ (47%), $PuPO_4$ (12%), $PuSO_4^+$ (12%), $Pu(OH)_2^+$ (9%), $PuCO_3^+$ (7%) (*)	Pu^{3+} (100%)
SR-270 NF	$PuOH^{2+}$ (60%), Pu^{3+} (36%)	$Pu(OH)_2^+$ (80%), $PuOH^{2+}$ (14%), Pu^{3+} (5%)

** Aqueous speciation in the absence of phosphates for the CR-10 NF groundwater calculated with TC/SIT:* $Pu(OH)^{2+}$ (56%), $PuSO_4^+$ (13%), $Pu(OH)_2^+$ (10%), $PuCO_3^+$ (9%).

Phosphates have been identified to form stable Pu(III) solid phases leading to lower Pu concentrations than those calculated considering equilibrium with $Pu(OH)_3$(s) and PuO_2(am) phases. Therefore, a Pu (III)-bearing phosphate solid phase can be the solid phase controlling the solubility in neutral and reducing waters if phosphates are present as in the case of the *CR-10 eq* (see Figure 26). The trivalent plutonium phosphate is stabilised over the tetravalent amorphous oxide when the lower redox potential groundwater (*CR-10 NF*) is considered.

In the absence of phosphates, as in the SR-*270 eq* and SR-*270 NF* groundwaters, or if phosphate precipitation is not taken into account, the solids $Pu(OH)_3$(s) and PuO_2(am) will be the solubility limiting phases depending on the redox conditions of the system (see Table 38). However for the SR-*270 eq* groundwater with the lowest pH (5.8) these hydroxide phases are more soluble and it can be considered that plutonium would not be solubility limited by any solid phase.

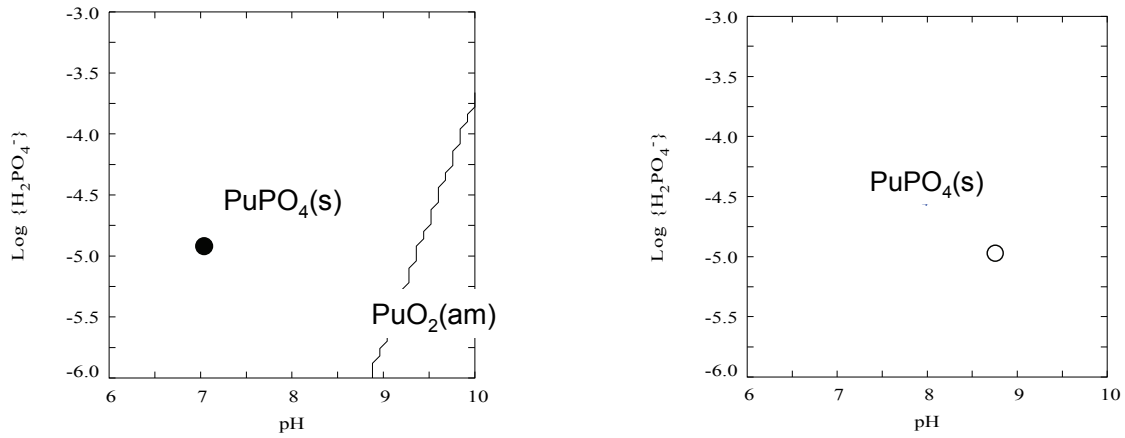

Figure 26. Stability fields of solid Pu phosphate and PuO_2(am) as a function of pH and phosphate concentration in solution under the conditions of the *CR-10 eq* (a, ●) and *CR-10 NF* groundwaters (b, ○).

Table 38 summarises the Pu solubility calculations for the different conditions of interest. The solubility limiting phases are the same for both databases although major differences are observed in the calculated radionuclide concentration in some cases. As in the previous cases, if the concentration of phosphate in the groundwater is given by equilibrium with hydroxyapatite, then the solubility of the Pu(III) solid phosphate increases, as shown in Table 38

Table 38: Pu solid phases and concentration values (m) under the different selected conditions and using both databases.

	Equilibrated (eq)		Bentonite + C-steel insert (NF)	
	TC / SIT	**YMP / PITZER**	**TC / SIT**	**YMP / PITZER**
CR-10	**$PuPO_4$** **$5.12 \cdot 10^{-12}$** **$PuO_2(am)$** **$1.50 \cdot 10^{-8}$** $PuPO_4$* $8.24 \cdot 10^{-11}$ -***	**$PuPO_4$** **$9.27 \cdot 10^{-13}$** **$PuO_2(am)$** **$7.01 \cdot 10^{-8}$** -***	**$PuPO_4$** **$8.12 \cdot 10^{-13}$** **$PuO_2(am)$** **$9.10 \cdot 10^{-8}$** $PuPO_4$* $3.2 \cdot 10^{-10}$ **$Pu(OH)_3$** **$2.47 \cdot 10^{-8}$**	**$PuPO_4$** **$4.26 \cdot 10^{-12}$** **$PuO_2(am)$** **$1.44 \cdot 10^{-5}$** **$Pu(OH)_3$** **$5.20 \cdot 10^{-6}$**
SR-270	n.s.l.**	n.s.l	$Pu(OH)_3$ $4.50 \cdot 10^{-5}$	$Pu(OH)_3$ $3.15 \cdot 10^{-5}$

* indicates the solubility if the concentration of phosphate in groundwater is fixed by equilibrium with hydroxyapatite

** n.s.l.: no solubility limit

*** Pu concentration in equilibrium with $Pu(OH)_3$ solid phase would give very high concentrations (> 10^{-4} m) under this conditions

From Table 38 we can see that the effect of the Pitzer calculations on the solubility of PuO_2(am) is very high for the bentonite and C-steel NF groundwater. After checking the calculations, we found that the logγ for the species Pu^{3+} in the *CR-10 eq* groundwater is -2.5, and it is -5 for *CR-10 NF* groundwater for the Yucca Mountain/Pitzer database. This means that the concentration calculated after applying the activity correction will be much higher for the bentonite and C-steel NF groundwater. At this point, it is relevant to quote some of the conclusions in Neck and Kim (2001):

> *"The simple SIT equation is preferred to the more elaborate Pitzer approach because the hitherto available data for An(IV) hydrolysis species are not sufficient to evaluate all necessary ion interaction coefficients. Some uncertainties arising from the estimation of SIT coefficients have no significant effect on the calculation of activity coefficients at I ≤ 0.1 mol/kg, whereas an estimated Pitzer coefficient $\beta^{(1)}$ has a considerable effect even at low ionic strength, in particular for ions of high charge."*

Therefore, for the solubility of PuO_2 (am), we recommend the results calculated by the SIT approach.

4.13 RADIUM

Radium is not a redox-sensitive element. No data on Ra are included in the YMP Pitzer database.

The main parameter affecting radium aqueous speciation under the selected groundwater compositions is the sulphate concentration for the CR-10 groundwater and the chloride concentration for the more saline SR-270 groundwater.

The aqueous speciation of radium is dominated by free Ra^{2+} with contributions of the species $RaSO_4$ for the CR-10 groundwater and the chloride species ($RaCl_2$ and $RaCl^+$) for the SR-270 groundwater (see Table 39). As we can see in Figure 27, the aqueous speciation and solubility of radium depends on sulphate aqueous concentration.

Table 39: Ra aqueous speciation under the different selected groundwater compositions.

	TC / SIT	YMP / PITZER
Equilibrated		
CR-10 eq	Ra^{2+} (77%), $RaSO_4$ (20%)	--
SR-270 eq	Ra^{2+} (50%), $RaCl_2$ (31%), $RaCl^+$ (19%)	
Bentonite + C-steel insert		
CR-10 NF	Ra^{2+} (54%), $RaSO_4$ (44%)	--
SR-270 NF	Ra^{2+} (49%), $RaCl_2$ (32%), $RaCl^+$ (19%)	

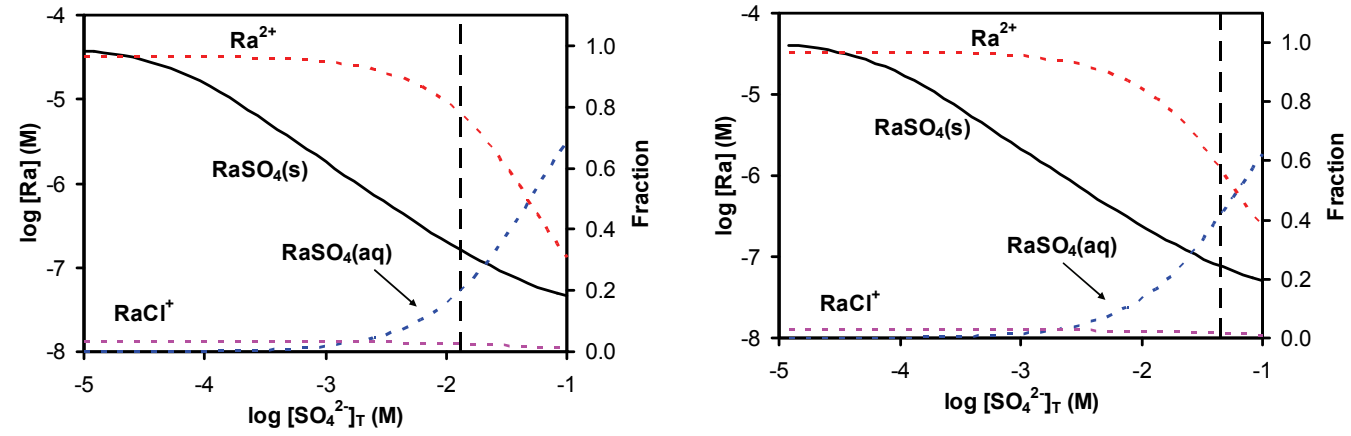

Figure 27: Calculated $RaSO_4$ (s) solubility and underlying aqueous speciation as a function of the total sulphate concentration of the contacting groundwater (a) *CR-10 eq* groundwater (I = 0.24); and b) *CR-10 NF* groundwater (I = 0.32). Verticle dashed line corresponds to the sulphate concentration defined for each groundwater

The main parameter affecting the radium solubility limiting phase under the selected groundwater compositions is the sulphate to carbonate concentration ratio (see Figure 28). We see that all groundwater compositions fall in the predominance field of $RaSO_4(s)$.

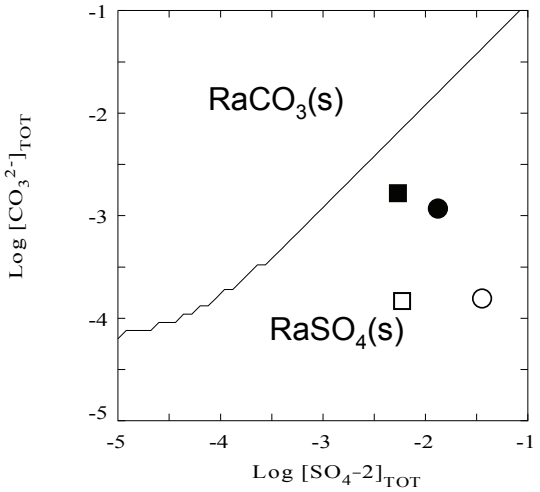

Figure 28. Predominance carbonate to sulphate diagram of Ra solid phases. Symbols stand for the carbonate and sulphate concentration of *CR-10 eq* (●), *CR-10 NF* (○), SR-270 eq (■) and SR-270 NF (□) groundwaters. The diagram has been calculated at the pH of the CR-10 eq groundwater.

Although the plot in Figure 28 has been calculated at the pH of the *CR-10 eq* groundwater (pH = 7.1; Eh = -194 mV), if sulphate to sulphide reduction is not allowed the diagram is very similar for all selected groundwaters. If the reduction of sulphate to sulphide is allowed, $RaSO_4(s)$ is destabilized relative to $RaCO_3(s)$ and the solubility controlling phase would the $RaCO_3(s)$.

Under all the selected conditions, the solid phase most likely to control the solubility of radium is $RaSO_4(s)$ (see Table 40). As we can see in Figure 27, the solubility of $RaSO_4(s)$ is strongly affected by the sulphate concentration of the contacting groundwater.

Table 40: Ra solid phases and concentration values (m) under the different selected conditions.

	Equilibrated (eq)		Bentonite + C-steel insert (NF)	
	TC / SIT	**YMP / PITZER**	**TC / SIT**	**YMP / PITZER**
CR-10	$Ra(SO_4)(s)$ $1.56 \cdot 10^{-7}$	--	$Ra(SO_4)(s)$ $7.12 \cdot 10^{-8}$	--
SR-270	$Ra(SO_4)(s)$ $1.68 \cdot 10^{-5}$	-	$Ra(SO_4)(s)$ $1.43 \cdot 10^{-5}$	-

One of the conceptual uncertainties to consider is the reduction of sulphate to sulphide. If sulphate were allowed to reduce to sulphide, the solubility of $RaSO_4(s)$ would considerably increase due to the lower sulphate concentration in solution.

Radium co-precipitation with Ba, Sr or Ca phases (such as carbonates or sulphates) may also be an important factor controlling radium solubility. Isomorphic substitution of Ca by Ra in calcite or in gypsum is possible, and the co-precipitation between radium isotopes and barite precipitates is well known (Bruno et al., 2007). The formation of this kind of solid solution may result in lower solubility values for Ra.

4.14 SELENIUM

Selenium is a redox-sensitive element with oxidation states -II, +IV and +VI in aqueous solution. Under anoxic and reducing conditions, Se(-II) prevails as HSe^- in a wide pH range, whereas the highly mobile oxyanion species (SeO_3^{2-} and SeO_4^{2-}) dominates the Se speciation under oxidising conditions (see Figure 29).

The YMP Pitzer database does not include thermodynamic data for selenium. Thermodynamic data for selenium in the ThermoChimie SIT database come basically from the NEA selection (Olin et al. 2005). The database includes SIT interaction coefficients for Se(IV) and Se(VI) species, but not for Se(-II) species.

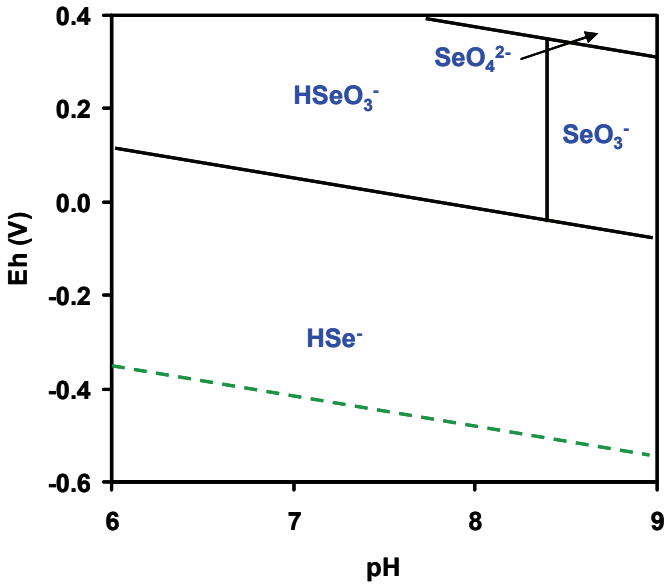

Figure 29: Aqueous predominance diagram (Eh-pH) of Se. $[Se]_T = 1 \cdot 10^{-7}$ M in water.

Selenium is mainly found as HSe^- under all studied conditions. One important parameter in the study of Se solubility is the presence of Fe(II) in the aqueous solution which may cause the precipitation of $FeSe_x$(s) solid phases (where x =1 or 2). The formation of $FeSe_x$(s) solid phases has been widely described in Olin et al. (2005) and this phase is expected to control Se solubility in reducing environments where Fe(II) is present.

Figure 30 shows the effect of both the Eh and iron concentration on the precipitation of iron selenide solid phases. Elemental selenium, Se(cr) could be stable under slightly reducing

conditions (Figure 30). According to Charlet et al. (2007) Se(VI) and Se(IV) are converted to Se(0) and reduced Se species in reducing environments. However, the mechanism is not well known and it seems that it proceeds via sorption onto Fe or Mn oxides, reductive dissolution of the latter minerals or mineralization of organic matter and that it finishes with the precipitation of Se(0), of ferroselite or Se-hosting pyrite. Se reduction can be either microbial or inorganic, with the latter reaction only observed in the presence of green rust. The authors studied the reduction of Se in Fe(II)-clay systems and observed important Se reduction for pH below 7 (where both Fe and Se sorb onto the mineral edges) and the formation of stable and insoluble Se(0). They suggest that other forms of Fe(II) may lead to the reductive precipitation of Se(0) as well and highlighted the need of investigating other geochemical parameters to determine the long-term stability of Se(0).

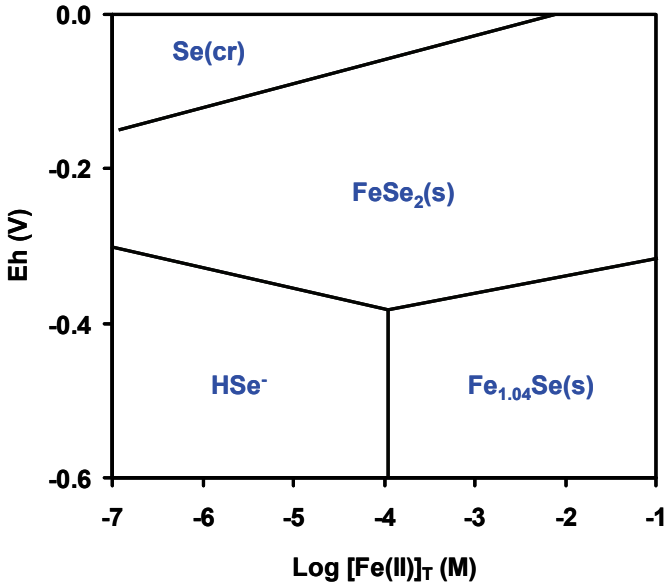

Figure 30: Predominance Eh vs log$[Fe]_T$ diagram of selenium at pH = 7.1, $[Se]_T = 1 \cdot 10^{-7}$ Mol/L, $[Mg]_T = 2.5 \cdot 10^{-3}$ Mol/L, $[Ca]_T = 5.6 \cdot 10^{-2}$ Mol/L, $[SO_4]_T = 1.3 \cdot 10^{-2}$ Mol/L, and $[CO_3]_T = 8.3 \cdot 10^{-4}$ Mol/L.

The expected solubility limiting solid phases for Se and the solubility values are summarised in Table 41. If the total iron concentration in solution is not varied in a very wide range, only small changes in selenium concentration in solution would be calculated. For *Cr-10 eq* , decreasing the total iron concentration from 8 to 1 ppm leads only to a small increase in the total selenium concentration in solution (from $1.15 \cdot 10^{-10}$ m to $3.60 \cdot 10^{-10}$ m).

Table 41: Se solid phases and concentration values (m) under the different selected conditions.

	Equilibrated		Bentonite + C-steel insert	
	TC / SIT	**YMP / PITZER**	**TC / SIT**	**YMP / PITZER**
CR-10	$FeSe_2(s)$ $1.15 \cdot 10^{-10}$	--	β-$Fe_{1.04}Se$ $1.26 \cdot 10^{-8}$	--
SR-270	$FeSe_2(s)$ $3.43 \cdot 10^{-9}$		β-$Fe_{1.04}Se$ $1.77 \cdot 10^{-9}$	

Co-precipitation processes with other major solid phases may also control Se concentration in groundwaters. Given the similarities between the ionic radius of Se^{2-} and that of S^{2-} (0.191 nm vs. 0.184 nm, (Shannon, 1976)) substitution of selenium for sulphur can occur. Mineralogical studies on sulphides report the incorporation of selenium into the crystalline lattice of sulphides to a maximum of 300 ppm in pyrite ($FeS_2(s)$) and 100 ppm in pyrrhotite (FeS(s)) (Vaughan and Craig, 1978). Thus the above calculated solubilities are likely higher than would occur if coprecipitation processes are considered.

4.15 TECHNETIUM

Technetium is a redox sensitive element which may appear in several redox states (+II to +VII), although the most stable redox states are Tc(+IV) under reducing conditions and Tc(+VII) under oxidizing conditions (see Figure 31).

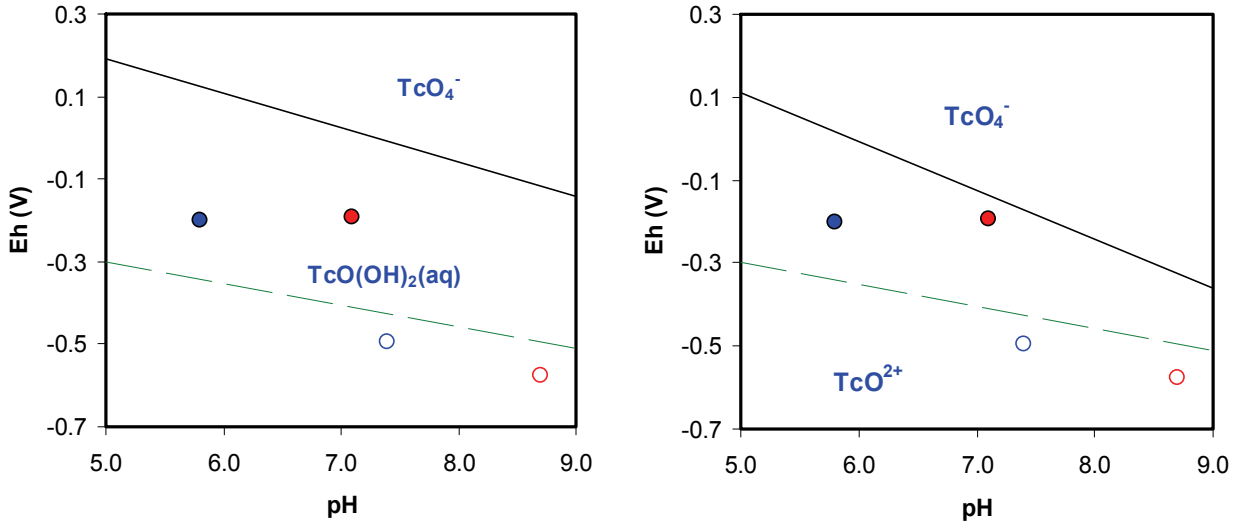

a) b)

Figure 31: Predominance diagram pH vs Eh of Tc in water using a)ThermoChimie V7.b/SIT and b) YMP Pitzer database. Symbols refers to *CR-10 eq* (●), *CR-10 NF* (○), *SR-270 eq* (●) and *SR-270 NF* (○) groundwater Eh and pH. $[Tc]_T = 1 \cdot 10^{-7}$ M. Dashed line: reduction of water to H_2

A complete set of thermodynamic data for Tc are not available in the YMP Pitzer database, where only the solid phases of technetium and the master species TcO_4^- and TcO^{2+} are selected (see Figure 31). For this reason, calculations are only done with ThermoChimiev.7b/SIT database.

The formation of technetium aqueous species and solid phases depends on the master variables Eh and pH. Under the reducing conditions of the selected groundwaters the main aqueous species for technetium is the hydroxocomplex $TcO(OH)_2$ (aq). Concerning the solid phases, the amorphous hydrous oxide $TcO_2 \cdot 1.6H_2O$ has been selected as the solid phase limiting the technetium solubility (see Table 42). More thermodynamically stable solid phases are pure techetium metal (Tc(cr)) and the crystalline oxide (TcO_2(cr)), although they have not been selected based on kinetic criteria.

Table 42: Tc solid phases and concentration values (m) under the different selected conditions using both databases.

	Equilibrated (eq)		Bentonite + C-steel insert (NF)	
	TC / SIT	**YMP / PITZER***	**TC / SIT**	**YMP / PITZER***
CR-10	TcO_2:1.6H_2O $4.01 \cdot 10^{-9}$	--	TcO_2:1.6H_2O $4.05 \cdot 10^{-9}$	--
SR-270	TcO_2:1.6H_2O $4.39 \cdot 10^{-9}$	--	TcO_2:1.6H_2O $4.39 \cdot 10^{-9}$	--

*Calculations are incorrect since no aqueous species are included in the database

4.16 THORIUM

Thorium is mainly found in the redox state +IV and can be considered a non redox sensitive radioelement.

The formation of aqueous species and solid phases depends on the pH as Th(IV) is strongly hydrolysed in water. Under acidic conditions, where hydrolysis is relatively unimportant, thorium forms strong complexes with fluoride. Thorium also forms very stable complexes with carbonate, which enhances significantly the solubility of Th in carbonate waters at near-neutral to alkaline pH values (Rand et al. 2009). However hydroxocarbonate thorium aqueous complexes are not included in the YMP Pitzer database and only the limiting carbonate complex $Th(CO_3)_5^{6-}$ is selected (see Figure 32).

Under the low carbonate concentration of the *CR-10 NF* groundwater, the aqueous chemistry of thorium is mainly dominated by the $Th(OH)_4$(aq) species and no major differences in the aqueous speciation are observed using the different databases (see Table 43).

Under higher carbonate concentrations, such as those of the *CR-10 eq* groundwater, the predominant aqueous species of thorium depends on the thermodynamic database used in the calculations. When using the ThermoChimie v.7b /SIT database, the species $Th(OH)_3(CO_3)^-$ is the main aqueous species. Hydrolysis species and other carbonate species ($Th(OH)_4$, $Th(OH)_3^+$, and $Th(OH)_2(CO_3)_2^{2-}$) are also present in minor amounts. When using the YMP Pitzer database, $Th(OH)_4$ (aq) is the dominant species for *CR-10 eq* groundwater, with minor contributions of the species $Th(OH)_3^+$ (see Table 43).

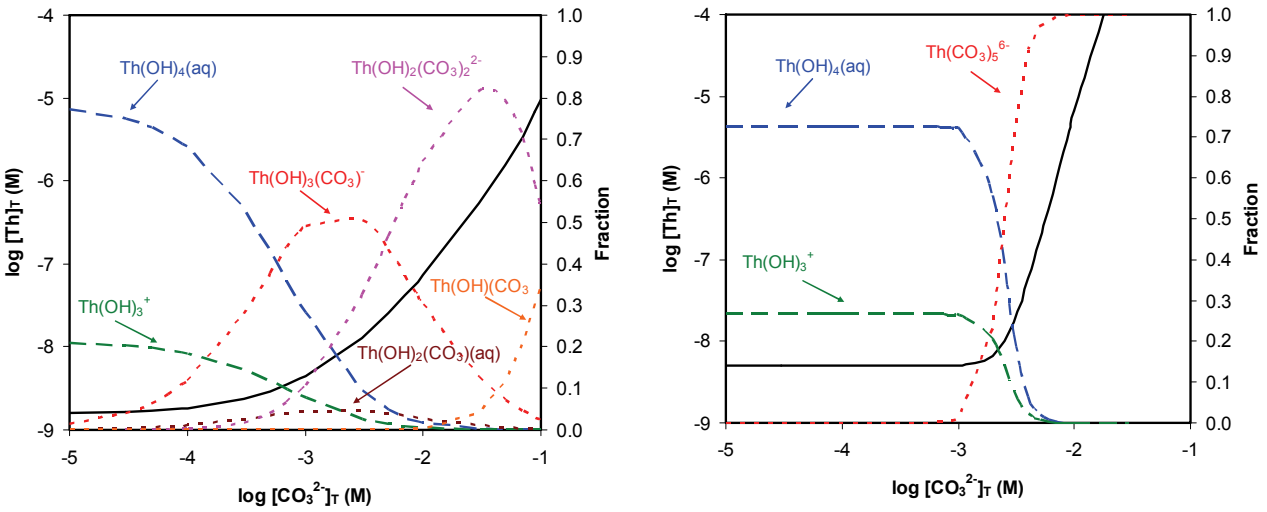

a) b)

Figure 32: Thorium solubility (black solid line) and underlying thorium aqueous speciation (dotted lines) as a function of carbonate concentration in solution at pH = 7.06. Calculations have been made using the a) ThermoChimie v 7.b/SIT database, and b) YMP Pitzer database.

Table 43: Th aqueous speciation under the different selected conditions using both databases

	TC / SIT	YMP / PITZER
Equilibrated		
CR-10 eq	$Th(OH)_3(CO_3)^-$ (46%), $Th(OH)_4(aq)$ (32%), $Th(OH)_3^+$ (10%), $Th(OH)_2(CO_3)_2^{2-}$ (8%)	$Th(OH)_4(aq)$ (70%), $Th(OH)_3^+$ (29%)
SR-270 eq	ThF_2^{2+} (35%), $Th(OH)_3^+$ (19%), ThF^{3+} (15%), $Th(OH)_2^{2+}$ (7%), $Th(OH)_2(CO_3)$ (6%), ThF_3^+ (5%), $Th(OH)_3(CO_3)^-$ (5%)	---[1]
Bentonite + C-steel insert		
CR-10 NF	$Th(OH)_4(aq)$ (90%), $Th(OH)_3(CO_3)^-$ (9%)	$Th(OH)_4(aq)$ (99%)
SR-270 NF	$Th(OH)_4$ (84%), $Th(OH)_3^+$(10%), $Th(OH)_3(CO_3)^-$ (6%)	---[1]

(1) No reliable results

In the case of calculations with the SR-270 groundwaters (both *SR-270 eq* and *SR-270 NF*) using the YMP Pitzer database, the Phreeqc calculations did not lead to consistent results. Calculations using this database indicate the formation of thorium polynuclear species

($Th_2(OH)_2^{6+}$ and in some cases $Th_4(OH)_{12}^{4+}$) which enhance thorium hydroxide solubility until it is totally dissolved.

LogK values for thorium polynuclear species included in the YMP Pitzer database have been obtained from Neck et al. (2002). In this study, Neck and his co-workers used the SIT approach. The inclusion of those polynuclear species when using the Pitzer approach results in a non-consistent thorium database that leads to doubtful results when applied to highly saline waters.

In order to check the consistency of the YMP Pitzer database regarding thorium solubility in highly saline waters, we have used both databases to model the experimental results of Felmy et al. (1991). Felmy et al. (1991) studied thorium hydroxide solubility at 3M NaCl (that is, in a saline water) at various pH values, covering the range relevant for *SR-270* groundwaters. Modelled results are shown in Figure 33. Results indicate that ThermoChimie v.7b/SIT is able to reproduce the experimentally measured solubility. In contrast, the YMP Pitzer database is not able to explain the results obtained at pH<8, where the model predicts an unrealistic high solubility for the solid phase. The Th speciation indicates that the YMP Pitzer database predicts the formation of $Th_2(OH)_2^{6+}$ at pH<8, which does not form under those conditions (Felmy et al. 1991, Neck at al. 2002). For this reason only results obtained with ThermoChimie SIT will be discussed.

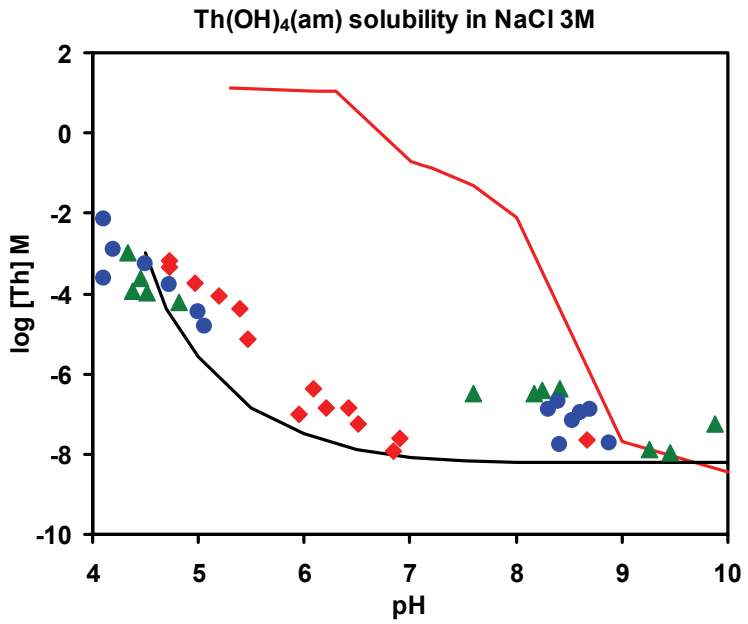

Figure 33: Hydrous Th(IV) hydroxide solubilities in 3.0 M NaCl, experimental data from Felmy et al. (1991). Different symbols represent 8 (red diamonds), 122 (green triangles) and 372 (blue circles) days of equilibration. Black line: model results using ThermoChimie SIT database. Red line: model results using YMP Pitzer database.

The thorium aqueous speciation in *SR-270 eq* groundwater is very different from that obtained in *CR-10 eq* groundwater. The more acidic pH in the *SR-270 eq* groundwater (pH= 5.8 for *SR-270 eq*, pH=7.1 for *CR-10 eq*) results in formation of the aqueous thorium fluoride complex

ThF_2^{2+} as the main aqueous species. Other fluoride, hydroxide and carbonate complexes are also present in minor proportion (see Table 43). Fluoride species are not present in *SR-270 NF* groundwater because of the higher pH in this groundwater (pH=7.4). In this case, $Th(OH)_4$ is the main aqueous species with minor contributions of other hydrolysis and carbonate species ($Th(OH)_3^+$, $Th(OH)_3(CO_3)^-$).

The amorphous oxides and hydroxides are the most likely solids controlling thorium solubility under the studied conditions, leading to thorium concentrations in solution in the order of 10^{-9} to 10^{-7} m (see Table 44). It can be seen that in both cases the databases reflect the wide variation of the solubility of thorium oxides and hydroxides due to the crystallinity variation, ageing effects, surface hydration, particle size variation and colloids formation. Note that ThO_2(aged) and ThO_2(fresh) are amorphous phases that represent different stages of the crystallitzation of ThO_2(am). ThO_2(am), which is the solid phase included in YMP Pitzer database, is a more amorphous phase than ThO_2(aged) or ThO_2(fresh).

Table 44: Th solid phases and concentration values (m) under the different selected conditions using both databases.

	Equilibrated (eq)		Bentonite + C-steel insert (NF)	
	TC / SIT	**YMP / PITZER**	**TC / SIT**	**YMP / PITZER**
CR-10	ThO_2(aged) $3.94\cdot10^{-9}$ ThO_2(fresh) $2.49\cdot10^{-8}$	$Th(OH)_4$(am) $5.23\cdot10^{-9}$ ThO_2(am) $1.68\cdot10^{-7}$	ThO_2(aged) $1.38\cdot10^{-9}$ ThO_2(fresh) $7.85\cdot10^{-9}$	$Th(OH)_4$(am) $3.69\cdot10^{-9}$ ThO_2(am) $1.14\cdot10^{-7}$
SR-270	ThO_2(aged) $2.39\cdot10^{-8}$ ThO_2(fresh) $1.45\cdot10^{-7}$	---(1)	ThO_2(aged) $1.10\cdot10^{-9}$ ThO_2(fresh) $6.93\cdot10^{-9}$	---(1)

(1) No reliable results

As we can see in Table 44, the solubility limiting phases do not differ significantly when using the two databases, although different radionuclide concentrations are calculated. Differences are attributed to the different stability constants for the aqueous and solid phases selected for each database. The thorium hydrolysis scheme is similar in both databases but Th-hydroxo-carbonate species are not present in the YMP Pitzer database.

One of the main uncertainties affecting the solubility assessment of thorium is the effect of phosphate. The YMP Pitzer database includes thermodynamic data for the formation of the thorium-phosphate solid $Th_{0.75}PO_4$(s) (equivalent to $Th_3(PO_4)_4$(s)). Formation of this solid may lead to thorium concentrations $\approx10^{-12}$ m in the case of *CR-10 eq* water and $\approx10^{-8}$ m in the case of CR-10 NF groundwater equilibrated with bentonite and the C-Steel insert. However, according to the NEA review (Rand et al., 2009), thermodynamic data for this solid should only be applied for scoping calculations, due to the uncertainties on the stoichiometry of this Th-phosphate solid and the lack of information about its formation at 25ºC.

4.17 TIN

Tin may exist in the redox states Sn(+II) and Sn(+IV) in aqueous solution. While the (+IV) state is particularly stable in natural environments, Sn(+II) appears only at very reducing conditions (see Figure 34).

No thermodynamic data are available for Sn in the YMP Pitzer database and only results obtained with ThermoChimie v.7b/SIT database are described.

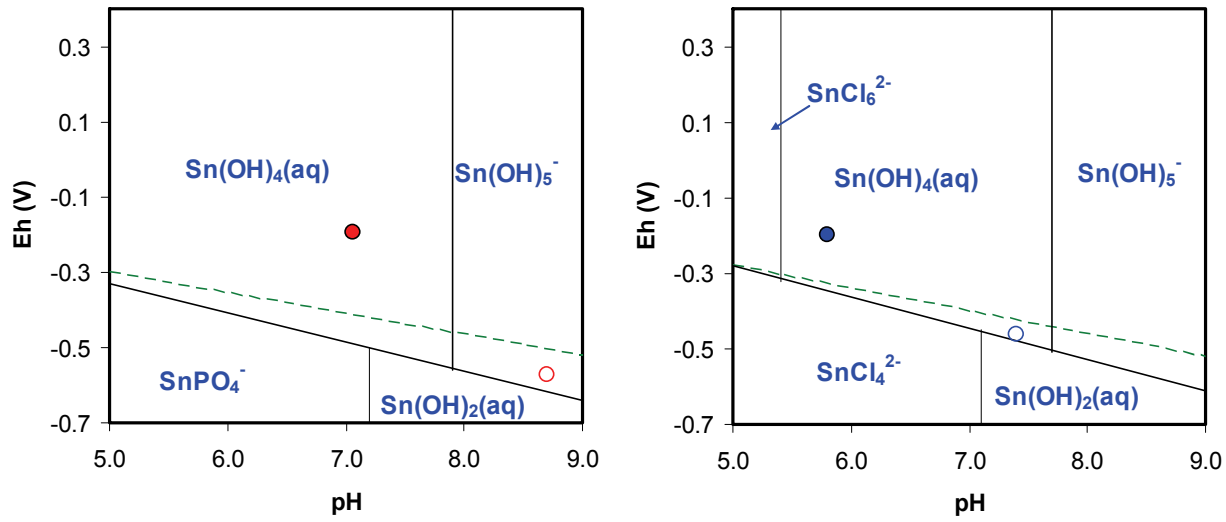

a) b)

Figure 34: Predominance diagram (Eh-pH) of Sn aqueous species: a) Composition of the CR-10 groundwater: *CR-10 eq* (●) and the *CR-10 NF* (○), and b) Composition of the SR-270 groundwater: *SR-270 eq* (●) and the *SR-270 NF* (○). $[Sn]_T = 1 \cdot 10^{-7}$ M. Dashed line: reduction of water to H_2.

The main parameters affecting tin aqueous speciation and solid formation are the pH and Eh of groundwater. However, there are other parameters such as the calcium concentration that can be significant in the formation of solid phases such as $Ca[Sn(OH)_6](s)$. Chloride could also affect tin aqueous speciation (see Figure 34). However, chloride species have only been observed for highly saline waters (Muller and Seward, 2001, Sherman et al. 2000) such as SR-270.

Under all the selected groundwater conditions Sn(+IV) hydrolysis species ($Sn(OH)_4$ and $Sn(OH)_5^-$) dominate the aqueous chemistry of tin (see Table 45). The Sn(+II) hydrolysis species $Sn(OH)_2$ is only present under the reducing conditions found for groundwaters reacted with the C-Steel insert (*CR-10 NF and SR-270 NF*). The proportion of each species depends on the pH and Eh of the selected groundwater. For SR-270 with high chloride concentration (4.75 M), the chloride species $SnCl_6^{2-}$ and $SnCl_4^{2-}$ are also present in minor proportion for *SR-270 eq* and *SR-270 NF* groundwaters, respectively.

Table 45: Sn aqueous speciation under different selected conditions.

	TC / SIT
Equilibrated	
CR-10 eq	$Sn(OH)_4$ (85%), $Sn(OH)_5^-$ (15%)
SR-270 eq	$Sn(OH)_4$ (94%), $SnCl_6^{2-}$ (5%)
Bentonite + C-steel insert	
CR-10 NF	$Sn(OH)_5^-$ (77%), $Sn(OH)_4$ (10%), $Sn(OH)_2$ (7%)
SR-270 NF	$Sn(OH)_4$ (40%), $Sn(OH)_2$ (35%), $Sn(OH)_5^-$ (17%), $SnCl_4^{2-}$ (7%)

Under the selected conditions, the expected solubility limiting solid phases for Sn and the solubility values are summarised in Table 46. The most likely solubility limiting phases under reducing conditions are Sn(+IV) oxide (SnO_2(am)). Under more alkaline conditions, such as for *CR-10 NF* groundwater, the solid phase $CaSn(OH)_6$(s) can be the solid phase controlling the solubility giving tin concentrations in solution of the same order of magnitude (see Table 46)

Table 46: Sn solid phases and concentration values (m) under the different selected conditions.

	Equilibrated (eq)		Bentonite + C-steel insert (NF)	
	TC / SIT	**YMP / PITZER**	**TC / SIT**	**YMP / PITZER**
CR-10	SnO_2(am) $5.81 \cdot 10^{-8}$	-	SnO_2(am) $4.85 \cdot 10^{-7}$ $CaSn(OH)_6$(s) $9.63 \cdot 10^{-7}$	-
SR-270	SnO_2(am) $3.91 \cdot 10^{-8}$	-	SnO_2(am) $9.06 \cdot 10^{-8}$	

Due to the formation of the solid phase $CaSn(OH)_6$(s) under slightly alkaline conditions, the availability of free calcium in the system will modify the concentration of Sn in equilibrium with $CaSn(OH)_6$(s). A slight increase in the Ca aqueous concentration will imply a decrease in the Sn concentration.

Another important uncertainty to take into consideration is the potential presence of sulphide species due to sulphate reduction. Indeed, if sulphate were reduced to sulphide, sulphide solid phases might exert the solubility control at reducing Eh values.

4.18 URANIUM

In the environment, uranium occurs in the oxidation states +III, +IV, +V and +VI. Under the redox conditions of the selected groundwater compositions, uranium will predominantly be in

the tetravalent state, although other redox states such as U(+VI) could coexist in solution (e.g U(+VI) carbonate complexes are very stable and may dominate the aqueous speciation even under slightly reducing conditions).

The uranium aqueous speciation is very dependent on the Eh and pH of the system, although other chemical parameters such as the carbonate content could be important for U(+VI) speciation (see Figure 35 and Figure 36). Under the very reducing conditions of the *CR-10 NF* and *SR-270 NF* groundwaters, the aqueous chemistry of uranium is mainly dominated by the $U(OH)_4$(aq) species and no differences in the aqueous speciation are observed using different databases (see Table 47).

Under less reducing conditions, such as for the *CR-10 eq* and the *SR-270 eq* groundwaters, at the pH and carbonate concentrations of interest, the predominant aqueous species of uranium depends on the thermodynamic database. When using the ThermoChimie v.7 /SIT database, the species $U(OH)_4$(aq) is the main aqueous species for both *CR-10 eq* and *SR-270 eq* groundwater compositions. A minor contribution of the species $U(OH)_3^+$ is observed for the *SR-270 eq* groundwater. On the other hand, when using the YMP Pitzer database, the species $U(OH)_4$ (aq) is the main aqueous species in solution with minor contributions of the species $UO_2(CO_3)_3^{4-}$ for the *CR-10 eq* and the species $UO_2(CO_3)_3^{4-}$, $U(OH)_3^+$, $U(OH)_2^{2+}$ for the *SR-270 eq* groundwater (see Table 47).

For *CR-10 eq* groundwater (with an ionic strength lower than that of *SR-270 eq* groundwater) differences are attributed to the different stability constants for the aqueous and solid phases selected in each database. In *SR-270 eq* groundwater, differences are attributed to differences in both the stability constants and the approach used to calculate ionic strength corrections.

Table 47: U aqueous speciation under the different selected conditions and using both databases.

	TC / SIT	**YMP / PITZER**
Equilibrated		
CR-10 eq	$U(OH)_4$ (92%), $UO_2(CO_3)_3^{4-}$ (4%)	$U(OH)_4$ (80%), $UO_2(CO_3)_3^{4-}$ (14%)
SR-270 eq	$U(OH)_4$ (70%), $U(OH)_3^+$(29%)	$U(OH)_4$ (37%), $UO_2(CO_3)_3^{4-}$ (29%), $U(OH)_3^+$ (28%), $U(OH)_2^{2+}$ (6%)
Bentonite + C-steel insert		
CR-10 NF	$U(OH)_4$ (100%)	$U(OH)_4$ (100%)
SR-270 NF	$U(OH)_4$ (99%)	$U(OH)_4$ (98%)

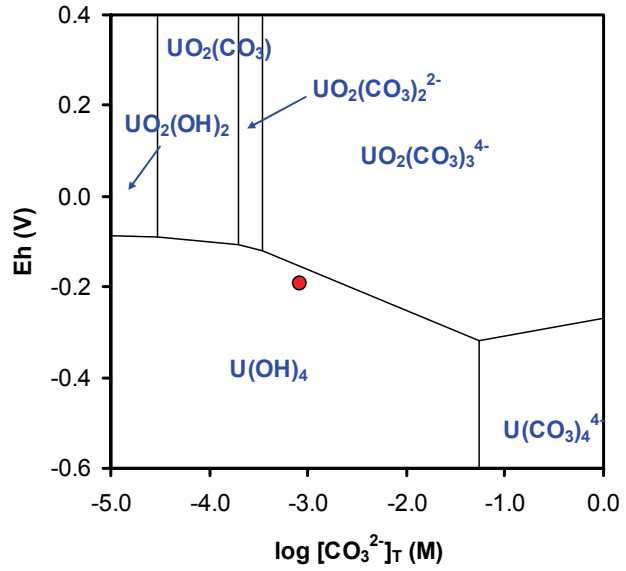

a) ThermoChimie, *CR-10 eq* (pH = 7.1)

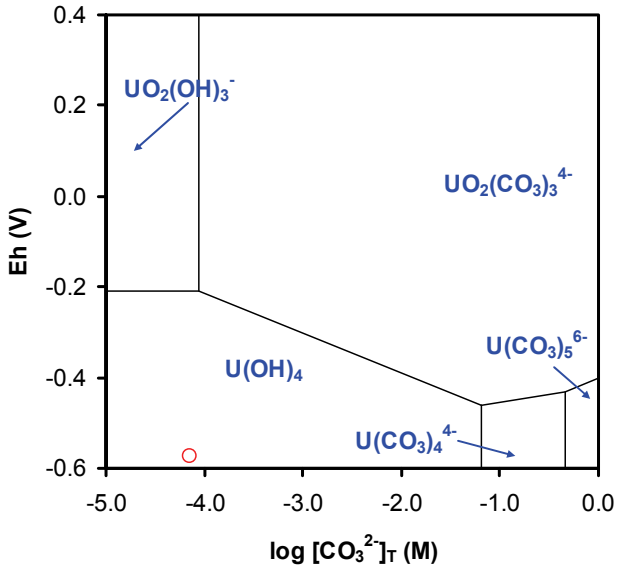

b)ThermoChimie; *CR-10 NF* (pH = 8.7)

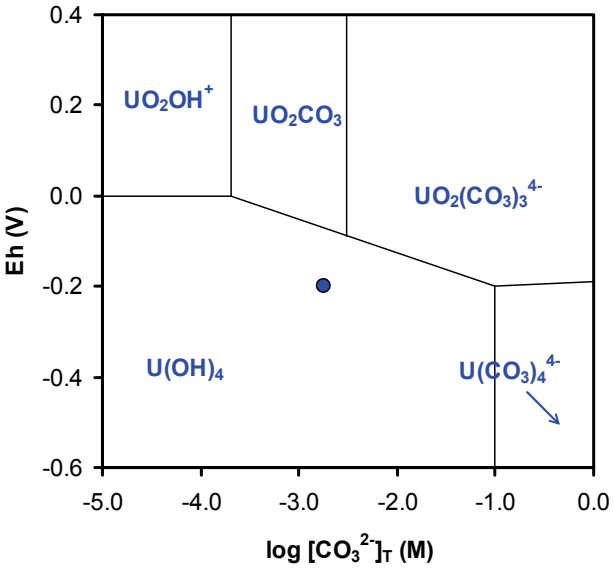

b)ThermoChimie; *SR-270 eq* (pH = 5.8)

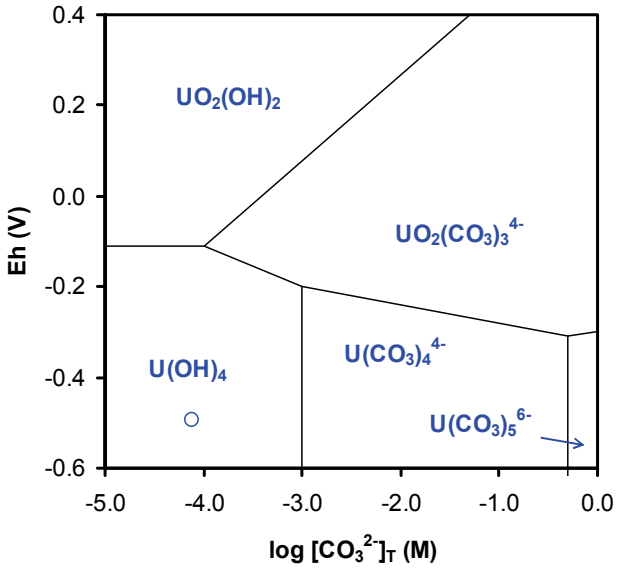

b)ThermoChimie; *SR-270 NF* (pH = 7.4)

Figure 35: Predominance diagram Eh vs log[CO_3^{2-}]$_T$ of uranium aqueous species under the different groundwater compositions calculated with the ThermoChimie SIT database. Symbols refers to *CR-10 eq* (●), *CR-10 NF* (○), *SR-270 eq* (●) and *SR-270 NF* (○) groundwater Eh and carbonate concentration. [U]$_T$=3·10^{-9} Mol/L.

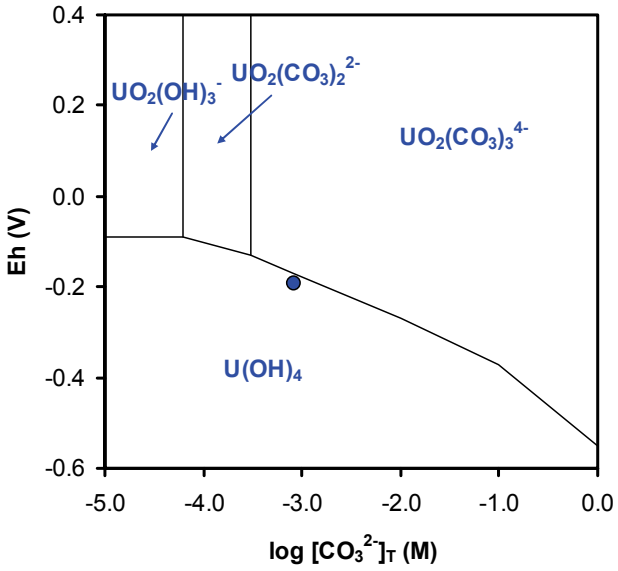

a) YMP database, *CR-10 eq* (pH = 7.1)

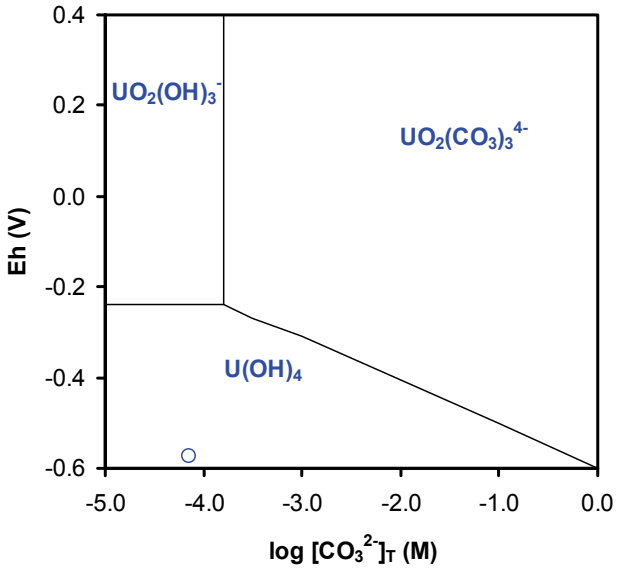

b)YMP database; *CR-10 NF* (pH = 8.7)

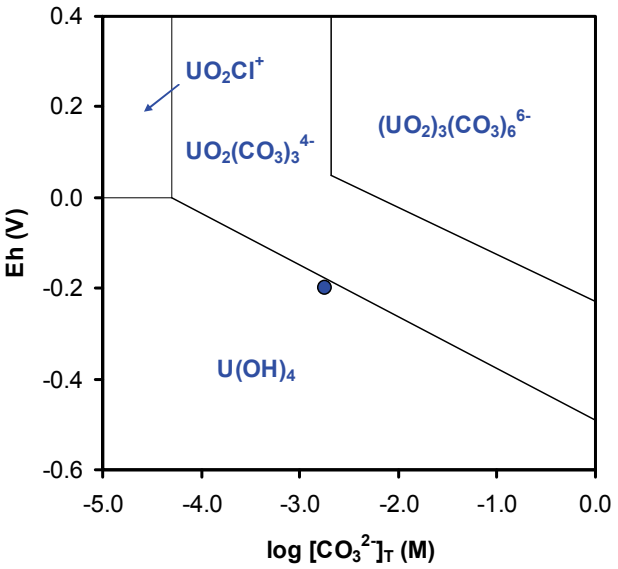

a) YMP database, *SR-270 eq,(* pH = 5.8)*

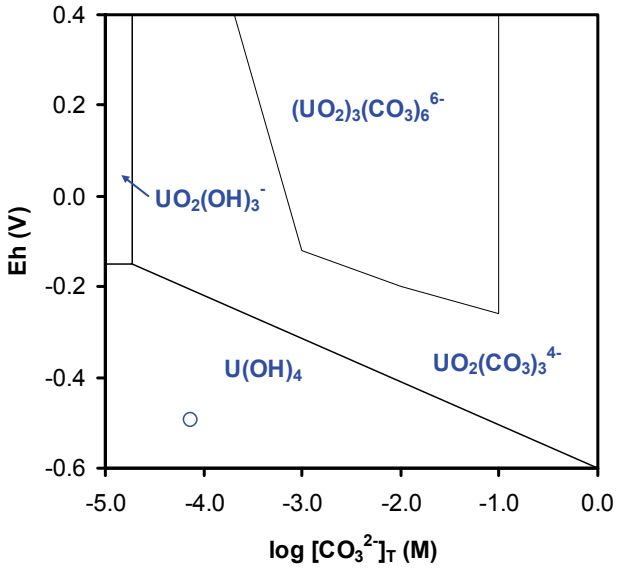

b) YMP database, *SR-270 NF* (pH = 7.4)*

Figure 36: Predominance diagram Eh vs log[CO_3^{2-}]$_T$ of uranium aqueous species under the different groundwater compositions calculated with the YMP Pitzer database. Symbols refers to *CR-10 eq* (●), *CR-10 NF* (○), *SR-270 eq* (●) and *SR-270 NF* (○) groundwater Eh and carbonate concentration. [U]=3·10^{-9} Mol/L. **The stabilization of the complex $(UO_2)_3(CO_3)_6^{6-}$ in SR-270 groundwaters is due to the high charge of the cation when using the Pitzer correction (*Neck and Kim, 2001).

Under the reducing conditions of the selected groundwaters, the solid phases likely to control the aqueous concentration of uranium are UO_{2+x} type solids (writed as hydroxide $U(OH)_4$(am) in

some databases). Calculated concentrations of uranium in equilibrium with the amorphous uranium oxide (UO_2(am) or $U(OH)_4$(am)) are summarized in Table 48.

Table 48: U solid phases and concentration values (m) under the different selected conditions and using both databases.

	Equilibrated (eq)		Bentonite + C-steel insert (NF)	
	TC / SIT	**YMP / PITZER**	**TC / SIT**	**YMP / PITZER**
CR-10	UO_2(am) $3.45\cdot10^{-9}$	$U(OH)_4$(am) $4.80\cdot10^{-9}$	UO_2(am) $3.16\cdot10^{-9}$	$U(OH)_4$(am) $3.82\cdot10^{-9}$
SR-270	UO_2(am) $4.52\cdot10^{-9}$	$U(OH)_4$(am) $1.03\cdot10^{-8}$	UO_2(am) $3.20\cdot10^{-9}$	$U(OH)_4$(am) $3.89\cdot10^{-9}$

As we can see in Table 48 the solubility limiting phases are similar for the two databases. However, the solubility of UO_2 (am) under the *SR-270 eq* is different when using the different databases due to the higher stabilization of ions with high charge (e.g., $UO_2(CO_3)_3^{4-}$ and $(UO_2)_3(CO_3)_6^{6-}$) in saline groundwaters when using Pitzer correction.

4.19 ZIRCONIUM

Zirconium is not a redox sensitive element, thus, it only appears in the Zr(+IV) oxidation state in solution.

Thermodynamic data for zirconium aqueous species are not available in the YMP Pitzer database where only the solid phase ZrO_2(s) (baddeleyite) is selected. Zirconium possesses a remarkable tendency to hydrolyze due to its large charge/size ratio and as a result hydrolysis species must be included in the solubility calculations in order to obtain reliable results. For this reason, only calculations done with ThermoChimie v.7b/SIT database will be discussed.

The main zirconium aqueous species in all selected groundwaters is the hydroxocomplex $Zr(OH)_4$ (aq). Concerning the solid phases, it is believed that ZrO_2(cr) appears to be the solubility controlling phase in low temperature natural waters (Brown et al. 2005). However and according to the Ostwald's principle we have selected the amorphous hydrous oxide as the solid limiting phase. This phase is very insoluble in the pH range of interest (pH between 6 and 9) (see Table 49). No effect of ionic strength on zirconium solubility would be expected for the selected conditions as only the uncharged $Zr(OH)_4$ aqueous species is present in solution.

Table 49: Zr solid phases and concentration values (m) under the different selected conditions.

	Equilibrated (eq)		Bentonite + C-steel insert (NF)	
	TC / SIT	**YMP / PITZER**	**TC / SIT**	**YMP / PITZER**
CR-10	**$Zr(OH)_4$(am, aged)** **$1.82 \cdot 10^{-8}$** ZrO_2(cr) 10^{-10}	(1)	**$Zr(OH)_4$(am, aged)** **$1.82 \cdot 10^{-8}$** ZrO_2(cr) 10^{-10}	(1)
SR-270	**$Zr(OH)_4$(am, aged)** **$1.82 \cdot 10^{-8}$** ZrO_2(cr) 10^{-10}		**$Zr(OH)_4$(am, aged)** **$1.82 \cdot 10^{-8}$** ZrO_2(cr) 10^{-10}	

(1) Not discussed due to the lack of Zr aqueous species in the database (see text).

One of the main uncertainties affecting the Zr solubility assessment is related with the crystallinity of the formed solid phase. The formation of the amorphous phase ($Zr(OH)_4$ (am)) has been favoured in this assessment, given that many of the processes of crystallization occur through a process of dehydration or re-structuring, which are favoured both with temperature and/or with time.

4.20 SUMMARY OF SOLUBILITY CALCULATIONS

In this work we present the solubility assessment of Am, As, Bi, C, Cu, Mo, Nb, Np, Pa, Pb, Pd, Pu, Ra, Se, Sn, Tc, Th, U and Zr at 25ºC in two reference groundwaters, CR-10 and SR-270 under two different cases:

A. **Equilibrated (CR-10 eq and SR-270 eq).** This case assumes that groundwater composition is the one resulting from the equilibration of the groundwater composition provided by NWMO with some major minerals (section 2.4)

B. **Bentonite + C-steel insert (CR-10-NF and SR-270-NF)**. This case assumes that groundwater composition is the one resulting from the interaction of the near field components with the equilibrated groundwaters (section 2.4 and 3.3)

We have used two different databases: the YMP Pitzer and the ThermoChimie v.7b /SIT. This second database has been used in order to check the influence of the database on the results and to calculate solubilities for elements for which there are no data or incomplete data in the YMP Pitzer database.

Assessment of the solubility of elements As, Bi, Nb, Pa, Pb, Pd, Ra, Se, Sn and Zr has been only done with the ThermoChimie v.7b/SIT database or with the thermodynamic data selected in this work (i.e., As and Bi), given that no thermodynamic data are available for these elements in the YMP Pitzer database. A summary of the results of the solubility assessment for these elements is presented in Table 50 and Table 52 for the CR-10 and SR.270 groundwater, respectively.

The solubility assessment for Am, C, Cu, Mo, Np, Pu, Tc, Th and U has been done using both databases. A summary of the results is shown in Table 51 and Table 53 for the CR-10 and SR 270 groundwater, respectively.

From the results obtained we can see that the YMP Pitzer database must be enlarged to incorporate data for missing elements and missing aqueous species of Cu, Mo and Tc. Under the salinity conditions of CR-10 groundwaters, with relatively low ionic strength (0.24 and 0.32 respectively), the differences in the calculated solubilities attributed to the activity corrections are not crucial, as shown in Table 51. In the case of the more saline groundwater such as SR-270, differences due to the activity correction have been observed for C, Am, Pu Th and U (Table 53). Differences are indicated by the different aqueous speciation calculated with each database.

Differences in the solubility values obtained using the two databases are below ± 1 logarithimic unit for all elements except Am, Cu, Mo, Tc, Pu and Th.

These differences are due to the following reasons:

- Lack of MoO_2(s) data in the YMP Pitzer database therefore a different solid phase has been selected as likely solubility limit ($CaMoO_4$(s))

- Lack of Cu(I) data in the YMP Pitzer database which is the redox state present under reducing conditions. As a consequence very low unrealistic solubilities are calculated

- Lack of Tc(IV) hydrolysis species data in the YMP Pitzer database. As a consequence very low unrealistic solubilities are calculated. The implementation of these data in the YMP Pitzer database would be difficult (no Pitzer parameters for Tc(IV) are described in the literature), but it would improve the dataset.

Some differences are only observed for a specific case. For the more reducing conditions of the CR-10 groundwater interacted with the near field components differences for Pu and Am are due to:

- The very high activity coefficients calculated for the dominant aqueous species of plutonium (Pu^{3+}) and americium (Am^{3+}) when using the Pitzer approach. The value of $\log\gamma$ at an ionic strength of 0.24 m is -2.5 while that calculated at an ionic strength of 0.32 is -5, causing an increase of 2 and 1.5 log units in the calculated concentration of plutonium and americium in solution, respectively. This is currently an unresolved issue, but it seems highly unrealistic that the activity corrections at such relatively low ionic strengths are as high as those calculated with the Pitzer approach used in the YMP Pitzer database.

For the saline groundwater SR-270 differences are attributed to:

- LogK values for thorium polynuclear species included in Yucca Mountain / Pitzer database obtained from Neck et al. (2002). In this study, Neck and its co-workers used the SIT approach. The inclusion of those polynuclear species when using Pitzer approach results in a non-consistent thorium database that leads to doubtful results when applied to highly saline waters.

Table 50: Calculated solubility limits and main associated uncertainties for As, Bi, Nb, Pa, Pb, Pd, Ra, Se, Sn and Zr using the ThermoChimie SIT database given the lack of data on these elements in the YMP Pitzer database. Solubilities are calculated for two groundwater compositions: CR-10 eq and CR-10 NF.

Element	GW	Solid phase	Solubility	Mainly sensitive to	Main uncertainty
As	CR-10 eq CR-10 NF	n.s.l[1]	-	pH	• formation of sulphide • co-precipitation or sorption onto major phases
Bi	CR-10 eq CR-10 NF	Bi_2O_3 (s)	$1.17 \cdot 10^{-5}$		• formation of sulphide
Nb	CR-10 eq	Nb_2O_5(s)	$1.07 \cdot 10^{-7}$	pH, calcium concentration	• Quality of thermodynamic data; • Lack of data for Ca solid phases
	CR-10 NF		$1.30 \cdot 10^{-5}$		
Pa	CR-10 eq	Pa_2O_5(s)	$2.22 \cdot 10^{-9}$	pH	• Scarcity of thermodynamic data
	CR-10 NF		$1.31 \cdot 10^{-9}$		
Pb	CR-10 eq	$Pb(CO_3)$ $Pb_3(CO_3)_2(OH)_2$ $Pb_3(PO_4)_2$(s)	$3.11 \cdot 10^{-6}$ $7.96 \cdot 10^{-6}$ $1.09 \cdot 10^{-6}$/ *$7.1 \cdot 10^{-6}$	pH, chloride, carbonate and phosphate concentration	• solid phase formed; • concentration of phosphate in the groundwater; • reduction of sulphate to sulphide
	CR-10 NF	$Pb_3(PO_4)_2$(s)	$2.54 \cdot 10^{-7}$/*$1.4 \cdot 10^{-5}$		
Pd	CR-10 eq	$Pd(OH)_2$(s)	$4.11 \cdot 10^{-6}$	Chloride concentration	• formation of sulphide
	CR-10 NF		$3.98 \cdot 10^{-6}$		
Ra	CR-10 eq	$Ra(SO_4)$(s)	$1.56 \cdot 10^{-7}$	Sulphate and carbonate concentration. Eh due to the reduction of sulphates	• Reduction of radiumsulphate would decrease the stability of sulphate and radium carbonate could become the limiting solid phase • Solid-solution formation with Ba, Sr or Ca phases would produce lower concentrations
	CR-10 NF		$7.20 \cdot 10^{-8}$		
Se	CR-10 eq	$FeSe_2$ (Ferroselite)	$1.15 \cdot 10^{-10}$	Eh and Fe concentration	• Incorporation into sulphide phases would decrease its solubility • Solid phase formed
	CR-10 NF	β-$Fe_{1.04}Se$	$1.26 \cdot 10^{-8}$		
Sn	CR-10 eq	SnO_2(am)	$5.81 \cdot 10^{-8}$	Eh, pH, calcium concentration	• Reduction of sulphate to sulphide may produce solid sulphides
	CR-10 NF	SnO_2(am) $CaSn(OH)_6$(s)	$4.85 \cdot 10^{-7}$ $9.63 \cdot 10^{-7}$		
Zr	CR-10 eq CR-10 NF	$Zr(OH)_4$(am) / ZrO_2(s)	$1.82 \cdot 10^{-8}$ / $6.4 \cdot 10^{-10}$		• Crystallinity of the solid phase formed

[1]:n.s.l.: no solubility limited; *Phosphate concentration given by equilibrium with hydroxoapatite.

Table 51. Calculated solubility limits and main associated uncertainties for Am, C, Cu, Mo, Np, Pu, Tc, Th and U using the ThermoChimie v.7b/SIT and the YMP Pitzer databases. Solubilities are calculated for two groundwater compositions: CR-10 eq and CR-10 NF.

Element	GW	Solid phase	Solubility TC	Solubility YMP	Mainly sensitive to	Main uncertainty
Am	CR-10 eq	$AmPO_4 \cdot xH_2O$ (am) $AmOHCO_3$(s)	$5.14 \cdot 10^{-12}$/*$8.2 \cdot 10^{-12}$ $2.23 \cdot 10^{-5}$	$7.94 \cdot 10^{-12}$ $8.51 \cdot 10^{-6}$	pH, phosphate and carbonate concentration	• solid phase formed: phosphates/carbonates/hydroxides
	CR-10 NF	$AmPO_4 \cdot xH_2O$ (am) $Am(OH)_3$(s)	$2.63 \cdot 10^{-12}$/*$1.06 \cdot 10^{-9}$ $1.51 \cdot 10^{-6}$	$3.64 \cdot 10^{-11}$ $2.8 \cdot 10^{-7}$		
C	CR-10 eq	$CaCO_3$ (calcite)	$8.29 \cdot 10^{-4}$	$8.98 \cdot 10^{-4}$	pH, Calcium concentration	• Reduction to methane/CO
	CR-10 NF		$7.01 \cdot 10^{-5}$	$8.80 \cdot 10^{-5}$		
Cu	CR-10 eq	Cu(s)	$1.36 \cdot 10^{-8}$	Unreliable results	Eh, chloride concentration	• formation of sulphide
	CR-10 NF		$5.22 \cdot 10^{-15}$			
Mo	CR-10 eq	MoO_2 (s)	$8.72 \cdot 10^{-9}$	Unreliable results	pH, Eh, Calcium concentration	• solid phase formed; • lack of thermodynamic data in both databases, specially in YMP TDB
	CR-10 NF		$3.64 \cdot 10^{-15}$			
Np	CR-10 eq	NpO_2(am)	$1.08 \cdot 10^{-9}$	$1.26 \cdot 10^{-9}$		
	CR-10 NF		$1.00 \cdot 10^{-9}$	$1.21 \cdot 10^{-9}$		
Pu	CR-10 eq	$PuPO_4$ PuO_2(am)	$5.12 \cdot 10^{-12}$/ *$8.24 \cdot 10^{-11}$ $1.50 \cdot 10^{-8}$	$9.27 \cdot 10^{-13}$ $7.01 \cdot 10^{-8}$	Eh, pH, phosphate concentration	• Phosphate concentration. Important influence on the database used.
	CR-10 NF	$PuPO_4$ PuO_2(am)	$8.12 \cdot 10^{-13}$/*$3.2 \cdot 10^{-10}$ $9.10 \cdot 10^{-8}$	$4.26 \cdot 10^{-12}$ $1.44 \cdot 10^{-5}$		
Tc	CR-10 eq	TcO_2:$1.6H_2O$	$4.01 \cdot 10^{-9}$	Unreliable results	Eh	• Lack of thermodynamic data in the YMP TDB for aqueous species
	CR-10 NF		$4.05 \cdot 10^{-9}$			
Th	CR-10 eq	ThO_2(aged/am)	$3.94 \cdot 10^{-9}$/$2.49 \cdot 10^{-8}$	$5.23 \cdot 10^{-9}$ /$1.68 \cdot 10^{-7}$	Carbonate concentration	• Crystallinity of the solid phase formed
	CR-10 NF		$1.38 \cdot 10^{-9}$/$7.85 \cdot 10^{-9}$	$3.69 \cdot 10^{-9}$ /$1.14 \cdot 10^{-7}$		
U	CR-10 eq	UO_2(am)	$3.45 \cdot 10^{-9}$	$4.80 \cdot 10^{-9}$	Eh, carbonate concentration	• Crystallinity of the solid phase formed
	CR-10 NF		$3.16 \cdot 10^{-9}$	$3.82 \cdot 10^{-9}$		

*Phosphate concentration given by equilibrium with hydroxoapatite.

Table 52: Calculated solubility limits and main associated uncertainties for As, Bi,Nb, Pa, Pb, Pd, Ra, Se, Sn and Zr using the ThermoChimie v.7b/SIT database. Solubilities are calculated for two groundwater compositions: SR-270 equilibrated with major minerals (SR-270 eq) and SR-270 interacted with the near field components (C-steel insert and bentonite) (SR-270 NF).

Element	GW	Solid phase	Solubility	Mainly sensitive to	Main uncertainty
As	SR-270 eq SR-270 NF	n.s.l[1]	-	pH	• formation of sulphide • co-precipitation or sorption onto major phases
Bi	SR-270 eq	n.s.l	-	pH, chloride concentration	• formation of sulphide
	SR-270 NF	Bi_2O_3 (s)	$9.33 \cdot 10^{-6}$		
Nb	SR-270 eq	Nb_2O_5(s)	$4.90 \cdot 10^{-9}$	pH	• Quality of thermodynamic data
	SR-270 NF		$2.01 \cdot 10^{-7}$		
Pa	SR-270 eq	Pa_2O_5(s)	$3.20 \cdot 10^{-8}$	pH	• Scarcity of thermodynamic data
	SR-270 NF		$1.72 \cdot 10^{-9}$		
Pb	SR-270 eq SR-270 NF	n.s.l.	-	Chloride concentration	• concentration of phosphate in the GW; • reduction of sulphate to sulphide
Pd	SR-270 eq SR-270 NF	n.s.l.	-	Chloride concentration	• formation of sulphide
Ra	SR-270 eq	$Ra(SO_4)$(s)	$1.68 \cdot 10^{-5}$	Sulphate, chloride and carbonate concentration. Eh due to the reduction of sulphates	• Reduction of sulphate would decrease the stability of sulphate and carbonate could become the limiting solid phase • Solid-solution formation with Ba, Sr or Ca phases would produce lower concentrations
	SR-270 NF		$1.43 \cdot 10^{-5}$		
Se	SR-270 eq	$FeSe_2$ (Ferroselite)	$3.43 \cdot 10^{-9}$	Eh and Fe concentration	• Incorporation into sulphide phases would decrease its solubility • Solid phase formed
	SR-270 NF	β-$Fe_{1.04}Se$	$1.77 \cdot 10^{-9}$		
Sn	SR-270 eq	SnO_2(am)	$3.91 \cdot 10^{-8}$	Eh, pH, chloride concentration	• Reduction of sulphate to sulphide may produce solid sulphides
	SR-270 NF		$9.06 \cdot 10^{-8}$		
Zr	SR-270 eq SR-270 NF	$Zr(OH)_4$(am) / ZrO_2(s)	$1.82 \cdot 10^{-8}$/ $4.7 \cdot 10^{-10}$		• Crystallinity of the solid phase formed

[1]:n.s.l.: no solubility limited

Table 53. Calculated solubility limits and main associated uncertainties for Am, C, Cu, Mo, Np, Pu, Tc, Th and U using the ThermoChimie v.7b/SIT and the YMP Pitzer databases. Solubilities are calculated for two groundwater compositions: SR-270 equilibrated with major minerals (SR-270 eq) and SR-270 interacted with the near field components (C-steel insert and bentonite) (SR-270 NF).

Element	GW	Solid phase	Solubility TC	Solubility YMP	Mainly sensitive to	Main uncertainty
Am	SR-270 eq SR-270 NF	n.s.l[1]	-	-	pH, chloride, phosphate and carbonate concentration	• solid solution formation with calcite
C	SR-270 eq	$CaCO_3$ (calcite)	$2.22 \cdot 10^{-3}$	$1.80 \cdot 10^{-3}$	pH, Calcium concentration	• Reduction to methane/CO
	SR-270 NF		$4.34 \cdot 10^{-5}$	$7.52 \cdot 10^{-5}$		
Cu	SR-270 eq	Cu (s)	$2.64 \cdot 10^{-5}$	Unreliable results	Eh, chloride concentration	• formation of sulphide
	SR-270 NF		$3.06 \cdot 10^{-10}$			
Mo	SR-270 eq	MoO_2 (s)	$2.34 \cdot 10^{-13}$	Unreliable results	pH, Eh, Calcium concentration	• solid phase formed; • lack of thermodynamic data in both databases, specially in YMP TDB
	SR-270 NF		$6.29 \cdot 10^{-17}$			
Np	SR-270 eq	NpO_2(am)	$1.72 \cdot 10^{-9}$	$2.73 \cdot 10^{-9}$	pH	
	SR-270 NF		$1.02 \cdot 10^{-9}$	$1.24 \cdot 10^{-9}$		
Pu	SR-270 eq	n.s.l.	-	-	Eh, pH, phosphate concentration	• Phosphate concentration. Important influence on the database used.
	SR-270 NF	$Pu(OH)_3$	$4.50 \cdot 10^{-5}$	$3.15 \cdot 10^{-5}$		
Tc	SR-270 eq	TcO_2:1.6H_2O	$4.39 \cdot 10^{-9}$	Unreliable results	Eh	• Lack of thermodynamic data in the YMP TDB for aqueous species
	SR-270 NF		$4.39 \cdot 10^{-9}$			
Th	SR-270 eq	ThO_2(aged/am)	$2.39 \cdot 10^{-8}$ /$1.45 \cdot 10^{-7}$	Unreliable results	pH and carbonate concentration	• Crystallinity of the solid phase formed • Non-consistent thermodynamic data in the YMP TDB for Th polynuclear aqueous species
	SR-270 NF		$1.10 \cdot 10^{-9}$ /$6.93 \cdot 10^{-9}$			
U	SR-270 eq	UO_2(am)	$4.52 \cdot 10^{-9}$	$1.03 \cdot 10^{-8}$	Eh, carbonate concentration	• Crystallinity of the solid phase formed
	SR-270 NF		$3.20 \cdot 10^{-9}$	$3.89 \cdot 10^{-9}$		

[1]:n.s.l.: no solubility limited

5. SUMMARY AND CONCLUSIONS

In this report we present:

- A study of the effects that the near field components of the nuclear waste repository (C-steel insert and bentonite barrier) can have on the SR-270 groundwater compositions
- Thermodynamic data selected to perform solubility calculations for As, Bi and Cu, which are incorporated in the ThermoChimie v7.b/SIT database.
- A solubility assessment of Am, As, Bi, C, Cu, Mo, Nb, Np, Pa, Pb, Pd, Pu, Ra, Se, Sn, Tc, Th, U and Zr for the two selected reference groundwater compositions, CR-10 and SR-270 under the various conditions of interest.

There are in principle two main uncertainties affecting these calculations: the thermodynamic database and the selected ionic strength correction approach. Due to this reason, the calculations presented in this report have considered different thermodynamic databases:

- ThermoChimie v.7b /SIT database
- YMP Pitzer database

Consequently, results have been also used to test the capabilities of each thermodynamic database.

Concerning the **effect that the near field components** can have on the SR-270 groundwater compositions; results show that both the bentonite barrier and the corrosion of the C-steel insert significantly affect the evolution of the groundwater. Due to corrosion of the C-steel insert, the pH increases and Eh decreases, achieving values around ~ 8 and ~-500mV, respectively. Bentonite is able to control the concentrations of the major cations (Na^+, K^+, Mg^{2+}) by exchange reactions. Calcium concentration is controlled by the precipitation/dissolution of the primary phases present in bentonite (calcite and gypsum). The Fe aqueous concentration is controlled by C-steel corrosion and siderite / magnetite precipitation. The role of pyrite is not significant in this system.

Concerning the **solubility assessment** of Am, As, Bi, C, Cu, Mo, Nb, Np, Pa, Pb, Pd, Pu, Ra, Se, Sn, Tc, Th, U and Zr under the different groundwater compositions of interest, we have used two different databases: the YMP Pitzer and the ThermoChimie v.7b /SIT databases

Assessment of the solubility of As, Bi, Nb, Pa, Pb, Pd, Ra, Se, Sn and Zr has been only conducted with the ThermoChimie v.7b/SIT database or by the thermodynamic data selected in this work (i.e., As and Bi), given that no thermodynamic data are available for these elements in the YMP Pitzer database. A summary of the results of the solubility assessment for these elements is presented in Figure 37.

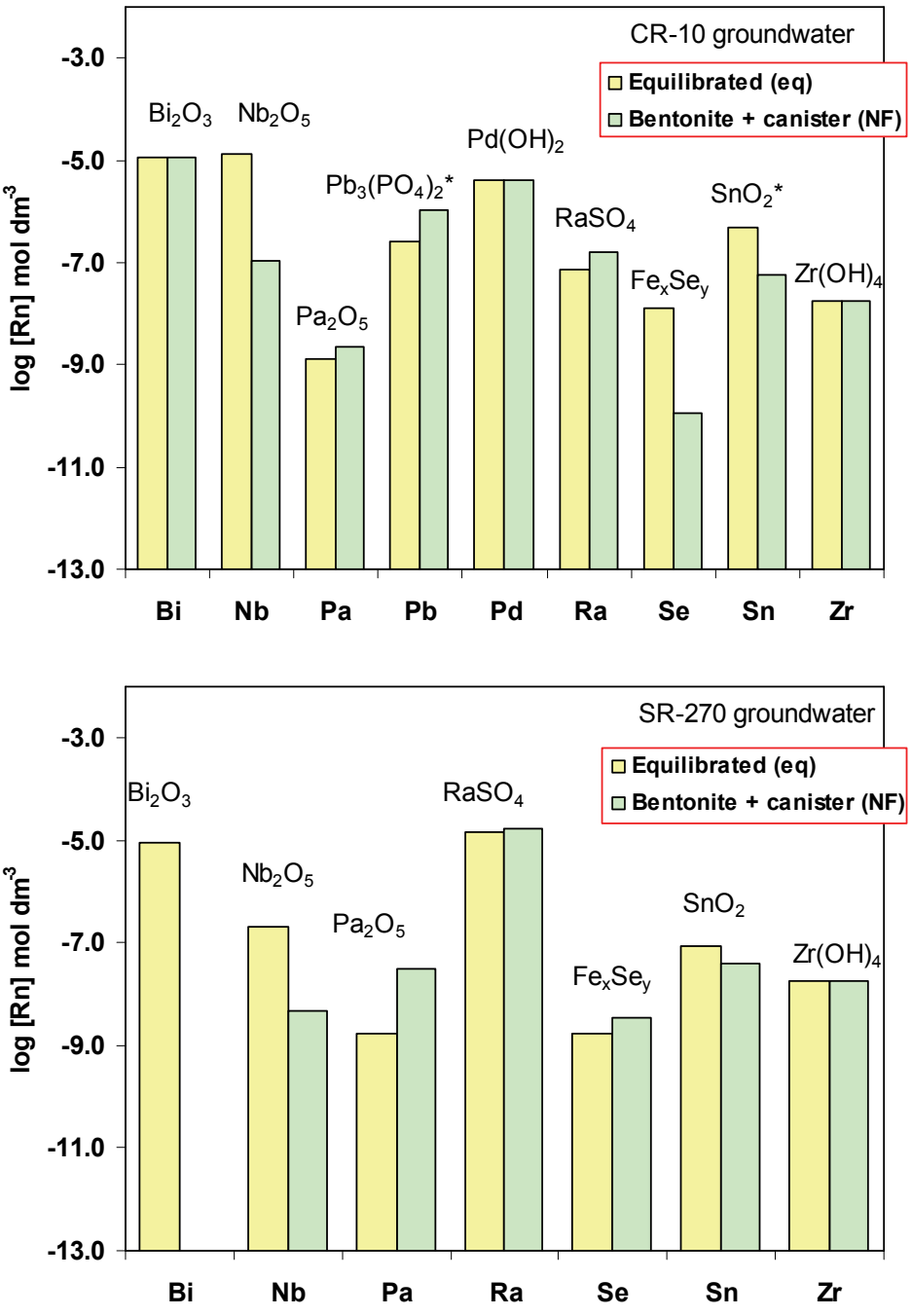

Figure 37. Solubility limiting phases and aqueous radionuclide concentrations calculated using the ThermoChimie v.7b/SIT for CR-10 (top) and SR-270 groundwater (down) compositions. *Other phases give similar concentrations. Elements that are not solubility limited are not represented.

The solubility assessment for Am, C, Cu, Mo, Np, Pu, Tc, Th and U was done using both databases. Differences in the solubility values obtained using the two different databases are below ± 1 logarithimic unit for all elements except Am, Cu, Mo, Tc, Pu and Th:

The differences for these elements are explained in detail in section 4.20

As the main conclusions of the present exercise, we can say that: (1) the incompleteness of the YMP Pitzer database prevents its application to many of the elements of interest in this solubility assessment and (2) the validity of the Pitzer activity corrections should be checked since for some elements these produce erroneous results especially at high ionic strengths.

Finally, the solubility limits discussed and selected in this work contain an important level of uncertainty. Sensitivity analyses, studying the influence of some key parameters on the solubility of radionuclides, and qualitative uncertainty analysis, describing the conceptual uncertainties that may affect the solubility limits of a radionuclide are summarised in Table 54. As we can see in Table 54, some parameters can significantly affect solubility values, generating a broad range of possible radionuclide solubilities depending on the selected groundwater conditions.

Table 54. Main geochemical parameters and conceptual uncertainties affecting to the solubility calculations of each radionuclide under study. Shadowed cells indicate that calculations have been done with both databases: ThermoChimie v.7b/SIT and YMP Pitzer.

	Geochemical parameters			Conceptual uncertainties	Concentration range*
Element	**pH**	**Eh**	**Ligands**		
As	✓			- Sulphide formation - Coprecipitation or sorption in major phases	n.s.l under all the studied conditions 10^{-4} – 10^{-6} m if sulphide formation is considered
Am	✓		- carbonate - chloride: *only for* high *saline waters* - phosphate	- Solid solution formation with calcite - Solid phase formed: phosphate, carbonate, hydroxides	Max: n.s.l (*low carbonate concentration*) Min: 10^{-12} m (*in presence of phosphate*)
Bi	*For pH < 6*		chloride	Sulphide formation	Max: n.s.l *(pH <6)* Min: 10^{-5} m *(pH > 6)*
C	✓		calcium	Reduction to methane /CO	Max:10^{-3} m (*equilibrated groundwaters*) Min: 10^{-5} m (*waters contacted with NF*)
Cu		✓	chloride	- Sulphide formation - YMP : No Cu(I) included in the database	Max:10^{-5} m *(high chloride content)* Min: 10^{-15} m (*low Eh*)
Mo	✓	✓	calcium	- Solid phase formed - Lack of thermodynamic data, specially YMP	Max: 10^{-9} (*higher Eh*) Min: 10^{-17} m (*lower Eh*)
Nb	✓		calcium: *Only for pH > 8.5*	- Lack of data for Ca solids - Quality thermodynamic data	Max: 10^{-5} m *(pH > 8.5)* Min: 10^{-9} m (pH between 7- 8.5)
Np	*For pH < 6*				10^{-9} m
Pa	✓			Scarcity thermodynamic data	Max:10^{-8} m *(pH <6)* Min: 10^{-9} m (pH between 7- 8.5)

Element	Geochemical parameters			Conceptual uncertainties	Concentration range*
	pH	Eh	Ligands		
Pb	✓		- chloride - carbonate: *Only for water with low chloride content* - phosphate: *Only for water with low chloride content*	- Solid phase formed - Sulphide formation	Max: n.s.l *(high chloride content)* Min: 10^{-6} m (*in presence of phosphate and carbonate*) 10^{-10} -10^{-12} m if sulphide formation is considered
Pd			chloride	Sulphide formation	Max: n.s.l *(high chloride content)* Min: 10^{-6} m
Pu	✓	✓	phosphate	Important influence of the database used	Max: n.s.l (*in absence of phosphate and pH <6*) Min: 10^{-12} m (in presence of phosphates)
Ra			- sulphate - carbonate - chloride: *only for* high *saline waters*	Reduction of sulphate	Max: 10^{-5} m *(high chloride content)* Min: 10^{-7} m
Se		✓	Iron	- Solid phase formed - Incorporation into sulphide phases	Max: 10^{-8} m Min: 10^{-10} m
Sn	✓	✓	calcium: *Only for pH > 8.5* *chloride: only for* high *saline waters*	Sulphide formation	Max: 10^{-7} m *(pH > 8.5)* Min: 10^{-8} m (pH between 7- 8.5)
Tc		✓		Lack of thermodynamic data in the YMP database	10^{-9} m
Th	*For pH < 6*		carbonate	Crystallinity of the solid phases	Max: 10^{-7} m (*cristallinity of the solid*) Min: 10^{-9} m (*cristallinity of the solid*)
Zr				Crystallinity of the solid phases	10^{-8} m
U		✓	carbonate	Crystallinity of the solid phases	Max:10^{-8} m (*higher Eh and presence of carbonate)* Min: 10^{-9} m

* Concentration range calculated for each radionuclide taking into account all the selected groundwater and conditions. The conditions under which the maximum and minimum concentrations of the range are obtained are specified in brackets.

ACKNOWLEDGEMENTS

The authors would like to acknowledge useful review comments and suggestions for improvements from Mark Gobien, Frank Garisto and Tammy Yang, NMWO.

REFERENCES

Akinfiev, N.N. and A. V. Zotov. 2001. Thermodynamic description of Chloride, Hydrosulfide, and Hydroxo complexes of Ag(I), Cu(I) and Au(I) at Temperatures of 25-500ºC and pressures of 1-2000 bar. Geochem. Int., 39, 990-1006.

Baes, C.F. Jr. and R.E Mesmer. 1976. The hydrolysis of cations. John Wiley and Sons, New York, USA.

Bard, A.J., R. Parsons, and J. Jordan. 1985. Standard potentials in aqueous solution, International union of pure and applied chemistry, Oxford, U.K.

Benbow, S, D. Savage, P. Wersin, and L.H. Johnson. 2000. Modelling thermal alteration of bentonite barriers in Opalinus Clay. Silica migration-SiO_2 and smectite kinetics, NAGRA internal report.

Bessinger, B., and J.A. Apps. 2003. The Hydrothermal Chemistry of Gold, Arsenic, Antimony, Mercury and Silver. Report LBNL-57395.

Beverskog, B. and I. Puigdomènech. 1997. Revised Pourbaix Diagrams for Copper at 25 to 300°C. J. Electrochem. Soc., 144, 3476-3483

Blanc, P., A. Lassin, and P. Piantone. 2007. Thermoddem a database devoted to waste minerals. BRGM, Orléans, France. http://thermoddem.brgm.fr

Bott, M. and R. K.Thauer. 1987. Proton-motive-force-driven formation of CO from CO_2 and H_2 in methanogenic bacteria. Eur J Biochem. 168, 407-412.

Bradbury, M. H. and B. Baeyens. 2002. Pore water chemistry in compacted re-saturated MX-Bentonite. Physico-chemical characterisation and geochemical modelling. PSI Bericht, Nr. 02–10.

Brown, P.L., Curti, E., Grambow, B., Ekberg, C. (OECD, NEA-TDB). 2005. Chemical Thermodynamics Vol. 8. Chemical Thermodynamics of Zirconium. Elsevier, Amsterdam, Netherlands.

Bruno, J., D. Bosbach, D. Kulik, and A, Navrotsky. 2007. Chemical Thermodynamics 10: Chemical Thermodynamics of Solid Solutions of interest in Radioactive Waste Management. A state-of-the-art report. Nuclear Energy Agency (NEA.OECD), Elsevier Science, Amsterdam, Netherlands.

Bruno, J., L. Duro, and M. Grivé. 2001. The applicability and limitations of the geochemical models and tools used in simulating radionuclide behaviour in natural waters. Lessons learned from the Blind Predictive Modelling exercises performed in conjunction with Natural Analogue studies. SKB TR-01-20. Stockholm, Swedish.

Cama, J, J. Ganor, C. Ayora, and A C Lasaga. 2000. Smectite dissolution kinetics at 80°C and pH 8.8. Geochim. Cosmochim. Acta, 64, 2701–2717.

Cao X., L. Q. Ma, S. P. Singh, and Q. Zhou. 2008. Phosphate-induced lead immobilization from different lead minerals in soils under varying pH conditions. Environmental Pollution 152, 184-192

Charlet, L., A. C. Scheinost, C. Tournassat, J. M. Greneche, A. Géhin, A. Fernández-Martínez, S. Coudert, D. Tisserand, and J. Brendle. 2007. Electron transfer at the mineral/water interface: Selenium reduction by ferrous iron sorbed on clay. Geochim. Cosmochim. Acta 71, 5731–5749.

Charlet, L. and C.Tournassat. 2005. Fe(II)–Na(I)–Ca(II) cation exchange on montmorillonite in chloride medium: Evidence for preferential clay adsorption of chloride – metal ion pairs in seawater. Aquatic Geochemistry, 11, 115–137.

Colàs, E, V. Montoya, X. Gaona, C. Domènech, M. Grivé, and L. Duro. 2007. Development of ThemoChimie database. Version 6. up-date. Prepared by Enviros Spain S. L. National Radiactive Waste Management Agency (ANDRA) report D. RP. 0ENQ.07.0001. Châtenay-Malabry cedex, France.

Curti, E. 1999. Coprecipitation of radionuclides with calcite: estimation of partition coefficients based on a review of laboratory investigations and geochemical data. Applied Geochem. 14, 433-446.

Duro, L., E. Cera, M. Grivé, C. Domènech, X. Gaona, and J. Bruno. 2006. Development of the ThermoChimie thermodynamic database. Janvier 2006, Prepared by Enviros Spain S. L. National Radiactive Waste Management Agency (ANDRA) report C.RP.0ENQ.06.0001, Châtenay-Malabry cedex, France.

Dyer, F. F. and G. W. Leddicote. 1961. The Radiochemistry of Copper, National Academy of Sciences, National Research Council, Washington, DC, USA

Eary, L.E. 1992. The solubility of amorphous As_2S_2 from 25 to 90°C. Geochim. Cosmochim. Acta 56, 2267-2280.

Felmy, A.R., D. Rai, and M.J. Mason. 1991. The solubility of hydrous Thorium(IV) oxide in chloride media: development of an aqueous ion-interaction model. Radiochim. Acta 55, 177-185.

Géhin, A., J. M. Grenèche, C. Tournassat, J. Brendlé, D. G. Rancourt, and L. Charlet. 2007. Reversible surface-sorption-induced electron-transfer oxidation of Fe(II) at reactive sites on a synthetic clay mineral. Geochim. Cosmochim. Acta, 71, 863-876.

Grenthe, I., J. Fuger, R. J. Konings, R.J. Lemire, A.B. Muller, C. Nguyen-Trung, and H. Wanner. 1992. Chemical Thermodynamics 1: Chemical Thermodynamics of Uranium, Vol. 1 of Chemical Thermodynamics, OECD Publishing, North-Holland, Amsterdam.

Grenthe, I. and I. Puigdomènech (eds.). 1997. Modelling in Aquatic Chemistry. Nuclear Energy Agency. Organisation for economic co-operation and development. Paris, France.

Grivé, M., O. Riba, V. Montoya, and L.Duro. 2009. Update of the thermodynamic database. Reporting of new data selection 2009, Amphos Internal report, Spain.

Guillaumont, R., J. Fanghänel, V. Neck, J. Fuger, D.A. Palmer, I. Grenthe, and M.H. Rand. 2003. Chemical Thermodynamics 5. Update on the Chemical Thermodynamics of Uranium, Neptunium, Plutonium, Americium and Technetium. NEA OECD, Elsevier.

Helz, G.R., J.A. Tossell, J.M. Charnock, R.A.D. Pattrick, D.J. Vaughan, and C.D. Garner. 1995. Oligomerization in As (III) sulfide solutions; theoretical constraints and spectroscopic evidence. Geochim. Cosmochim. Acta 59, 4591-4604.

Hinkle, S. R. and D. J. Polette. 1999. Arsenic in Ground Water of the Willamette Basin, Oregon. United States Geological Survey. Water-Resources Investigations Report 98-4205, Portland, Oregon.

Jove-Colon, C., Wolery T, Rard, J, Wijesinghe, A, Jareck, and R, Helean K: 2007. Pitzer database development: Description of the Pitzer geochemical thermodynamic database data0.ypf.R2. Appendix I. In In-Drift Precipitates/Salts Model, Report ANL-EBS-MD-000045 REV 03, DOC.20070306.0037 Las Vegas, Nevada: Sandia National Laboratories.

Kamei, G., C. Oda, S. Mitsui, M. Shibata, and T. Shinozaki. 1999. Fe(II)–Na ion exchange at interlayers of smectite: adsorption–desorption experiments and a natural analogue. Eng. Geol., 54, 15–20.

Karnland, O. 1995. Salt redistribution and enrichment in compacted bentonite exposed to a thermal gradient. SKB AR-95-31, Svensk Kärnbränslehantering AB., Stockholm, Swedish.

Karnland, O., S. Olsson, and U. Nilsson. 2006. Mineralogy and sealing properties of various bentonites and smectite-rich clay materials. SKB TR-06-30, Stockholm, Swedish

King, F. 2007. Overview of a carbon steel container corrosion model for a deep geological repository in sedimentary rock. NWMO TR-2007-01 report. Ontario Canada.

Krupp, R.E. 1990. Comment on “As (III) and Sb (III) sulfide complexes: An evaluation of stoichiometry and stability from existing experimental data” by N.F. Spycher and M.H. Reed. Geochim. Cosmochim. Acta 54, 3239-3240.

Kudo, K., and K. Komatsu. 1999. Reduction of alkali metal carbonate to methane with water in presence of Raney alloy. J. Mol. Catal. A:chemical, 145, 159-167.

Lemire, R.J. and F. Garisto. 1989. The Solubility of U, Np, Pu, Th and Tc in a Geological Disposal Vault for Used Nuclear Fuel. Atomic Energy of Canada Limited, Report AECL-10009. Pinawa, Manitoba, Canada.

Licht, S. 1988. Aqueous Solubilities, Solubility Products and Standard Oxidation-Reduction Potentials of the Metal Sulfides. J. Electrochem. Soc., 135, 2971-2976

Lothenbach, B., M. Ochs, H. Wanner, and M. Yui. 1999. Thermodynamic data for the speciation and solubility of Pd, Pb, Sn, Sb, Nb and Bi in aqueous solution. JNC TN8400 99-011, Japan.

Madsen, F.T. 1998. Clay mineralogical investigations related to nuclear waste disposal. Clay Minerals 33, 109–129.

Mandal, B.D. and K. T. Suzuki. 2002. Arsenic round the world: a review. Talanta, 58, 201-235.

Martell, A.E. R.M. Smith, and R.J. Motekaitis. 2004. NIST critically selected stability constants of metal complexes. NIST Standard Reference Database 46, Version 8.0.

Mironova, G.D. and A.V. Zotov. 1980. Solubility studies of the stability of As (III) sulfide complexes. Geochem. Intern, 17, 46-54.

Mironova, G.D., A.V. Zotov, and N.I. Gul'ko. 1984. Determination of the solubility of orpiment in acid solutions at 25-150°C. Geochem. Intern., 53-59.

Montoya, V., A. Tamayo, X. Gaona, M. Grivé, and L. Duro. 2008. Update of the ThermoChimie database. Reporting of new data selection 2007 Project ANDRA-TDB6-Task 1. Prepared by Amphos 21. Amphos 21 Progress Report vs.01, Barcelona, Spain.

Muller, B. and T.M.Seward. 2001. Spectrophotometric determination of the stability of tin(II) chloride complexes in aqueous solution up to 300ºC., Geochim. Cosmochim. Acta, 65, 4187-4199

Neck, V. and J.I. Kim. ,2001. Solubility and hydrolysis of tetravalent actinides. Radiochim. Acta 89, 1216 (2001).

Neck, V., R. Müller, M. Bouby, M. Altmaier, J. Rothe, M. A. Denecke, and J. I. Kim. 2002. Solubility of amorphous Th(IV) hydroxide – application of LIBD to determine the solubility product and EXAFS for aqueous speciation. Radiochim. Acta 90, 485–494.

Ochs, M, B. Lothenbach, H. Wanner, H . Sato, and M. Yui. 2001. An integrated sorption-diffusion model for the calculation of consistent distribution and diffusion coefficients in compacted bentonite. J. Contam. Hydrol., 47, 283–296.

O'Day, P. 2006. Chemistry and mineralogy of Arsenic. Elements, 2, 77-83.

O'Day, P. A., D. Vlassopoulos, R. Root, and N.Rivera. 2004. The influence of sulphur and iron on dissolved arsenic concentrations in the shallow subsurface under changing redox conditions. Proceedings of the National Academy of Sciences, 101, 13703-13708.

Olin, A., B. Noläng, E. G. Osadchii, L. O. Öhman, and E. Rosén. 2005. Chemical Thermodynamics 7: Chemical Thermodynamics of Selenium. Nuclear Energy Agency (NEA.OECD), Elsevier.

Palit, A. and S. O Pehkonen, 2000. Copper corrosion in distribution systems: evaluation of a homogeneous Cu2O film and a natural corrosion scale as corrosion inhibitors. Corrosion Science, 42, 1801-1822

Parkhurst, D.L. and C.A.J. Appelo. 2001. User's guide to PHREEQC (version 2.4.6) A computer program for speciation, batch reaction, one dimensional transport and inverse geochemical calculations. U. S. Department of the Interior. U. S. Geological Survey. Water Resources Investigations, Reston, Virginia, USA.

Pedersen, K. 2000. Microbial processes in radioactive waste disposal. Prepared by Göteborg University, SKB technical report TR-00-04, Svensk Kärnbränslehantering AB. Stockholm, Sweden.

Puigdomènech, I. and C. Taxén. 2000. Thermodynamic data for copper. Implications for the corrosion of copper under repository conditions. Technical Report SKB TR-00-13

Puigdomènech, I. 2002. MEDUSA (Make Equilibrium diagrams using sophisticated algorithms) Windows interface to the MS-DOS version of INPUT, SED and PREDOM (FORTRAN programs drawing chemical equilibrium diagrams. Royal institute of Technology, Stockholm, Sweden.

Rand, M., J. Fuger, I. Grenthe, V. Neck, and D. Rai. 2009. Chemical Thermodynamics 11: Chemical Thermodynamics of Thorium, Vol. 11 of Chemical Thermodynamics, OECD Publishing.

Robby, R.A. and B.S. Hemingway. 1995. Thermodynamic Properties of Minerals and Related substances at 298.15 K and 1 Bar (105 Pa) Pressure and at Higher Temperatures. U.S. Geological survey Bulletin 2131.

Sherman, D.M., K. V. Ragnarsdottira, E.H. Oelkers, and C.R. Collins. 2000. Speciation of tin (Sn^{2+} and Sn^{4+}) in aqueous Cl solutions from 25°C to 350°C: an in situ EXAFS study. Chemical Geol. 167, 169-176

Shannon, R.D. 1976. Revised Effective ionic Radii and Systematic Studies of Interatomic Distances in Halides and Chalcogenides. Acta Crystallog. A32, 751-767.

SKB. 2004. Interim main report of the safety assessment SR-Can. SKB TR-04-11, Svensk Kärnbränslehantering AB.

SKB. 2004b. Interim Process Report for the Safety Assessment SR-Can. SKB R-04-33,Svensk Kärnbränslehantering AB.

Smart, N.R, D. J. Blackwood, and L. Werme. 2001. The anaerobic corrosion of carbon steel and cast iron in artificial groundwaters. SKB TR-01-22. Stockholm, Swedish.

Smart, N.R., D. J. Blackwood, G. P. Marsh, C. C. Naish, T. M. O'Brien, A. P. Rance, and M. I. Thomas. 2004. The Anaerobic Corrosion of Carbon and Stainless Steels in Simulated Cementitious Repository Environments: A Summary Review of Nirex Research, AEAT/ERRA-0313

Smart, N.R. and A.R. Hochs. 2006. A survey of steel and zircaloy corrosion data for use in the SMOGG gas generation model. Serco report SA/ENV-0841.

Spycher, N.F. and M.H. Reed. 1989. As(III) and Sb(III) sulfide complexes; an evaluation of stoichiometry and stability from existing experimental data. Geochim. Cosmochim.Acta 53, 2185-2194.

Sriram, R and D. Tromans. 1985. Stress corrosion cracking of carbon steel in caustic aluminate solutions - Crack propagation studies. Metall. Trans. 16A, 979-986.

Talerico, C. M. Ochs, E. Giffaut. 2004. Solubility of niobium(V) under cementitious conditions: importance of Ca-niobate. Mat. Res. Soc. Symp. Proc., 824, 443-448

Var'yash, L. N. 1989. Equilibria in the Cu-Cu0-H_20 System at 150-450°C. Geochem. Int., 26, 80-90.

Vaughan, D. J. and J.R. Craig. 1978. Mineral Chemistry of metals sulfides. Cambridge University Press, New York, USA

Vines, S.P. 2002. Report of a workshop to discuss the electrochemical potential in a radioactive waste repository. Nirex report N/072, UK.

Wagman, D.D., W.H. Evans, V.B. Parker, R.H. Schumm, I. Halow, S.M. Bailey, K.L. Churney, and R.L. Nuttall. 1982. The NBS tables of chemical thermodynamic properties, selected values for inorganic and c1 and c2 organic substances in SI units. J. Phys. Chem. Ref. Data, V. 11, supp. 2, 392p.

Webster, J.G. 1990. The solubility of As_2S_3 and speciation of As in dilute and sulphide- bearing fluids at 25 and 90°C. Geoch. Cosmochim. Acta 54, 1009-1017.

Welch, A.H., M. S. Lico, and J. L. Hughes. 1988. Arsenic in ground water of the Western United States: Ground Water, 26, 333–347.

Welch, A. H., R. S. Oremland, J. A. Davis, and S. A. Watkins. 2006. Arsenic in Ground Water: A Review of Current Knowledge and Relation to the CALFED Solution Area with Recommendations for Needed Research, San Francisco Estuary and Watershed Science, 4, 1-32

West, J. M. and I.G. McKinley. 2001. Progress in the Geomicrobiology of Radioactive Waste Disposal Mat. Res. Soc. Symp. Proc., 663, 657-664

Williamson, M. A. and J.D. Rimstidt. 1994. The kinetics and electrochemical rate-determining step of aqueous pyrite oxidation. Geochim. Cosmochim. Acta, 58, 543–5454.